

AN ABSTRACT OF THE DISSERTATION OF
PERCY L. DONAGHAY for the degree of DOCTOR OF PHILOSOPHY
in Biological Oceanography presented on September 14, 1979
EXPERIMENTAL AND CONCEPTUAL APPROACHES
TO UNDERSTANDING ALGAL-GRAZER INTERACTIONS

Redacted for Privacy

Abstract approved: _____
Dr. Lawrence F. Small

An eventual objective of the study of grazing processes is to be able to predict both quantitatively and qualitatively what a copepod (species and life history stage) will ingest in any given situation, and subsequently to predict how that ingestion will affect copepod growth and reproduction. This objective can best be met by addressing the questions of how do the animals select and why do they select one food over another. Only once such patterns are known, can one predict the effects of grazing, and associated nutrient regeneration, on phytoplankton productivity and species succession. Attempts to model planktonic marine ecosystems have clearly demonstrated the critical nature of the coupling between the first and second trophic levels.

It is the premise of this thesis that accurate prediction is based on (1) the development of methods to determine the selective capabilities of an animal, and what elicits a particular response, (2) development of methods to distinguish between those patterns of behavior that are expected from mechanical properties of the feeding mechanism and those that require active choice, (3) development of conceptually consistent and mathematically correct indices for describing observed

patterns of behavior, and (4) development of a general theoretical model of copepod grazing that considers alternate methods whereby selection can occur and the reasons why a copepod should or should not be selective in a given situation. Each of these four major areas will be considered in one of the four chapters of this thesis. Although each chapter has been written as a separate paper (the first two of which are published), all the chapters are highly interrelated. Review of the pertinent literature in each of these areas is considered in the appropriate chapter. In addition, the theoretical paper (Chapter 4) is designed to integrate the work described in previous chapters with the existing literature on grazing.

EXPERIMENTAL AND CONCEPTUAL APPROACHES TO UNDERSTANDING
ALGAL - GRAZER INTERACTIONS

by

Percy L. Donaghay

A DISSERTATION
submitted to
Oregon State University

in partial fulfillment of
the requirements for the
degree of

Doctor of Philosophy

June 1980

APPROVED:

Redacted for Privacy

Professor of Oceanography in Charge of Major

Redacted for Privacy

Dean of School of Oceanography

Redacted for Privacy

Dean of Graduate School

Date thesis is presented September 14, 1979

Typed by Pam Wegner for Percy L. Donaghay

ACKNOWLEDGEMENTS

I would like to gratefully acknowledge the financial support of the National Science Foundation through NSF Grants OCE 76-10347 and OCE 78-08635. I would like to thank all those people who contributed in their own special way to this thesis. Contributions to particular chapters of this thesis are acknowledged at the end of the respective papers. Special thanks goes to my wife Karen whose emotional support made this thesis possible and to my major professor Larry Small whose friendship and unfailing willingness to discuss and become excited about new ideas and results made this thesis more enjoyable. I would like to also thank Drs. David Nelson, Charles Warren, and Louis Gordon for serving on my committee.

I would like to thank R. D. Leatham, J. M. DeManche, B. L. Dexter, and R. Malouf for the many discussions which helped hone the ideas in this thesis. Their friendship is also greatly appreciated.

I would like to thank Dr. S. Skopik for introducing me to the excitement of scientific discovery, Dr. D. Frankenberg for introducing me to biological oceanography and interdisciplinary thought, and Drs. J. Beers and C. E. Warren for helping me develop a strong research perspective and some concept of the interactions of theory and experiment in science.

TABLE OF CONTENTS

		<u>Page</u>
CHAPTER I	FOOD SELECTION CAPABILITIES OF THE ESTUARINE COPEPOD <u>ACARTIA CLAUSI</u>	1
	Abstract	2
	Introduction	2
	Existing viewpoints	2
	Theoretical considerations	3
	Methods and Materials	5
	Results	7
	Discussion	8
	Literature Cited	10
CHAPTER II	GRAZING INTERACTIONS IN THE MARINE ENVIRONMENT	12
	Abstract	13
	Acknowledgements	27
	References	28
CHAPTER III	A COMPARISON OF GRAZING FUNCTIONS FROM PHYTOPLANKTON AND ZOOPLANKTON VIEWPOINTS: AN ALGORITHM	29
	Abstract	30
	Introduction	31
	Exponential assumptions	33
	Mathematical Formulation of Grazing Indices	37
	Net effect indices	37
	Growth rate indices	39
	Ingestion rate indices	43
	Filtration rate indices	45
	Capture rate indices	54
	Electivity indices	58
	Experimental intercomparison of grazing indices	65
	Net effect indices	67
	Growth rate indices	71
	Ingestion rate indices	75
	Filtration rate indices	75
	Capture rate indices	84
	Electivity indices	91
	Acknowledgements	94
	References	95
CHAPTER IV	CONCEPTUAL APPROACHES TO THE CONTROL OF FEEDING BEHAVIOR IN COPEPODS	101
	Abstract	102
	Introduction	104

TABLE OF CONTENTS (continued)

	<u>Page</u>
Part I Capture Process Control of Feeding Behavior	106
Feeding mechanisms: an overview	106
Types of feeding	106
Types of selection	111
Filter model: factors affecting encounter and combing selection	113
Effects of critical elements of model on feeding behavior	118
1) effects of pattern of pore spacing	119
2) effects of δ	119
3) effects of cross filter flow, ϵ	122
4) effects of combing	122
5) effects of hydrodynamics	124
Factors in affecting post combing selection	126
Steps in evaluating feeding mechanisms	128
1) analysis of feeding appendage morphology	129
2) analysis of predicted shapes of filtering curves	137
3) experimentally defined selective capabilities	162
4) codevelopment of structure and behavior with ontogeny	163
Part II Assimilatory control of feeding behavior	166
Theoretical basis for I* hypothesis	170
Evidence supporting the I* hypothesis	177
Critical conditions necessary for experimental test of I* hypothesis	182
Part III Ecological and Evolutionary Implications of Alternative Feeding Behaviors	190
References	210

LIST OF ILLUSTRATIONS

<u>Figure</u>		<u>Page</u>
Chapter I		
1	Filtering efficiency curve for <u>Acartia clausi</u> and relative position of particle distributional peaks relative to filtering efficiency curve.	4
2	Hierarchical experimental design used to test between alternative feeding mechanisms.	6
3	Ingestion behavior and effects of preconditioning on feeding behavior on different particle mixes.	8
Chapter II		
1	Particle selectivity curve for <u>Acartia clausi</u> .	15
2	Experimentally derived filtering rate-particle size curve for <u>Calanus pacificus</u> .	16
3	Filtering rates for <u>Acartia clausi</u> fed a mixture of 14 μm <u>Thalassiosira fluviatilis</u> and 5 μm <u>Thalassiosira pseudonana</u> .	18
4	Effects of preconditioning on ingestion behavior of <u>Acartia clausi</u> .	20
5	Varying types of filtration curves derived for <u>Acartia clausi</u> .	23
Chapter III		
1	Exponential assumptions test.	36
2	Dark growth test.	47
3	Theoretical relationship between filtering efficiency and apparent filtering rate and particle size expressed as the natural log of equivalent particle diameter.	51
4	Percentage based indices.	63
5	The net effect indices shown for the four cases.	68
6	The growth rate indices.	72
7	Ingestion rate indices.	76
8	The F_{max} based filtration rate indices.	78

LIST OF ILLUSTRATIONS (continued)

<u>Figure</u>		<u>Page</u>
9	Regression based filtration rate indices for cases 2 and 3.	81
10	F_{\max} based capture indices.	85
11	Regression based capture indices plotted for cases 2 and 3.	89
12	Electivity indices.	92
 Chapter IV		
1	Feeding mechanisms in herbivorous and omnivorous copepods.	107
2	Design of the hypothetical filter.	115
3	Second maxillae of <u>Acartia clausi</u> adult female.	131
4	Variability in setule spacing as affected by different normalization procedures.	132
5	Comparison of patterns of setule spacing for all setae for all animals.	136
6	Properties of theoretical filtering efficiency curves.	139
7	Possible relevant combinations of ϕ , δ , combing, axis of variance and λ .	142
8	Expected filtering efficiency curves if minimal intersetal distance is greater than maximum intersetule distance (Case 1, Fig. 6).	143
9	Expected filtering efficiency curves if minimal intersetal distance is approximately equal to minimal intersetule distance.	148
10	Expected "filtering curves" for raptorial feeding copepods.	150
11	Expected filtering curve for "Strickler motion."	150
12	Shape of experimentally derived filtering curves for <u>Acartia clausi</u> .	156

LIST OF ILLUSTRATIONS (continued)

<u>Figure</u>		<u>Page</u>
13	Serial hypothesis test used to define selective capabilities of a copepod.	164
14	Functional relationship of ingestion rate and filtering rate to food concentration.	167
15	Relationship between digestive enzyme activity and the concentration of the appropriate substrate in the field environment from which the copepods were collected.	171
16	Ingestion rate curves determined six days apart on <u>Pseudocalanus sp.</u> from Bedford Basin, N.S.	171
17	Relationship between ingestion rate and particle concentration for all levels of food at or below that from which the animals were collected.	171
18	Hypothesized ingestion rate relationships.	173
19	Hypothesized relationship between I^* and enzyme activity.	173
20	Hypothesized alternative forms of the ingestion rate function.	175
21	Hypothesized relationships between I^* and natural field particle concentrations, I^* and all possible concentrations to which the animals have been acclimated in the laboratory, and animals growth rates measured in the laboratory and acclimated food concentrations.	175
22	Seasonal ingestion rates of <u>Acartia clausi</u> .	178
23	Preconditioning effects on ingestion rate curves.	181
24	Expected ingestion rate - concentration relationships for copepods exposed to changing phytoplankton concentration with time.	185
25	Hypothesized relationship between I^* and k_a and enzyme activity and k_a .	187
26	Potential interactions of filter design and particle size spectra in coastal waters.	205

CHAPTER 1

FOOD SELECTION CAPABILITIES OF THE ESTUARINE COPEPOD ACARTIA CLAUSI

by

Percy L. Donaghay
and
Lawrence F. Small
School of Oceanography
Oregon State University
Corvallis, Oregon 97331

Reprinted from Marine Biology, Vol 52, pages 137-146, 1979.
Copyright 1979 by Springer-Verlag and reprinted by permission of the
copyright owner.

Food Selection Capabilities of the Estuarine Copepod *Acartia clausi*

P.L. Donaghay and L.F. Smell

School of Oceanography, Oregon State University, Corvallis, Oregon, USA

Abstract

Existing viewpoints and theories of selective grazing by copepods are briefly reviewed in order to formulate explicit hypotheses to be tested experimentally. Based on these hypotheses, a series of grazing experiments was run to determine (1) the extent of the selective ingestion capabilities of *Acartia clausi* and (2) how these capabilities were affected by previous feeding histories. Groups of copepods were separately preconditioned on a small diatom (*Thalassiosira pseudonana*), a large diatom (*T. fluviatilis*), or a plastic sphere. The ingestive behavior was then examined on various combinations of spheres and food particles. Spheres offered alone were not ingested. In mixtures of diatoms and spheres, the copepods avoided ingesting spheres intermediate in size between the sizes of the diatoms. The copepods either ingested particles on either side of the spheres, or ignored all particles less than the size of the largest spheres. The pattern observed depended upon the size of the preconditioning food. However, if the spheres were larger than the largest food particles, the copepods still selectively ingested the food particles. The above results demonstrate that *A. clausi* has a complex grazing behavior consisting of (1) more efficient grazing on larger particles within its particle-size ingestion range; (2) the ability to alter "effective" setal spacing to optimize feeding behavior (i.e., the ability to increase efficiency of capture of food particles, and to avoid non-food particles); and (3) the ability for post-capture rejection of non-food particles when they interfere with the ingestion of food particles on which the copepod has been preconditioned. The behavioral patterns observed depend heavily on the food preconditioning and the presence or absence of non-food particles. These results clearly indicate that a simple "mechanistic" explanation of selective grazing is insufficient.

Introduction

Two general points of view have developed in recent years concerning selective grazing by copepods: the behavioral and the mechanistic. The behavioral view is that preferential removal of certain size classes of particles is the result of either (1) selection of particles by actively altering the setal spacing on the copepod's filtering appendages, or (2) post-capture rejection of unwanted particles. The mechanistic viewpoint is that all apparent selective grazing is the result of fixed mechanical properties of the copepod's filter. We shall briefly review the evidence behind each of these viewpoints, present a method

for testing the resulting alternative hypotheses, and discuss the results of our experiments.

Existing Viewpoints

The behavioral view originated from Wilson's (1973) observation that in short-term experiments *Acartia tonsa* selectively ingested the largest sphere offered in a mixture of various sizes of inert spheres. Wilson suggested, therefore, that *A. tonsa* actively alters its setal spacing to optimize capture of the largest particles present. Wilson's hypothesis allows for greater ingestion rates on larger particles, but does not permit selection against large particles.

Donaghay and Small (1979) suggest that rejection of large particles can be explained by post-capture rejection, in which rejection of particles by the mouth parts takes place after capture on the filtering appendages.

The mechanistic viewpoint derives from efforts to relate particle selection to the physical properties of copepod filtering appendages. Nival and Nival (1973, 1976) showed that there is variance in setule spacing along the setae of the principle filtering appendages. They suggested that this variance should result in increasing filtration efficiency for particles up to, but not above, the maximum setule spacing (i.e., the maximum pore size). Thus, increasing filtering efficiency for large particles could be explained by the assumption that large particles would be trapped at all pore sizes along the filter surface, but small particles would only be retained by the filter area having pore sizes smaller than the diameter of the small particles. Boyd (1976), however, suggested that if particles were trapped both by the setules and across the setae, increasing filtering efficiency with increasing particle size would be expected for all sizes of particles within the particle size ingestion range of the grazer. Assuming that particles were trapped on both the setules and setae, Boyd (1976) and later Lam and Frost (1976) and Lehman (1976) suggested that apparent selection for large particles could be predicted from the physical characteristics of the filter, and that active adjustment of setal spacing as per Wilson (1973) need not be invoked. This purely mechanistic viewpoint was supported by the early data of Frost (1972), which showed that the maximum filtering rates in unialgal food suspensions increased with increasing particle size. Lam and Frost (1976) proposed a mechanistic model of grazing wherein the copepod has a fixed setal spacing with a known variance, and only the filtering rate is variable. Based on this model, the relative efficiency of capture of a particle is a fixed function of that particle's diameter. As a result, the ingestion and filtration rates observed are solely functions of the particle size and the concentration of particles.

Neither the behavioral viewpoint of varying setal spacing nor the mechanistic viewpoint offer a sufficient explanation for the often complex selective behavior observed on natural food suspensions (Poulet, 1973, 1974; Storm, 1974; Schnack, 1975; Richman *et al.*, 1977; Conover, *in press*) or in some complex

multifood laboratory studies (Marshall and Orr, 1955; Conover, 1966; Donaghay and Small, 1979). Some of the field data can be disputed as evidence for selective ingestion because of possible particle modification (Poulet, 1973) or interference from inert particles (Frost's 1977 interpretation of Poulet, 1973, 1974). However, the particle counting data of Richman *et al.* (1977) and Conover, *in press*), and the gut content analyses of Schnack (1975), cannot be disputed on these grounds because the data have been microscopically confirmed. Several points are relevant here. Firstly, neither the variable nor fixed setal spacing viewpoint can explain how copepods can ingest particles at multiple locations (particle sizes) within their particle size ingestion range without ingesting intermediate sizes (Storm, 1974; Schnack, 1975; Richman *et al.*, 1977; Conover, *in press*). Secondly, neither viewpoint can explain how previous feeding history can alter the selective behavior of copepods (Harvey, 1937; Marshall and Orr, 1955; Conover, 1966). Thirdly, neither viewpoint addresses the question of why grazers should be so selective in mixed food suspensions in the first place. Finally, neither viewpoint offers an explanation for the variability in Ivlev-type ingestion curves (Frost, 1972; O'Connors *et al.*, 1976). The overall variability in Ivlev-type curves is much larger than the variability expected from experimental replicability (Donaghay and Small, 1979).

Three explanations can be offered for the insufficiencies of the fixed and variable setal spacing arguments: (1) copepods have a large repertoire of behavioral responses, only a few of which have been tested by previously used laboratory experimental designs (i.e., the copepods' full spectrum of selective capabilities is undefined); (2) species differences are involved so that responses of one species need not apply to a different species; (3) the discrepancy between field and laboratory data is the result of complex interactions between selective behavior and nutrient regeneration by the copepods, and the physical and physiological characteristics of the algal food.

Theoretical Considerations

Each of the above explanations undoubtedly has some validity, either individually or in concert. However, in this paper we shall examine only the first possible explanation: definition of the selective capabilities of a given cope-

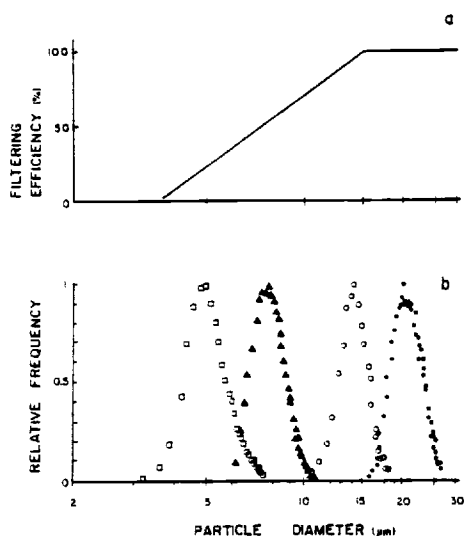


Fig. 1. *Acartia clausi*. (a) Filtering efficiency curve ("Nival curve"); redrawn from Nival and Nival (1976). (b) Relative volume distributions of *Thalassiosira pseudonana* (squares), nominally 8 μ m diameter latex spheres (triangles), *T. fluviatilis* (open circles), and nominally 20 μ m diameter latex spheres (filled circles), showing positions of the distributional peaks relative to the Nival curve; note separation between peaks

pod species. The three alternative mechanisms for selective grazing can be explicitly stated: (1) copepods cannot vary the setal spacing but have a known variance in setule spacing; (2) copepods can vary the "effective" setal (and thereby "effective" setule) spacing and have variance in setal spacing; (3) copepods with or without variable setal spacing can post-capture reject food that is of low quality. We use the word "effective" with the second alternative above because, as will be shown in the discussion, other mechanisms can be suggested that will give the same result as physically altering setal spacing.

If copepods are offered two food particles and a non-food particle (e.g. any particle with no assimilatory value such as a plastic sphere) within their particle-size ingestion range, and with the sizes of these offered particles relative to the filtering efficiency curve ("Nival curve") as given in Fig. 1, then it is possible to discriminate between the above three alternative mechanisms using the following rationale.

If copepods can alter their setal spacing and if Wilson's (1973) argument for the advantage of eating larger particles is valid, then copepods offered a large food particle for some period of time should set their setal spacing for the larger sized particles. If the small food particles are subsequently added to the food suspension, the small particles should be ignored or eaten at a very low rate. Conversely, if copepods are conditioned to eating the small food, they should set their setae for that food if they can alter their setal spacing. If subsequently offered a larger food along with the small food, they should eat both, because the larger food will be captured on any filter set for the small food. However, if the copepods have a lower capture efficiency on the small food, then the ingestion rate on the larger food should be higher than for individuals preconditioned on the larger food.

On the other hand, if the copepods cannot alter their setal spacing, they should always eat both foods in proportions defined by the filtration rate-particle diameter function of Frost (1972, 1977), and the filtering rate should be independent of previous feeding history.

If copepods avoid non-food particles, as Lehman's (1976) model implies, then two possibilities exist for copepods encountering plastic spheres placed between two food distribution peaks (as in Fig. 1b). If they cannot post-capture reject these inert spheres but can alter their setal spacing, they should alter their setal spacing to avoid the spheres (thereby avoiding the small food as well), regardless of previous feeding history. If the copepods cannot alter setal spacing but continue to feed, spheres will be ingested. If the grazers can post-capture reject, they presumably do not need to alter their setal spacing and can continue to eat both large and small foods. Instead of altering setal spacing, they should simply discard spheres up to some limit. Presumably there is some high concentration of spheres beyond which rejection becomes energetically unfeasible. The copepods must then either eat all particles they encounter including the spheres, or alter their setal spacing to filter only the large food particles. Post-capture rejection might also be demonstrated if, after the copepods are offered any food plus larger plastic spheres, only the food is ingested. The experiments described below were designed to test each of the above alternative hypotheses.

Materials and Methods

Two diatoms which do not form chains (*Thalassiosira pseudonana*, Clone 3H from the collection of R.R.L. Guillard, and *T. fluviatilis*, Clone Actin from the Guillard collection) were chosen as the food species because their sizes placed them respectively at the lower and upper end of the Nival curve for *Acartia clausi* (Fig. 1). Such a distribution should maximize capture efficiency differences between particles, if they exist. Inert latex spheres of intermediate size between food distribution peaks (8 μm diameter), or larger than the *T. fluviatilis* peak (20 μm diameter), were used to test for particle rejection capabilities. Any combination of these four distributional peaks can be separated on the Coulter Counter (Fig. 1b).

Acartia clausi females (large-sized form of O'Connors et al., 1976) were collected in September from Yaquina Bay, Oregon, USA, and sorted into filtered sea water. These copepods were then preconditioned on either *Thalassiosira pseudonana* or *T. fluviatilis* for at least 3 days to allow any adjustment of feeding behavior to occur for that food. The food volume concentration was maintained at about $3 \times 10^6 \mu\text{m}^3 \text{ml}^{-1}$ during this preconditioning period. All grazing experiments were performed in 2 or 4 replicate 900 ml flasks containing 50 *A. clausi* females and the appropriate food mix. Multiple control vessels were used in all experiments for determining phytoplankton growth rates. All experiments were performed at 12°C (the bay temperature) in a low light intensity ($\approx 50 \mu\text{E m}^{-2} \text{sec}^{-1}$) which is sufficient to maintain low growth rates of the phytoplankton species used. In order to minimize possible nutrient regeneration effects, all experiments were run with excess nutrients and the algae were taken from a mixed culture of algae and *A. clausi*. This ensured that the phytoplankton had been exposed to nutrient regeneration during the previous 24 h. As a result, differences in nutrient regeneration effects between grazed and control vessels should have been minimized. All vessels were gently stirred several times daily with a plunger-stirrer, which adequately kept both food particles and plastic spheres in suspension.

Samples were taken at the beginning of each grazing period and approximately 24 h later from each grazed and control flask. Each sample was counted and sized using a Coulter Model ZBI Particle Counter® with a Coulter P-64 Channelizer®. The channelizer was directly interfaced to a PDP8e minicomputer, allowing direct

calculation of particle number and volume distributions and of total particle number and volume for each particle-size distribution peak in each sample. The details of this method are being prepared for another publication. Instrument settings were adjusted to optimize counting of each peak separately, as in Donaghay and Small (1979). Filtering rates (F) and ingestion rates (I) were calculated using equations given in Frost (1972). Values of F and I were computed for each total phytoplankton or sphere peak, and for different size classes within any peak.

The general experimental design is summarized in Fig. 2. The experiments were designed so that the previous feeding history of the copepods was defined at all times, and so the chances for detection of the feeding capability being tested for were optimized. Copepods that were preconditioned separately on either *Thalassiosira pseudonana* or *T. fluviatilis* were separated into 4 replicate flasks of 50 copepods each (Fig. 2b). This procedure resulted in 4 replicate groups of *T. pseudonana*-preconditioned individuals, and 4 replicate groups of *T. fluviatilis*-preconditioned individuals. Twenty-four hour ingestion experiments were performed using the phytoplankton species to which the grazers had been preconditioned (Fig. 2c). Although each food volume concentration was about $3 \times 10^6 \mu\text{m}^3 \text{ml}^{-1}$ (Table 1A), there were many more cells of *T. pseudonana* than *T. fluviatilis* (Table 1A). After these single-food experiments, the copepods were removed from the grazing chambers (maintaining food-preconditioned groups separately) and the *T. pseudonana* and *T. fluviatilis* from the grazer flasks were diluted and re-mixed to form a suspension containing both species. The resulting volume and number concentrations of each species in the mix (Table 1B) were lower than concentrations in the single-food experiments (Table 1A). This was done so that, if the copepods did not alter their feeding behavior, ingestion rates could not be maintained without increasing filtering rates. The copepods were re-added to the grazing chambers and a second set of 24 h ingestion experiments was performed to determine the effects of food preconditioning on grazing in the presence of two food peaks (Fig. 2d). At the end of these ingestion experiments, the copepods from each flask were again removed, still maintaining food-preconditioning lines. This time, two food mixes were prepared (Table 1C): (1) the same mix of *T. pseudonana* and *T. fluviatilis* as in the two-food experiments (but at a volume concentration of about $3 \times$

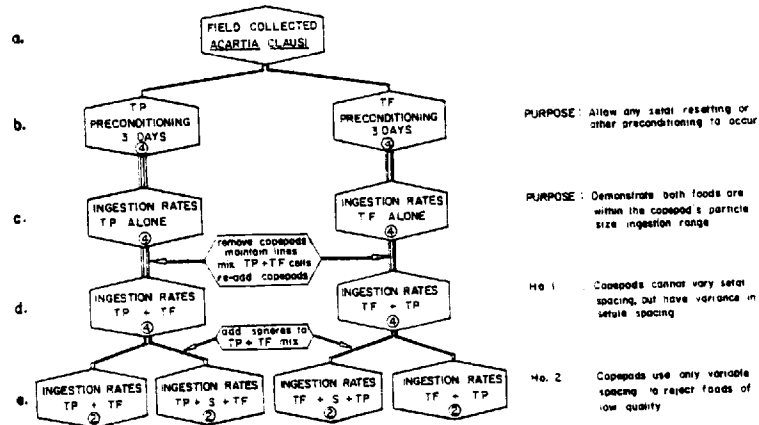


Fig. 2. *Acartia clausi*. Hierarchical experimental design used to test between alternative feeding mechanisms. (a) through (e) indicate the successive treatments. The purpose or hypotheses (designated Ho. 1 or Ho. 2) for each treatment are shown to the right of the figure. TF, TP, and S stand for, respectively, *Thalassiosira pseudonana*, *T. fluviatilis*, and 9 μ m diameter inert spheres. Circled numbers represent number of replicate grazing flasks at each step. Number of lines connecting the hexagons represent number of separate groups of copepods transferred from one step to the next

106 μ m³ ml⁻¹ for each species); and (2) the same mix as above, but with 2.8 x 106 μ m³ ml⁻¹ of 8 μ m diameter spheres added. The spheres were intermediate in size between the two food distribution peaks in order to determine if the copepods could reject particles after capture on their filters. Essentially equal total particle volumes of each type particle were used. Copepods preconditioned on *T. pseudonana* and copepods preconditioned on *T. fluviatilis* were then added to the appropriate flasks containing the two particle mixes. Replicate flasks for each experimental subset were always run. During the next 2 days ingestion rates were determined for each particle type and copepod preconditioning line (Fig. 2e).

In addition to the above experiments, an experiment was designed specifically to test post-capture rejection of unwanted particles. A group of copepods was preconditioned on *Thalassiosira fluviatilis*, a second group on 20 μ m diameter spheres, and a third group on a mixture of *T. fluviatilis* plus spheres (Table 2). Preconditioning time was 24 h. During the experimental period both types of particles were offered in nearly equal numbers so that the copepods would have nearly equal probability of capture for both spheres and the food (taking into account the higher expected mechanical capture rate of larger particles). As a

Table 1. *Acartia clausi*. Initial concentrations of food (*Thalassiosira* spp.) and latex spheres in each grazing situation

Situation	Volume (106 μ m ³ ml ⁻¹)	Numbers (cells ml ⁻¹)
(A) Single food		
<i>T. pseudonana</i>	3.10	36,061
<i>T. fluviatilis</i>	3.47	2,135
(B) Two foods		
<i>T. pseudonana</i>	2.40	25,513
<i>T. fluviatilis</i>	1.60	1,068
(C) Two foods, with or without spheres		
<i>T. pseudonana</i>	2.98	67,835
<i>T. fluviatilis</i>	2.34	1,869
Sphere	2.76	10,588

result, spheres should always have been present on the filter with the food. Because the spheres averaged almost four times larger than the food particles by volume per particle during the experimental period (Table 2), the failure to reject each sphere should have resulted in the exclusion from the gut of 4 food particles, a reasonable penalty. The grazing response was tested on each particle type offered singly and when offered as a mix. In these experiments, four replicates were run using 50 *Acartia clausi* in each 900 ml grazing flask.

Table 2. *Acartia clausi*. Initial concentrations of *Thalassiosira fluviatilis* (Tf) and 20 μ m diameter latex spheres (S 20) in experiment to test post-capture rejection of non-food particles

Period and preconditioning particle type	Initial conditions		
	Particle type measured	Volume ($10^6 \mu\text{m}^3 \text{ ml}^{-1}$)	Numbers (particles ml^{-1})
Preconditioning period (24 h)			
Tf	Tf	5.58	4,162
S 20	S 20	11.38	2,348
Tf + S 20	Tf	5.05	3,553
Tf + S 20	S 20	15.13	3,020
Experimental period			
Tf-preconditioned	Tf	2.47	1,911
Tf-preconditioned	S 20	5.28	1,057
S 20-preconditioned	Tf	2.38	1,840
S 20-preconditioned	S 20	5.54	1,105
Tf + S 20-preconditioned	Tf	5.18	4,077
Tf + S 20-preconditioned	S 20	14.85	2,970

Results

By comparing ingestion rates of *Acartia clausi* on each food species offered separately, we could determine if the copepods could feed on both particle sizes equally well. At equal particle volume concentrations of food, the ingestion rate on *Thalassiosira fluviatilis* (the larger cell) was higher than on *T. pseudonana* by about 40%, but substantial quantities of both were eaten (Table 3). This result was to be expected from the relative position of the two food peaks on the Nival curve for *A. clausi* (Fig. 1). Results between flasks replicated well.

A comparison of ingestion rates for copepods in multiple food experiments is shown in Fig. 3. The length of each bar represents the volume of *Thalassiosira fluviatilis* ingested as a percentage of the total particle volume ingested of both food species. When copepods preconditioned on the large food (*T. fluviatilis*) were offered both the large and small food (*T. pseudonana*) they ate only the large food (>98%) (Fig. 3a1). In contrast, copepods preconditioned on *T. pseudonana*, and then offered both large and small cells, ate both foods (Fig. 3a2). Almost 80% of the food volume ingested was derived from *T. fluviatilis*, however. Furthermore, the absolute ingestion rate (not %) on *T. fluviatilis* by the copepods preconditioned on *T. pseudonana* averaged higher than for the *T. fluviatilis*-preconditioned individuals (Table 4). As with the single-food grazing experiments, the results replicated well.

These results show that food preconditioning strongly controlled the feed-

Table 3. *Acartia clausi*. Ingestion rates on *Thalassiosira pseudonana* and *T. fluviatilis* when the two foods are offered separately

Replicate	Ingestion rate ($10^6 \mu\text{m}^3 \text{ copepod}^{-1} \text{ day}^{-1}$)	
	<i>T. pseudonana</i>	<i>T. fluviatilis</i>
1	8.1	12.8
2	6.1	12.2
3	7.8	12.5
4	6.0	10.1
Mean	7.0	11.8

Table 4. *Acartia clausi*. Effects of preconditioning on ingestion rates ($\mu\text{m}^3 \times 10^6 \text{ copepod}^{-1} \text{ day}^{-1}$) of *Thalassiosira* spp.

Replicate no.	<i>T. pseudonana</i> -preconditioned	<i>T. fluviatilis</i> -preconditioned
<i>T. pseudonana</i>		
1	1.8	0.0
2	1.6	0.0
3	1.9	0.0
4	1.6	0.0
mean	1.7	0.0
<i>T. fluviatilis</i>		
1	6.0	5.0
2	6.0	4.4
3	5.9	4.7
4	5.6	5.9
mean	5.9	5.0

ing behavior of copepods both quantitatively (as determined by differences in ingestion rates) and qualitatively (as determined by which food peaks were selected). Further, the results imply that the copepods not only effectively adjusted their feeding behavior to optimize for a food (i.e., their Nival curve was shifted), but they also maintained this behavior for some time period after the food environment was changed. The observed adjustments can be explained by either a physical resetting of setal spacing or by post-capture rejection of particles. The sphere-addition experiments allow us to test for post-capture rejection.

In the sphere-addition experiments (Fig. 3b), the flasks without spheres served as both controls for the sphere-addition experiments and as an extension in time of the two-food experiments (Fig. 3a). The percentage of the ration composed of *Thalassiosira pseudonana* increased in time in both the *T. fluviatilis*-preconditioned individuals and the *T.*

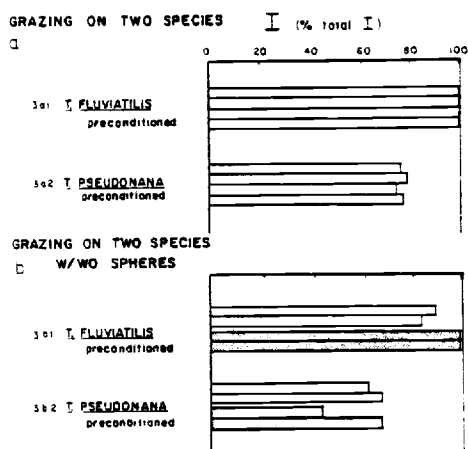


Fig. 3. *Acartia clausi*. Ingestion (I) behavior and effects of preconditioning on different foods, using *Thalassiosira fluviatilis* (Tf), and *T. pseudonana* (Tp) as foods, and 8 μ m diameter spheres (S) as inert particles. Lengths of bars represent percent (volume) of total food ingestion (Tf plus Tp) due to ingestion of Tf alone. Each bar in a group represents 4 replicates. (3a1) Tf-preconditioned copepods grazing on Tf plus Tp, (3a2) Tp-preconditioned copepods grazing on Tf plus Tp; (3b1) Tf-preconditioned copepods grazing on Tf plus Tp with S absent (open bars) and S present (stippled bars), (3b2) Tp-preconditioned copepods grazing on Tf plus Tp with S absent (open bars) and S present (stippled bars)

pseudonana-preconditioned individuals (compare Fig. 3a1 with Fig. 3b1, open bars, and Fig. 3a2 with Fig. 3b2, open bars). This percentage increase was probably because the *T. pseudonana* were increasing more rapidly in abundance than the *T. fluviatilis* (i.e., *T. pseudonana* had a higher apparent specific growth rate under these conditions). In the flasks with spheres added (Fig. 3b, stippled bars), two widely divergent results were observed for copepods preconditioned on *T. pseudonana* and *T. fluviatilis*. With *T. fluviatilis*-preconditioned individuals, neither *T. pseudonana* nor spheres were eaten (Fig. 3b1, stippled bars). These results can be interpreted to suggest that the copepods set their setal spacing just below *T. fluviatilis* in particle size to allow the spheres to pass through the filter, and therefore did not ingest and perhaps did not capture any *T. pseudonana*. In contrast, *T. pseudonana*-preconditioned individuals ingested both *T. pseudonana* and *T. fluviatilis* (Fig. 3b2, stippled bars); however, the inter-

mediate-sized spheres were not ingested. Thus, the *T. pseudonana*-preconditioned copepods did not reset their setae to avoid the spheres and thereby cease capturing *T. pseudonana*, but rather in some fashion must have rejected the spheres after capturing them. The rejection of these spheres is based both on the Coulter Counter measurements showing that the sphere peak was not altered during grazing, and on the very low frequency of occurrence of spheres in fecal pellets (1 to 3 spheres in less than 5% of the feces).

Rejection of spheres was also observed in our experiments in which copepods were preconditioned on 20 μ m diameter spheres, on *Thalassiosira fluviatilis*, or on both, and then offered an equal-number mix of *T. fluviatilis* cells and spheres. Although the copepods remained active during the 24 h preconditioning in the sphere suspension, no ingestion of spheres was detectable with the Coulter Counter, and feces and egg production ceased immediately. When these individuals, or individuals preconditioned on *T. fluviatilis*, were offered the mix of *T. fluviatilis* and spheres, again very few spheres were eaten. If non-preconditioned copepods were offered *T. fluviatilis* and spheres, some spheres were initially eaten; however, ingestion of spheres rapidly decreased with time while grazing on *T. fluviatilis* continued. As *T. fluviatilis* was smaller than the 20 μ m diameter spheres, ingestion of *T. fluviatilis* without concomitant ingestion of spheres was interpreted as post-capture rejection of spheres.

Ingestion rates were somewhat depressed in all experiments in which post-capture rejection occurred. The *Thalassiosira pseudonana*-preconditioned copepods, for example, had ingestion rates that were suppressed an average of 19% compared to control individuals which were not offered 8 μ m diameter spheres. Conversely, when post-capture rejection was not needed to avoid spheres (e.g. when *T. fluviatilis*-preconditioned copepods ingested *T. fluviatilis* but not 8 μ m diameter spheres or *T. pseudonana*), no depression of ingestion rates was detectable.

Discussion

The above results demonstrate that *Acartia clausi* has a complex grazing behavior consisting of (1) more efficient grazing on larger particles within its particle-size ingestion range; (2) the ability to alter "effective" setal spacing to optimize feeding behavior (i.e., to increase efficiency of capture of food particles

and to avoid non-food particles); and (3) the ability for post-capture rejection of non-food particles when they interfere with the ingestion of food particles on which the copepod has been preconditioned. The behavioral patterns observed depend heavily on the food preconditioning and the presence or absence of non-food particles. It was also observed that *A. clausi* will definitely avoid eating spheres after the first few minutes; in fact, this copepod apparently will starve rather than continue to ingest such particles.

The evidence both for alteration of "effective" setal spacing and for post-capture rejection may be interpreted as evidence for two different types of post-capture rejection. The above results do not necessarily require that setal spacing be altered; in fact, the data can be explained if the copepods selectively comb particles from their filter appendages. For example, the avoidance of both spheres and *Thalassiosira pseudonana* by *T. fluviatilis*-preconditioned individuals presented with the mix of all three particles can be explained if they comb the filter starting at pore sizes larger than the size of the spheres, and then simply discard any residual particles remaining on the filter. Further, if particles are sorted along the filter axis during the actual filtering process, the rejection of spheres located between two food peaks can conceivably be explained by multiple entry and exit of the combing appendage along the filter, or by particle-by-particle post-combing rejection. The derivation of the particle sorting concept and the discussion of the difference between combing and post-combing rejection will be considered in detail elsewhere.

Evidence for food preconditioning on different food sizes and types has existed for some time, although the potential impact on grazing dynamics perhaps has not been fully appreciated. The evidence also suggests that the phenomenon is not limited to *Acartia clausi*. For example, Conover (1966) observed that *Calanus hyperboreus*, preconditioned on large cells then subsequently offered a mix of small and large cells, did not ingest the small cells. Conversely, copepods fed small cells first ignored the large cells when offered a mix of both. This is a much stronger preconditioning response than we have observed with *A. clausi*, because it requires rejection of the presumably more easily filtered large food particles. In an experiment similar to Conover's, using *Ditylum brightwelli* and *Lauderia borealis* as the large

and small cells, Harvey (1937) observed that when *C. finmarchicus* was preconditioned on the smaller food and then fed both foods, the filtering rates on the small food increased and the filtering rates on the large food decreased relative to copepods preconditioned on the large food. The amount of small food that was ingested increased sharply, but never to the exclusion of the large food. Harvey's data indicate that *C. finmarchicus* altered its effective setal spacing, assuming that the lower filtration rates on the large cells were brought about by "closing down" the filter area to maximize filtration efficiency on the small cells. At the other extreme from Conover's observations, Mullin (1963) was unable to detect food preconditioning effects for *C. helgolandicus*. We have observed that *Eurytemora* sp. shows essentially the same preconditioning response as *A. clausi*, yet has a filtration pattern very different from *A. clausi*. *Eurytemora* sp. sets up a current through a fixed filter, while *A. clausi* moves its maxillae through the water like a seine (Conover, 1956).

The effects of preconditioning are also implied from field experiments. Gamble et al. (1977) compared the grazing responses of zooplankton taken from large *in situ* plastic columns and fed particle suspensions from a variety of sources. They observed that ingestion rates were always higher when animals were allowed to graze on suspensions from which they were collected rather than on natural suspensions from other sources. It also seems probable that preconditioning has been at least partly responsible for the variability in ingestion responses (Ivlev curves) for other field-collected animals (Frost, 1972; O'Connors et al., 1976). If the test foods used to develop Ivlev curves were radically different from the foods eaten in the field, little or no ingestion might be expected to occur over the time courses of the grazing experiments. Certainly, the development of single-food Ivlev curves should be coupled with some knowledge of the types and sizes of foods being eaten by animals in the field. Companion field experiments (Richman et al., 1977) or gut-content analyses (Schnack, 1975) can provide this information.

In addition to the problem of Ivlev-curve variance, food preconditioning might also explain observations of ingestion of non-food particles by copepods. Three possibilities may be suggested. First, certain non-food particles might interfere with the copepods' sensory mechanism, or they might chem-

ically mimic good food (Friedman and Strickler, 1975). Ingestion of such items as tar balls (Conover, 1971) might be explained in this way. A better knowledge of the sensory mechanism of copepods is clearly needed. Secondly, very tiny non-food particles might not be energetically worthwhile rejecting. For example, Schnack (1975) has observed that only inorganic "sand" particles of less than 4 μ m diameter were ever found in the gut contents of 5 copepod species. These very small particles, with their large surface to volume ratios, might even have been bacteria-covered and eaten as a result of this coating. Finally, ingestion of non-food particles by copepods taken from the field might simply reflect their previous feeding history. For example, if copepods had been actively ingesting particles in, say, the 10 to 20 μ m size range, and were then offered a different food suspension, poor or non-food particles might be ingested before the grazing behavior shifted. D.R. Heinle (personal communication) might have observed such events in the field. When copepods from one depth were offered a food suspension from a different depth, feeding continued in the particle size ranges appropriate for the original food suspension, regardless of the food composition of the new particle suspension.

If in future work we find that food preconditioning responses are widespread among copepods, then some rethinking of theoretical models seems appropriate. The functional basis of preconditioning almost certainly lies in both the filtering mechanism and in the assimilatory processes of the animal. The filtering mechanism can be examined through both structural analysis (Nival and Nival, 1973, 1976; Schnack, 1975) and through analysis of the mechanics of operation of filtering appendages (Strickler and Rosenberg, 1977). The assimilatory processes might be examined using enzyme techniques (Mayzaud and Conover, 1976; Mayzaud and Poulet, 1978). Further theoretical development of these ideas will be considered elsewhere.

Our observations of preconditioning, and the ingestion rates reported here, are not in conflict with the idea that the maximum filtering rate increases with increasing particle size (Frost, 1972; Lam and Frost, 1976; Frost, 1977). However, our data, as well as those of Poulet (1973, 1974), Richman et al. (1977), Mayzaud and Poulet (1978) and Conover (in press), seem to conflict with the assumption that the energy of filtration (Lam and Frost, 1976) is "the" critical energy cost for copepods. It

may be argued that the crucial "objective" for copepods is to maximize the assimilation of food in order to maximize growth and reproduction (Lehman, 1976). This requires not only that the capture energetics be as low as possible, but also that (1) copepods eat foods that can be rapidly digested using the enzymes induced as a result of their previous feeding history (Mayzaud and Conover, 1976; Mayzaud and Poulet, 1978); (2) copepods avoid filling their guts with non-food particles, by some selective mechanism if necessary; and (3) the foods eaten have the proper nutritional properties. Our data and the field results cited above suggest that filtering costs are secondary to the nutritional gains of being selective. Conover's (in press) observations that copepods avoid the large dinoflagellate *Ceratium tripos* while eating all other phytoplankton size groups, coupled with the knowledge that these same copepods could ingest but not digest the dinoflagellates because they did not possess the required cellulase enzyme (P. Mayzaud, personal communication), is perhaps a good example of food selection under nutritional or assimilatory "control". Some revisions of existing theories of filter-feeding are needed to include the consideration of more than just the energetics of filtration in understanding filter-feeding in copepods.

Acknowledgements. We acknowledge the support of NSF Grants OCE 76-10347 and OCE 78-08635, and the discussions with, and many helpful comments on the manuscript by, J.M. DeManche, R.D. Leatham and B.L. Dexter. We wish to thank C.S. Miller for his editorial comments.

Literature Cited

- Boyd, C.M.: Selection of particle sizes by filter-feeding copepods: a plea for reason. *Limnol. Oceanogr.* 21, 175-180 (1976)
- Conover, R.J.: Oceanography of Long Island Sound, 1952-1954. VI. Biology of *Acartia clausi* and *A. tonsa*. *Bull. Bingham Oceanogr. Coll.* 15, 156-233 (1956)
- Feeding on large particles by *Calanus hyperboreus* (Krøyer). In: *Some contemporary studies in marine science*, pp 187-194. Ed. by H. Barnes. London: George Allen & Unwin Ltd. 1966
 - Some relations between zooplankton and bunker C oil in Chedabucto Bay following the wreck of the tanker Arrow. *J. Fish. Res. Bd Can.* 28, 1327-1330 (1971)
 - Feeding interactions in the pelagic zone. *J. Cons. int. Explor. Mer* (in press)

P.L. Donaghay and L.F. Small: Food Selection Capabilities of *Acartia*

- Donaghay, P.L. and L.F. Small: Long-term food modification by *Acartia clausi*: a preliminary view. *Mar. Biol.* 52, 129-136 (1979)
- Friedman, M.M. and J.R. Strickler: Chemoreceptors and feeding in calanoid copepods (Arthropoda: Crustacea). *Proc. natn. Acad. Sci. U.S.A.* 72, 4185-4188 (1975)
- Frost, B.: Effects of size and concentration of food particles on the feeding behaviour of the marine planktonic copepod *Calanus pacificus*. *Limnol. Oceanogr.* 17, 805-815 (1972)
- Feeding behaviour of *Calanus pacificus* in mixtures of food particles. *Limnol. Oceanogr.* 22, 472-491 (1977)
- Gamble, J.C., J.M. Davies and J.H. Steele: Loch Ewe bag experiment, 1974. *Bull. mar. Sci.* 27, 146-175 (1977)
- Harvey, W.H.: Note on selective feeding by *Calanus*. *J. mar. biol. Ass. U.K.* 22, 97-100 (1937)
- Lam, R.K. and B.W. Frost: Model of copepod filtering response to changes in size and concentration of food. *Limnol. Oceanogr.* 21, 490-500 (1976)
- Lehman, J.T.: The filter-feeder as an optimal forager, and the predicted shapes of feeding curves. *Limnol. Oceanogr.* 21, 501-516 (1976)
- Marshall, S.M. and A.P. Orr: The biology of a marine copepod, 188 pp. London: Oliver & Boyd 1955
- Mayzaud, P. and R.J. Conover: Influence of potential food supply on the digestive enzyme activity of neritic copepods. *Proc. 10th Eur. mar. Biol. Symp.* 2, 415-427 (1976). (Ed. by G. Persoone and E. Jaspers. Wetteren, Belgium: Universa Press)
- and S.A. Poulet: The importance of the time factor in the response of zooplankton to varying concentrations of naturally occurring particulate matter. *Limnol. Oceanogr.* 23, 1144-1154 (1978)
- Mullin, M.M.: Some factors affecting the feeding of marine copepods of the genus *Calanus*. *Limnol. Oceanogr.* 8, 239-250 (1963)
- Nival, P. et S. Nival: Efficacite de filtration des copepods planctoniques. *Annls Inst. océanogr., Paris (N.S.)* 49, 135-144 (1973)
- - Particle retention efficiencies of an herbivorous copepod, *Acartia clausi* (adult and copepodite stages): effects on grazing. *Limnol. Oceanogr.* 21, 24-38 (1976)
- O'Connors, H.B., L.F. Small and P.L. Donaghay: Particle-size modification by two size classes of the estuarine copepod *Acartia clausi*. *Limnol. Oceanogr.* 21, 300-308 (1976)
- Poulet, S.A.: Grazing of *Pseudocalanus minutus* on naturally occurring particulate matter. *Limnol. Oceanogr.* 18, 564-573 (1973)
- Seasonal grazing of *Pseudocalanus minutus* on particles. *Mar. Biol.* 25, 109-123 (1974)
- Richman, S., D.R. Heinle and R. Huff: Grazing by adult estuarine calanoid copepods of the Chesapeake Bay. *Mar. Biol.* 42, 69-84 (1977)
- Schnack, S.: Untersuchungen zur Nahrungsbiologie der Copepoden (Crustacea) in der Kieler Bucht, 144 pp. Dissertation, Universität Kiel 1975
- Storm, S.: Selective feeding, ingestion and assimilation rates and distribution of the copepod *Acartia* in Chesapeake Bay, 162 pp. Baltimore. Ph.D. Thesis, John Hopkins University 1974
- Strickler, J.R. and G. Rosenberg: Visual observation of filter-feeding by copepods. *A. Mtg. Am. Soc. Limnol. Oceanogr. Abstr.* (June 1977), p. 56 (1977). (East Lansing, Michigan: Michigan State University)
- Wilson, D.S.: Food size selection among copepods. *Ecology* 54, 909-914 (1973)

Dr. Percy L. Donaghay
School of Oceanography
Oregon State University
Corvallis, Oregon 97331
USA

Date of final manuscript acceptance: December 3, 1978. Communicated by J.M. Pérés, Marseille

CHAPTER 2

GRAZING INTERACTIONS IN THE MARINE ENVIRONMENT

by

Percy L. Donaghay
School of Oceanography
Oregon State University
Corvallis, Oregon 97331

Presented at the Symposium

on

"Structure of Zooplankton Communities"

Held at Dartmouth College

August 20-25, 1978

in Press in Proceedings of the International Symposium on Zooplankton
Community Structure, New England Press, 1979.

Abstract

The physical properties of copepods filtering appendages suggest an increasing filtering capacity for large versus small particles. This prediction agrees with laboratory data for some species, but does not agree with field experiments or laboratory experiments for other species. The expected results for Acartia clausi are shown to be modified by (1) previous feeding history, (2) presence of non food particles, and (3) food quality. Important interactions exist between each of these factors. Alteration of patterns of filter movement, combing rejection, and post combing rejection are considered as possible mechanisms for modification of expected filtering patterns. An experiment with food and non food particles of identical size is used to demonstrate that A. clausi can post comb reject unwanted particles.

Careful study of the morphology of the feeding appendages of copepods has shown that pore size formed by the setae and setules are approximately normally distributed (Nival and Nival 1973, 1976). Copepod filtering appendages can be used to directly capture particles [as in the raptorial feeding behavior for Acartia (Conover 1956)] or to act as a concentrating device without direct contact [as for the cladoceran, Daphnia (Porter, unpubl.)]. Regardless of whether particles are trapped on the filter or only concentrated by it, a filtering efficiency curve can be calculated from the variance in setule spacing (Fig. 1a) (Nival and Nival 1973, 1976). These filtering-efficiency curves can be used to predict relative filtering rates as a function of particle size.

Such expected filtering rate-particle size relationships may also be derived experimentally as has been done by Frost for Calanus pacificus (Frost 1972). These curves are developed by determining filtering rates over a variety of concentrations and for a variety of different-sized particles. The maximum filtering rates (observed at low concentrations) provide an estimate of the relative efficiency of filtering for those sized particles. These maximum filtering rates can then be plotted versus particle size to form a filtration efficiency curve (Fig. 2). Such experimentally derived relationships most accurately reflect only the mechanical properties of the filter when the different-sized particles used are of equal food quality and identical particle shape (nearly spheroid in shape). These conditions can be met by using size clones of a single species of algae as was done by Frost (1972).

The strictly mechanical properties of the filter will result in higher filtering and ingestion rates for larger particles, providing the

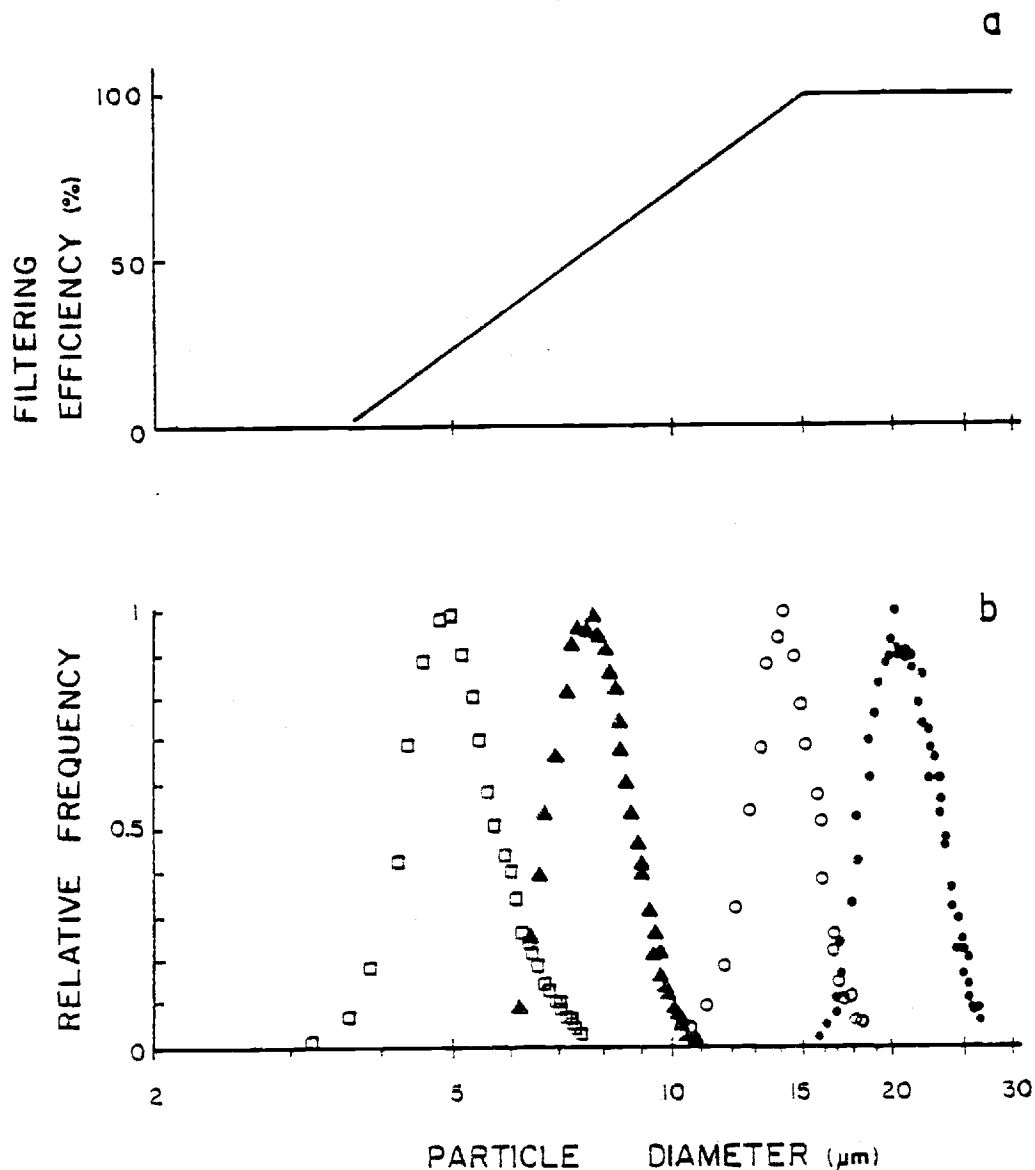


Fig. 1. a. Particle selectivity curve for *Acartia clausi* (redrawn from Nival and Nival, 1976).
 b. Size distribution of the algae *T. pseudonana* (□), 8 μm sphere (▲ ranging in size from 6 to 11 μm,) *T. fluviatilis* (○), and 20 μm spheres (● 95% > 15μm) showing relative position of particle size peaks relative to theoretical Nival function. Size distribution peaks are relative volume distributions of particles used in experiments. Not separation between peaks (redrawn from Donaghay and Small 1979).

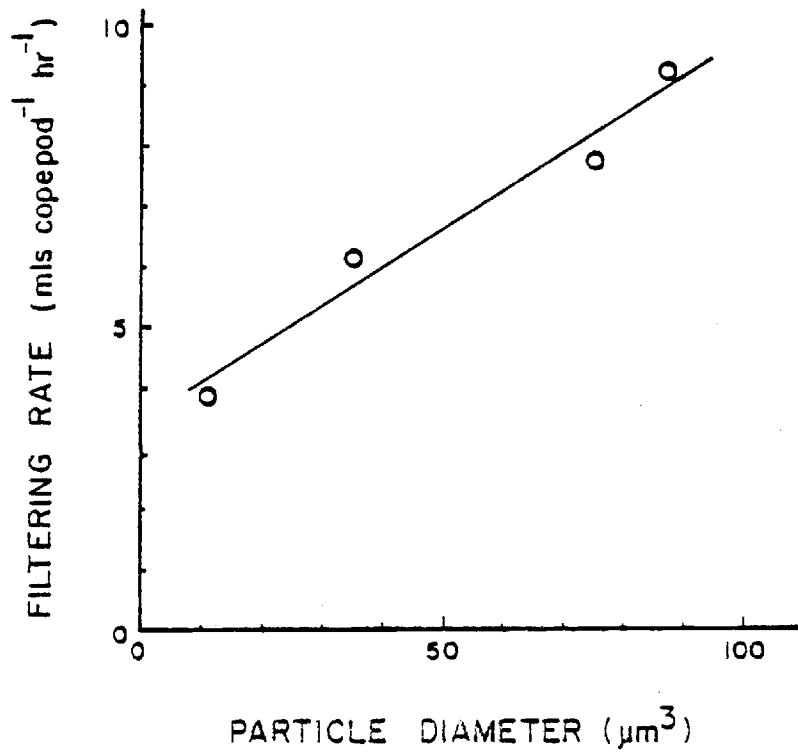


Fig. 2. Experimentally derived filtering particle size for Calanus pacificus (redrawn from Frost 1972).

particles are of equal quality. It should be noted that this is a purely passive selection and requires no behavioral response by the copepod. Hereafter I shall term this "passive selection" to distinguish it from "active selection." Any deviation of the observed filtering responses from those expected based on the physical properties of the filter requires some behavioral response on the part of the animal and is thus "active selection." As has been pointed out by Boyd (1976), Lam and Frost (1976), and Lehman (1976), passive selection can be used to explain apparent selection for larger particles over smaller ones. This is true for inert spheres (Wilson 1973) or for foods of equal value (Frost 1977). It can also be shown to be true for Acartia clausi when fed two different-sized species of Thalassiosira (Fig. 3).

Recent experiments in our laboratory (Donaghay and Small 1979) and field experiments (Richman et al. 1977) clearly demonstrate that the results expected from the mechanical properties of the filter can be strongly modified by the type of food spectra, the animals' previous feeding history, and by presence of non food particles. Richman et al. (1977) have demonstrated that filtering curves can be altered by the types of natural particle spectra offered. The responses reported by them range from generally increasing filtration rates with increasing size (as expected from passive selection) to feeding in only very narrow sections of the particle spectra. It must be assumed that these patterns are the result of differing food quality associated with individual sections of the particle spectra and of the resultant active selection by copepods for certain food types.

Previous feeding history can also be shown to modify filtering

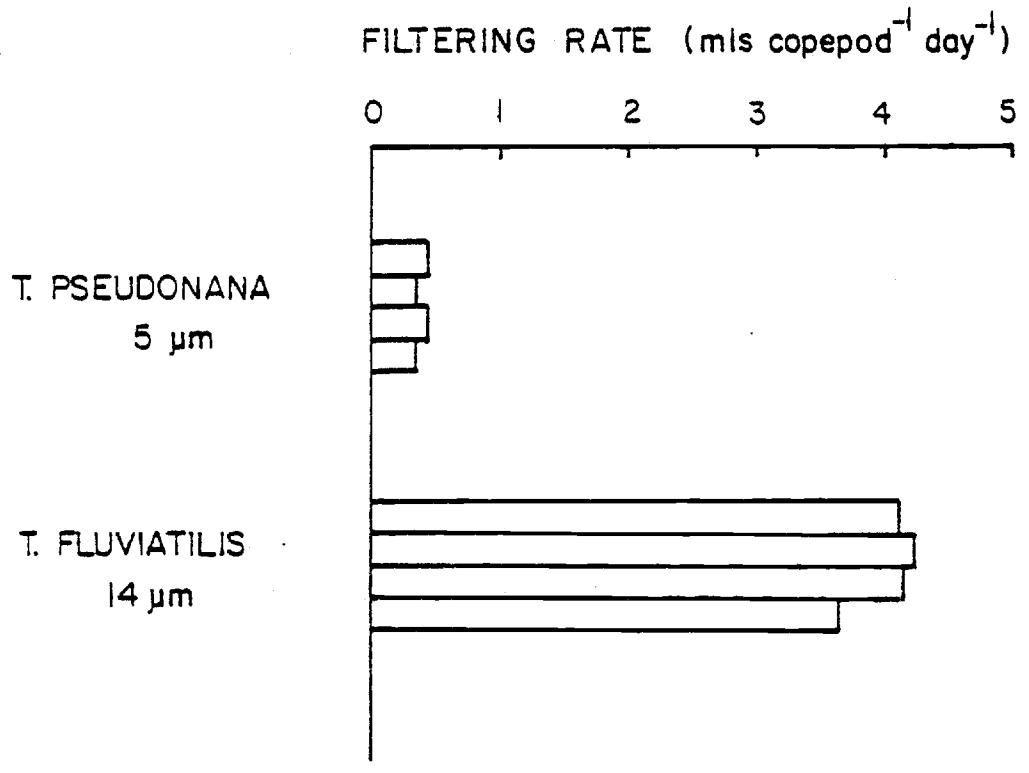


Fig. 3 Filtering rates for Acartia clausi fed a mixture of 14 μm Thalassiosira fluviatilis and 5 μm T. pseudonana. Bars represent separate replicate experiments.

responses for Acartia clausi. Donaghay and Small (1979) preconditioned Acartia females on equal concentrations of Thalassiosira pseudonana (5 μm) and Thalassiosira fluviatilis (15 μm) (see Fig. 1b for sizes relative to the filtering function). Both species are small, single celled centric diatoms. The animals were preconditioned on each food for 4 days to ensure that the copepods would be fully acclimated to those foods and so that any alteration of setal spacing (as suggested by the model of Wilson 1973) would have occurred. The ingestion response was then examined on both foods separately and together (Fig. 4). Figure 4a shows that ingestion of the small cell occurred only with Thalassiosira pseudonana preconditioned animals, but animals with both preconditionings ingested the larger cell, Thalassiosira fluviatilis. These results demonstrate that previous feeding history can modify the expected responses of copepods based on filter structure alone. These results are also consistent with the setal spacing alteration mechanism suggested by Wilson (1973).

The presence of non food particles was also shown by Donaghay and Small (1979) to modify expected mechanical filtering responses. After performing the above experiment, inert latex spheres of 8 μm size were added to the food suspension of 5 and 15 μm Thalassiosira cells (Fig. 1b). This experiment tested the hypothesis that alteration of setal spacing was the animals only mechanism for rejecting unwanted particles. In all cases spheres were avoided.

However, the feeding patterns showed a clear interaction with previous feeding history (Fig. 4b). Animals preconditioned on the large food avoided spheres by not ingesting either spheres or Thalassiosira

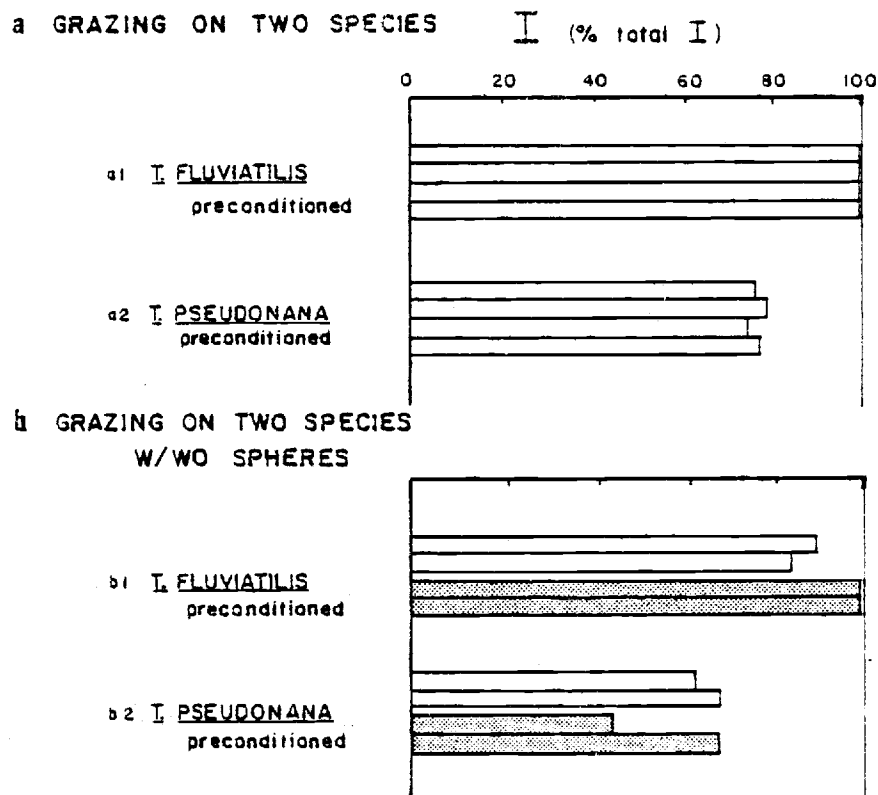


Fig. 4. a. Effects of preconditioning or ingestion behavior of Acartia clausi. Bars represent percent of total ingestion represented by ingestion of T. fluviatilis calculated as:

$$I_{T.f.} = \frac{\text{Ingestion rate of T.f.}}{\text{Ingestion rate of T.p.} + \text{Ingestion rate of T.f.}} \times 100$$

a1 T. fluviatilis preconditioned animals grazing on T. pseudonana plus T. fluviatilis;

a2 T. pseudonana preconditioned animals grazing on T. pseudonana plus T. fluviatilis.

b. Grazing on two food peaks with or without spheres present. Two replicate flasks without spheres are open bars; two replicate flasks with spheres represented by striped bars.

b1 T. fluviatilis preconditioned animals;

b2 T. pseudonana preconditioned animals (redrawn from Donaghy and Small 1979).

pseudonana. Those preconditioned on small cells ingested both food species but no spheres. Since altered setal spacing cannot explain the latter behavior, the Thalassiosira pseudonana preconditioned animals must have rejected the spheres after capture on the filter using a post capture rejection mechanism. This experiment demonstrates that Acartia clausi has a post capture rejection mechanism and that presence of non food particles strongly interacts with previous feeding history to modify responses based on mechanical properties of the filter.

More recently Poulet and Marsot (1978) have demonstrated that food quality can alter the expected filtering pattern. They offered microencapsulated particles containing either phytoplankton or a non phytoplankton derived material. The animals repeatedly selected the phytoplankton-containing particles regardless of whether they were the larger or smaller sized particles offered.

Both the results of Poulet and Marsot (1978) and Donaghay and Small (1979) can be interpreted as evidence for either of two types of post capture rejection. Donaghay and Small (1979) suggested that their data could be explained either by the selective removal of particles of a given size by the multiple entry and exit of the combing appendage along the filter or by particle by particle post combing rejection (after removal of those particles from the maxillae). The first type of rejection, termed "combing selection" is possible because the variance in pore size is oriented along the filter axis and allows the animal to select a certain sized particle by combing at the appropriate place along the filter (Donaghay in prep.).

In order to test between these two hypothesis and to further inves-

tigate how expected filtering curves could be modified, a rejection experiment was run this summer. Both hypothesized mechanisms for particle rejection will have identical results except when food and non food particles of identical size are offered together. Under these conditions, both foods and non foods will occur at similar positions along the filter and therefore size based rejection will not be possible. Thus, rejection of the inert spheres in this situation will be a clear demonstration of a post combing rejection mechanism. To test the hypothesis that combing rejection is the only mechanism, six replicate groups of 20 Acartia clausi females each were fed a mix of 15 μm Thalassiosira fluviatilis and 15 μm spheres. The relative sizes and abundances of these particles (Fig. 5) were such that the sphere distribution completely overlapped the food distribution. As a result, spheres were equal to or greater in number than the food in all size classes. After 1, 2, and 24 hours, two groups of animals were removed from the grazing chambers. The animals were preserved and prepared for gut content analysis using the methods of Schnack (1975). The feces were collected on 35 μm Nitex and preserved, and the number of spheres per feces were counted on an inverted microscope. At the end of 24 hours, grazed and control suspensions were counted and sized with a Coulter Counter (after Donaghay and Small 1979) and filtering rate curves were calculated using the equations of Frost (1972). When the resulting filtering curves are compared to those obtained with pure Thalassiosira fluviatilis suspensions (Fig. 5b and d), it is clear that the presence of non food particles altered the filtering function from an increasing function with size to a uniform rate at all sizes. In a similar experi-

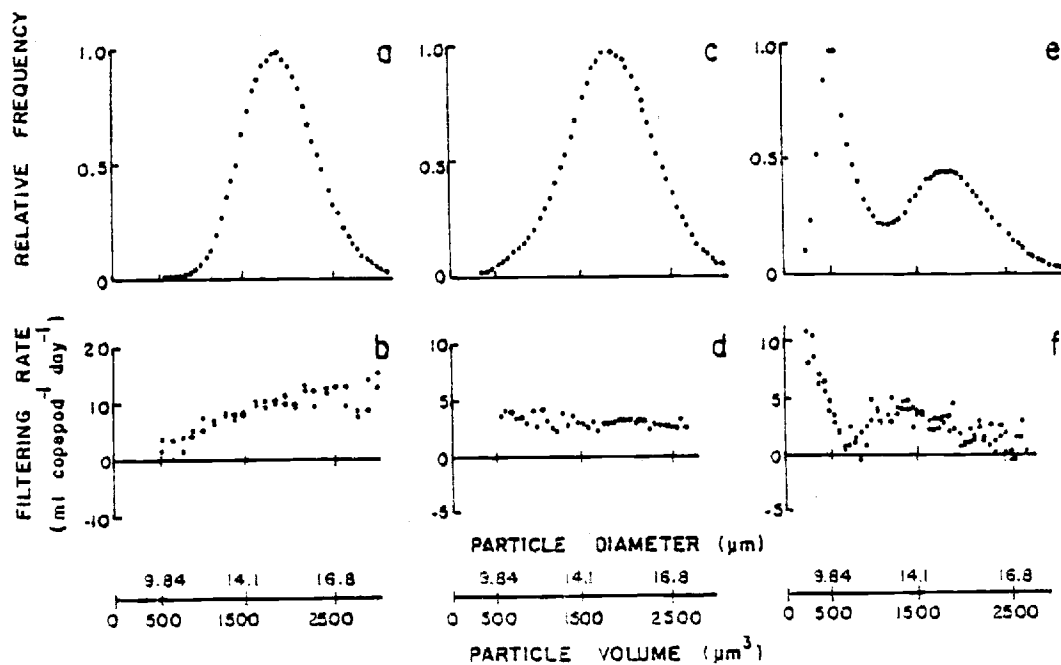


Fig. 5. Varying types of filtration curves (b,d,f) derived from *Acartia clausi* grazing on particle distribution composed of pure 15 μm *Thalassiosira fluviatilis* (b); approximately equal numbers of 15 μm *T. fluviatilis* and 15 μm inert plastic spheres (d) and a mix of 11 μm *T. fluviatilis*, and the same equal number mix of 15 μm *T. fluviatilis* and 15 μm spheres as in b (f). Relative frequency (relative particle number distributions) for each of these experiments is shown directly above filtering curves in a, c, and e respectively. Circles represent means of 4 replicate experiments for d and individual pairs of replicates for b and f.

ment with food particles also present at a smaller size (in addition to the food sphere mix at 15 μm), the filtering curve became maximal at the smallest sizes (Fig. 5e and f). In this case, the observed filtering rate is a decreasing function of particle size. Thus, the presence of non food particles in the same size range as a food will result in significant modification of the mechanistic filtering function.

The above filtering curves tell us only that the observed filtering pattern was modified. They tell us nothing about whether the non food particles were ingested and nothing about the mechanism involved. In order to answer these questions, the numbers of spheres in the animal guts and in the feces were counted and the total number of spheres ingested per flask was calculated. These totals were divided by the number of animals per flask to determine the number of spheres ingested per animal per day (Table 1). Based on the 24 hour data, each animal ingested an average of 101 spheres per day. This number is very small when compared to the total number of particles ingested per day (22,000 per animal per day). Also, recall that the food and spheres were equally abundant, and thus approximately equal numbers of both food and spheres should have been eaten. The difference between the observed and expected results shows a clear post combing rejection capability for Acartia with an error rate of only 1 in 200. This is a rather impressive capability. The filtering rate data, particularly from the two peak experiments, indicates that although Acartia can reject unwanted particles on a one by one basis, it also responds to the presence of a non food by shifting its filtering activity to other parts of the particle spectrum.

Table 1. Acartia clausi grazing on particle mixes of Thalassiosira fluviatilis and spheres.

Particle mix 1: 11 μ m cells: 0
 15 μ m cells: 2426
 15 μ m spheres: 2629

Replicate	Particle Ingestion (particles/copepod/day)	Sphere Ingestion (spheres/copepod/day)
1	19560	143
2	22089	94
3	29149	95
<u>4</u>	<u>21755</u>	<u>73</u>
Mean	23138	101

Error rate: $\frac{\text{number of spheres ingested}}{\text{number of spheres handled}} = \frac{101}{24063} = 0.42\%$

or 1 sphere ingested per 238 handled.

Particle mix 2: 11 μ m cells: 2358
 15 μ m cells: 1302
 1410 spheres: 1410

Replicate	Particle Ingestion (particles/copepod/day)	Sphere Ingestion (spheres/copepod/day)
1	10357	79
2	9328	47
3	11021	82
<u>4</u>	<u>11631</u>	<u>59</u>
Mean	10584	67

Error rate: $\frac{\text{number of spheres ingested}}{\text{number of spheres handled}} = \frac{67}{11132} = 0.6\%$

or 1 error in 166 encounters.

The above demonstration of a particle by particle post capture rejection capability does not disprove the use of alteration of setal spacing, combing rejection, or other behavioral actions as mechanisms for modification of feeding patterns. However, since post combing rejection is a more sophisticated mechanism, visual observations will be required to confirm these other mechanisms, if they exist. Visual observations of a variety of copepods feeding in different types of particle suspensions suggest that the way in which the filter is used to remove particles from the water may be altered in response to changes in that particle spectra. For example, after feeding on a suspension containing both spheres and food, A. clausi stops using a seining motion (Conover 1956) and switches to very brief bursts of feeding activity. These changes in filter motion must almost certainly affect the way particles are captured and handled and thereby must affect the observed filtering curves.

In conclusion, it appears that by using a variety of behavioral tools A. clausi can radically modify the filtering behavior expected from the morphology of the filter. The observed feeding patterns on complex particle mixtures are strongly controlled by food quality and preconditioning. In our efforts to understand the capabilities of A. clausi, it has become apparent that the Coulter Counter is but one of several powerful tools needed to solve grazing problems. Careful study of feeding appendage morphology, gut content, fecal pellet analysis, and behavioral observation all play important roles. Their combined use, where appropriate, is often more powerful than any one alone.

Care should be taken in extrapolating these results to all species.

Work in our laboratory with Eurytemora and Calanus marshallae has shown that while Eurytemora has many of the capabilities that Acartia has, Calanus appears to be much more limited in the extent to which behavior may be used to modify filtering patterns. As a result, much more work is needed before we can attempt to develop a universal feeding model. The differences observed between species may be an important element in controlling population dynamics of these species and in generating observed community structures.

ACKNOWLEDGEMENTS

We acknowledge the support of NSF Grants OCE 76-10347 and OCE 78-08635. We also acknowledge discussion with and assistance in performing these experiments by S. Schnack, R. D. Leatham, and B. L. Dexter.

References

- Boyd, C. M. 1976. Selection of particle sizes by filter feeding copepods: A plea for reason. *Limnol. Oceanogr.* 21:175-180.
- Conover, R. J. 1956. Oceanography of Long Island Sound, 1952-1954. VI Biology of Acartia clausi and A. tonsa. *Bull. Bingham Oceanogr.* 15:156-233.
- Donaghay, P. L. In prep. Conceptual and experimental approaches to grazing behavior in copepods.
- Donaghay, P. L. and L. F. Small. 1979. Food selection capabilities of the estuarine copepod Acartia clausi. *Marine Biology* 52:137-146.
- Frost, B. 1972. Effects of size and concentration of food particles on the feeding behavior of the marine planktonic copepod Calanus pacificus. *Limnol. Oceanogr.* 17:805-815.
- _____. 1977. Feeding behavior of Calanus pacificus in mixtures of food particles. *Limnol. Oceanogr.* 22:472-491.
- Lam, R. K. and B. W. Frost. 1976. Model of copepod filtering response to changes in size and concentration of food. *Limnol. Oceanogr.* 21:490-500.
- Lehman, J. T. 1976. The filter-feeder as an optimal forger, and the predicted shapes of feeding curves. *Limnol. Oceanogr.* 21:501-516.
- Nival, P. and S. Nival. 1973. Efficacite de filtration des copepodes planctoniques. *Ann. Inst. Oceanogr.* 49:135-144.
- _____ and _____. 1976. Particle retention efficiencies of an herbivorous copepod Acartia clausi (adult and copepodite stages): Effects on grazing. *Limnol. Oceanogr.* 21:300-308.
- Porter, K. G. and J. R. Strickler. In prep. The mechanisms of selective feeding in Daphnia.
- Poulet, S. A. and P. Marsot. 1978. Chemosensory grazing by marine calanoid copepods (Arthropoda: Crustacea). *Science* 200:403-405.
- Richman, S., D. R. Heinle, and R. Huff. 1977. Grazing by adult estuarine copepods of the Chesapeake Bay. *Mar. Biol.* 42:69-84.
- Schnack, S. 1975. Untersuchungen zur nahrungsbilogie der Copepoden (Crustacea) in der Kieler Bucht. Ph.D. thesis, Kiel. 144 p.
- Wilson, D. S. 1973. Food size selection among copepods. *Ecology* 54:909-914.

CHAPTER 3

A Comparison of Grazing Functions from Phytoplankton and
Zooplankton Viewpoints: An Algorithm

Percy L. Donaghay

Lawrence F. Small

Rae Deane Leatham

and

J. Michael DeManche

School of Oceanography, Oregon State University

Submitted to Limnology and Oceanography

Abstract

Selective grazing by copepods is widely recognized as an important process to both phytoplankton and zooplankton. Our ability to understand and interpret the results of grazing experiments depends on the use of indices of grazing behavior that precisely describe the effects of grazing from both phytoplankton and zooplankton points of view. These indices must be free of artifacts resulting from both conceptual and mathematical errors in their formulation. An examination of existing indices showed (1) that only indices from a zooplankton viewpoint existed, (2) that for those indices most often used (i.e. filtering rate, ingestion rate, and Ivlev's electivity), a great diversity of formulation existed, and (3) that some of the formulations were correct and equivalent, but some were invalid for conceptual or mathematical reasons. Using the primary production equation as a base, a series of grazing indices is mathematically derived and intercompared. The performances of these indices are compared using the results from grazing experiments under four very different conditions. The results of these comparisons show that from a phytoplankton point of view the growth rate indices (derived herein) are most useful. From a zooplankton point of view, ingestion rate and filtering rate indices (when correctly formulated) are most useful for examining general grazing behavior and testing theoretical models. When particle rejection events are occurring, a series of newly derived indices for measuring encounter rate, capture rate, and rejection rate is very useful in understanding the mechanisms of grazing behavior. The widely used electivity indices were found to provide little new information and to be subject to a great variety of problems.

Introduction

Selective grazing by copepods is an important process to both zooplankton and phytoplankton. Zooplankton biologists often view selective grazing from three perspectives: 1) how do copepods selectively graze (i.e., what are the mechanisms) (Strickler and Rosenberg, 1977; Porter and Strickler, 1977; Frost, 1972; Lam and Frost, 1976); 2) why do they do it (i.e., what are the benefits to the animal of being selective) (Mayzaud and Conover, 1976; Mayzaud and Poulet, 1978; Conover, 1976; Donaghay and Small, 1979b); and 3) what will they do to a given particle suspension (Parsons, 1969; Poulet, 1973, 1974, 1976; Richman, et al., 1977; Allan, et al., 1977). Phytoplankton biologists are beginning to ask a different set of questions: 1) what are the effects of zooplankton selectivity on phytoplankton population species composition and succession; and 2) what are the effects of selection and nutrient regeneration on the physical and physiological characteristics of a particular phytoplankton species. In light of these different viewpoints it is not surprising that a variety of different ways of expressing selective grazing have evolved: the Ivlev electivity index (Poulet, 1974; Frost, 1977; Storm, 1974) size class specific filtering and ingestion rates (Richman, et al., 1977; Allan, et al., 1977; Frost, 1977; Donaghay, 1979a); and net grazing effect index and net selective pressure index (O'Connors, et al., 1976; Donaghay and Small, 1979a). A critical problem occurs when one tries to reinterpret existing data from one's own viewpoint without knowing how a particular index is related to a different set of indices. For example, how are filtering rate and Ivlev electivity indices related, and do they have the same sensitivity

to various factors and the same information content? In addition, if one is interested in the effects of selective grazing on phytoplankton populations, none of the existing indices provide particularly useful information, i.e., information on grazing effects on phytoplankton size class specific growth rates. While trying to interpret experiments on particle rejection by copepods (Donaghay and Small, 1979a,b) we realized that such rejection could perhaps be best interpreted, or best visualized, by using capture indices already proven useful by animal behaviorists but not yet used to describe copepod grazing.

In an effort to solve the above problems, we have explicitly set down the equations most frequently used in the grazing literature, and have introduced a series of new indices designed to redress the inadequacies in the existing indices. These equations were compiled into a computerized grazer algorithm that allows us to calculate and plot all of the indices for multi-size-classed data (particle counter data) generated in a grazing experiment.

In this paper, we shall define each index, describe its derivation, and examine the assumptions implicit in its use. Then we shall examine the potential information content and utility of each index in describing the results of four very different yet representative types of grazing experiments.

The algorithm described herein was designed for use with our linear based particle counting system. However, it is applicable to any linear or log based system with minor program modifications. In our system, particles are sized using a model ZBI Coulter Counter^R, and separated into 64 size classes by a Coulter model P-64 Channelizer. The 64 chan-

nels are set up in such a way that the mean particle size in each channel is a simple linear multiple of the channel number and the counter sensitivity (i.e., a linear system as described by Sheldon and Parsons, 1966). Our channelizer has been interfaced to a PDP-8-E minicomputer so that data can be directly transferred and processed in real time. Once data are transferred to the minicomputer, particle number and volume distributions are calculated. These distributions are then plotted and stored on paper tape. After an experiment is completed (or between samples during a long-term experiment), the data tapes are re-entered into the computer, and processed by our grazer algorithm program.

The equations that are described herein are designed for use under all conditions where changes in phytoplankton concentration occur with time in either grazing or control vessels or both. This eliminates the requirement to run grazing experiments in the dark in order to make the assumption that growth of phytoplankton does not occur (Gauld, 1951). As will be shown below the assumption of true zero growth in the dark is almost never correct. In this paper we shall consider experiments that are run under conditions of light that are sufficient to support algal growth ranging from zero to maximum rates (compensation intensity to supersaturation).

Exponential Assumptions:

The exponential equations for grazing derive from the basic production equations (see Steele and Frost, 1978 and Kremer and Nixon, 1978 for recent reviews):

$$\frac{1}{N} \frac{dN}{dt} = a - r - e - w - g - s \quad \text{eq. a}$$

where N = phytoplankton population size, t = time, and the phytoplankton specific rates are as follows: a = assimilation, r = respiration, e = excretion, w = dilution, g = grazing and s = sinking losses. In a simple grazing situation (a closed, well mixed vessel) w and s are zero, and the term $a-r-e$ is set equal to k , the specific growth rate. Equation 1 then simplifies to

$$\frac{1}{N} \frac{dN}{dt} = k - g. \quad \text{eq. b}$$

In any typical grazing experiment, k is measured as the growth rate in a control vessel with no grazers (we shall term it k_c), $\frac{1}{N} \frac{dN}{dt}$ is measured as the apparent (i.e., observed) growth rate in a vessel with grazers (we shall call this the apparent growth rate, k_a), and g is calculated as the difference (for consistency we shall call it k_g) thus,

$$k_a = k_c - k_g \quad \text{eq. c}$$

The phytoplankton concentration at any time t during the experiment in the grazed flask is:

$$N_t = N_0 [e^{(k_a t)}] \quad \text{eq. d}$$

These growth rate terms can be specified for the i^{th} size class by adding a subscript (k_{ai} , k_{ci} , k_{gi}). These are the fundamental equations upon which all subsequent calculations in the algorithm are made.

Thus far we have assumed that the specific rate of grazing removal is exponential. This will be true, if during the course of the grazing period, the animals filter the water at a constant rate and the food particles remain evenly distributed in the water. Experiments by Mullin (1963) and McAllister (1970) showed that for copepods starved for 24 hrs the filtering rate decreases at a decreasing rate with time.

Experiments by Frost (1972) and Donaghay and Small (1979a) using non-starved copepods suggest that these changes in filtration rates are the result of pre-starvation and subsequent reacclimation to the presence of food. Changes from one food type to another might also elicit transient responses that result in non-exponential specific rate of particle removal. If the particle biomass in the grazed flask were to change in something other than an exponential fashion, some equation other than the exponential (eq. c) should be used. In order to test the assumption that the specific rate of removal is exponential, we preconditioned Acartia clausi for three days on $3 \times 10^6 \mu\text{m}^3 \text{ml}^{-1}$ of the diatom Thalassiosira fluviatilis. After this conditioning period, grazing was observed over a 24 hr period under low light with repetitive samples from well mixed control and grazing vessels. Exponential growth in terms of particle volume is easily observed for phytoplankton in the absence of grazers or in their presence (Fig. 1a). Exponential "growth" in the grazed vessel was negative in this case. Because the assumption of exponentiality held, k_a and k_c and therefore k_g were constant under these conditions of constant low light and preconditioned animals. Thus the exponential assumption is valid for grazing experiments in constant low light with preconditioned animals. The constancy of k_a , k_c and k_g can also be shown to be true for each particle size class within the distribution (Fig. 1b,c,d,e,f,g). The exponential assumption should be rechecked if either the animals or the phytoplankton are exposed to transient conditions (alteration of food levels or types, light levels, nutrients, etc.). There are no a priori reasons to assume that the specific rate of grazing removal will remain exponential under transi-

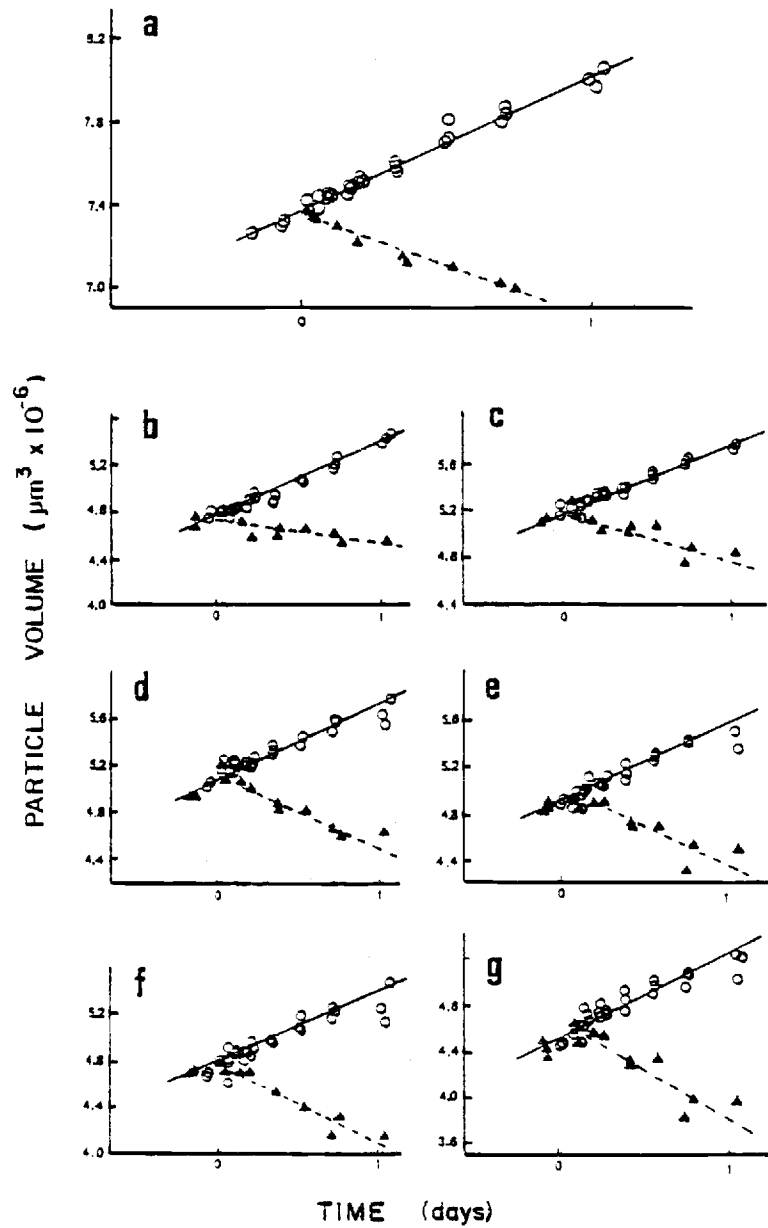


Fig. 1. Exponential assumptions test: (a) total particle volume from a control (o) and a grazed (\blacktriangle) flask taken repeatedly over 24 hour grazing experiment. Parts (b) through (e) are particle volume in size classes 10 through 15 from the same grazing experiment. Symbols same as in (a).

ents; in fact there is significant evidence to suggest otherwise (Donaghy, et al., in prep.).

We have emphasized the validation of the exponential assumption for a special reason other than the fact that it is almost always made implicitly in grazing experiments. As long as this assumption holds, a "ghosted" particle size distribution or concentration can be calculated at any time during a grazing experiment. In addition to needing such ghosted particle size distributions for the calculation of ingestion and capture rates, the ability to calculate such distributions can be used to modify experimental designs and enhance statistical precision of our estimates of grazing rates.

Mathematical Formulations of Grazing Indices

In this section we shall consider the mathematical formulation of the grazing indices and how they are mathematically related. In those cases where a variety of different mathematical formulations have been used for a particular index, the effects of such different formulations will be examined. In the following discussion, it will be assumed that data being analyzed is from a grazing experiment where initial and final samples are available from both grazed and control flasks. It will further be assumed that this data is in the form of particle volume in each of 64 particle size classes. Although particle number data may be used with the following equations, the interpretation of those indices will in some cases be very different.

1. Net effect indices

Net grazing effect ($G_i - C_i$) is calculated as the difference be-

tween particle volume in the i^{th} particle size class in the grazed and control vessels at the end of the grazing period. This index was first used by O'Connors, et al. (1975) and later Donaghay and Small (1979a) to express the net effect of grazing when particle modification was important. Positive values of this index are clear proof of particle production resulting from the disruption of large chains by grazing activity. This index has the advantages that it is both simple to calculate and requires no assumptions about the exponentiality of grazing; however, if the index is to be used to compare results from different experiments, great care must be taken to insure that (1) all experiments are of identical length, (2) the initial values for both grazed and control vessels are identical, and (3) both grazed and control samples are taken as closely together as possible.

(2) Relative removal pressure index $\left(\frac{G_i - C_i}{C_i}\right)$ was first used by Donaghay and Small (1979a) to examine the effect of copepod selectivity on phytoplankton from an algal point of view. The index measures the relative removal pressure exerted on the i^{th} particle size class independent of that particle size class' growth rate. This index has both the same advantage and restrictions as the net grazing effect index.

The limitations on the use of the above two indices can be greatly reduced by modifications of experimental design and normalization of the resulting data to a common time period. Identical initial particle concentrations can be achieved in both grazed and control vessels by splitting a single well mixed particle suspension into both grazed and control vessels and then adding copepods without altering that suspension. We normally do this by sorting copepods into cages suspended in a

similar particle mix, then transferring the cage and copepods to the grazed vessel. The copepod cages are made by gluing nitex just small enough to retain the copepods to the end of plexiglas cylinders. Similar cages without copepods are added to the controls. If for some reason, it is not possible to have identical initial concentrations (size distributions must be identical), the effect of such initial differences on the net effect indices can be mathematically resolved. Under such conditions the initial and final values from the control are used to calculate k_{ci} , then using the initial values of the grazed flask, and k_{ci} determined from the control flask, a final control distribution can be calculated at the same time as the final grazed distribution was measured. Since in many grazing experiments it is very difficult to obtain all final samples exactly 24 hours after the start of grazing, intercomparison of results with net effect indices is greatly facilitated by calculating final control (C_i' , eq. 3, Table 1) and final grazed (G_i' , eq. 4, Table 1) ghosted to 24 hours. These distributions are normally plotted. These 24 hour corrected final control and grazed distributions are then used to calculate 24 hour corrected net effect indices (eq. 5 and 6, Table 1). These 24 hour corrected indices have the same problems as indices 1 and 2, except that they are directly comparable among experiments.

2. Growth rate indices

The three growth rate indices (k_{ci} , k_{ai} , and k_{gi}) are critically involved in the calculations of the other indices, but, to our knowledge, have not previously been explicitly calculated and plotted. k_{ci} , the volume based phytoplankton specific growth rate in each size class

Table 1. Grazing Equations.

1.	NET GRAZING EFFECT	$\mu\text{m}^3 \text{ ml}^{-1}$	$G_i - C_i$	$G_i = v_{it} \text{grazed}$ $C_i = v_{it} \text{control}$ where $t = 1$
2.	RELATIVE REMOVAL PRESSURE	relative units	$\frac{G_i - C_i}{C_i}$	
3.	24 HOUR GRAZED	$\mu\text{m}^3 \text{ ml}^{-1}$	$G_i' = v_{it_0} e^{(k_{ai})}$	k_{ai} from eq. 8
4.	24 HOUR CONTROL	$\mu\text{m}^3 \text{ ml}^{-1}$	$C_i' = v_{it_0} e^{(k_{ci})}$	k_{ci} from eq. 7
5.	NET GRAZING EFFECT (24 hour)	$\mu\text{m}^3 \text{ ml}^{-1}$	$G_i' - C_i'$	
6.	RELATIVE REMOVAL PRESSURE	relative units	$\frac{G_i' - C_i'}{C_i'}$	
7.	SPECIFIC GROWTH RATE (size class specific)	days ⁻¹	$k_{ci} = \frac{\ln\left(\frac{v_{it_1}}{v_{it_0}}\right)}{t_1 - t_0}$	v_{it} from controls
8.	APPARENT GROWTH RATE (size class specific)	days ⁻¹	$k_{ai} = \frac{\ln\left(\frac{v_{it_1}}{v_{it_0}}\right)}{t_1 - t_0}$	v_{it} from grazed
9.	SPECIFIC GRAZING RATE (size class specific)	days ⁻¹	$k_{gi} = c_i - k_{ai}$	
10.	mean time in grazing period	day	$t^* = \frac{t_1 + t_0}{2}$	
11.	exponential mean biomass (grazed vessel)	$\mu\text{m}^3 \text{ ml}^{-1}$	$v_{it^*} = v_{it_0} e^{[k_{ai}(t^* - t_0)]}$	
12.	TOTAL GRAZING FLUX LOSS	$\mu\text{m}^3/\text{vessel}/\text{day}$	$G_{fi} = k_{gi}(v_{it^*})(v_o)$	$v_o = \text{vessel volume}$
13.	INGESTION RATE	$\mu\text{m}^3/\text{copepod}/\text{day}$	$I_i = \frac{G_{fi}}{A}$	$A = \text{animal numbers}$

14.	APPARENT FILTERING RATE	$\mu\text{l}/\text{copepod}/\text{min}$	$F_{ai} = \frac{I_i}{1440(\bar{v}_{it^*})}$	
15.	EQUIVALENT SPHERICAL DIAMETER (natural logarithm)	μm	$\ln d = \frac{(\ln 1.9085 \bar{v}_i)}{3}$	$\bar{v}_i = \text{mean particle volume in } i^{\text{th}} \text{ size class}$
16.	APPARENT FILTERING RATE AT MAXIMUM INTERSEPTULE PORE SIZE	$\mu\text{l}/\text{copepod}/\text{min.}$	$F_{ad} = \alpha' \ln(d_s) - F'_{ai}$	
17.	FILTERING EFFICIENCY		$F_{ei} = \frac{F_{ai}}{F_{ad}}$	
18.	NORMALIZED APPARENT FILTERING RATE		$F_{nai} = \frac{F_{ai}}{F_{\max}} = \frac{F_{ai}(w_2^{-w_1+1})}{\sum_{i=w_1}^{i=w_2} (F_{ai})}$	w_1 and w_2 are operator defined
19.	EXPECTED FILTRATION RATE for $d < d_u$ (regression based)	$\mu\text{l}/\text{copepod}/\text{min.}$	$\hat{F}_{ai} = \alpha'(\ln d) + F'_{ai}$	
20.		for $d \geq d_s$ $\mu\text{l}/\text{copepod}/\text{min}$	$\hat{F}_{ai} = \beta'(\ln d) + F_{ad}$	
21.	EXPECTED FILTRATION RATE for $i < w_1$ (F_{\max} based)	$\mu\text{l}/\text{copepod}/\text{min.}$	$\hat{F}_{ai} = F_{ai}$	
22.		for $i \geq w_1$ $\mu\text{l}/\text{copepod}/\text{min.}$	$\hat{F}_{ai} = F_{\max}$	
23.	EXPONENTIAL MEAN PARTICLE NUMBER	particles/ml	$N_{it^*} = \frac{V_{it^*}}{\bar{v}_i}$	
24.	ENCOUNTER RATE	particles/copepod/min.	$E_{ri} = \hat{F}_{ai}(N_{it^*})$	
25.	CAPTURE RATE	particles/copepod/min.	$G_{ri} = \frac{I_i}{1440 \bar{v}_i} = F_{ai}(N_{it^*})$	
26.	REJECTION RATE	particles/copepod/min	$R_{ri} = E_{ri} - G_{ri}$	
27.	IVLEV ELECTIVITY		$E_i = \frac{\frac{G_{ri}}{\sum G_{ri}} - \frac{N_{it^*}}{\sum N_{it^*}}}{\frac{G_{ri}}{\sum G_{ri}} + \frac{N_{it^*}}{\sum N_{it^*}}}$	
28.	JACOBS ELECTIVITY		$D_i = \frac{\frac{G_{ri}}{\sum G_{ri}} - \frac{N_{it^*}}{\sum N_{it^*}}}{\frac{G_{ri}}{\sum G_{ri}} + \frac{N_{it^*}}{\sum N_{it^*}} - 2 \left(\frac{G_{ri}}{\sum G_{ri}} \right) \left(\frac{N_{it^*}}{\sum N_{it^*}} \right)}$	

is calculated from particle size class data from the control flask(s) (eq. 7, Table 1). We have found that the precision of all the subsequent indices is highly dependent on the precision of the estimate of k_{ci} . As a result, k_{ci} is normally determined by using many samples taken from the control flasks with these samples spread over a period of time slightly longer than the 24 hour grazing period. Such a procedure maximizes the precision of the estimate of k_{ci} . The apparent size-class-specific growth rates (k_{ai}) in the grazed flask are then calculated from the initial and final values in the grazed flask. If the grazed and control flasks have the same initial concentrations (as described above) then the particle size distributions will change in an identical way in both the control and grazed flasks until grazers are added to the grazed flask. As a result, k_{ci} from the control flask can be used to calculate the particle size distribution in the grazed flask at the exact time grazers are added. This ghosted initial grazed value can then be used with the measured final grazed value(s) to calculate k_{ai} (eq. 8, Table 1) with the greatest precision. If the initials in the grazed and control flasks are not identical, then k_{ai} must be calculated based on measured initial and final particle distributions taken from the grazed flask. If this latter procedure is used, it is critical that the initial and final samples from the grazed vessel be collected at exactly the time the grazers are added or removed from the flask. Significant errors may result if grazers are not present in the grazed flask over the entire time interval between initial and final measurements.

From a phytoplankton point of view these are the three most impor-

tant indices in that they (1) illustrate the direct effect of grazing on phytoplankton and (2) unravel possible algal grazer interactions (i.e., the effects of grazing on the physical and physiological characteristics of the phytoplankton). Each of the indices describes an important effect: k_{ci} describes if and how the growth rate of the phytoplankton is particle size class dependent; k_{ai} describes the net selective pressure on the phytoplankton population (assuming grazing stays constant) and determines how the particle size distribution (in the grazed vessel) will change with time; k_{gi} describes the net effect of grazing removal on the apparent growth rate of each particle size class. Knowledge of these rates allows the direct testing of a series of very important hypotheses, including (1) is k_{ci} size-class independent? (2) is k_{gi} a function of k_{ci} , i.e., do grazers preferentially ingest faster growing cells; (3) do the combined effects of grazing and phytoplankton growth both of which may be size-class dependent, cause a highly size-class dependent selective pressure on the population (i.e., are grazing removal and phytoplankton growth additive, multiplicative or neutralizing in their effects)?

3. Ingestion rate indices

Once the specific grazing rate (k_{gi}) is calculated, ingestion rates can be determined. We have divided the computation of ingestion rates into a series of explicit stages. First, the average particle volume (biomass) concentration (in each particle size class) to which the animals were exposed in the grazing vessel during the grazing period must be calculated. If the mean time in the experiment is designated as t^* (eq. 10, Table 1) then the exponential mean biomass in the i^{th} size

class at t^* can be given as:

$$V_{it^*} = V_{it_0} e^{[k_{ai}(t^* - t_0)]}$$

(eq. 11, Table 1) in exactly the same fashion and with exactly the same assumptions as the final 24 hour grazed and control distributions (eq. 3 and 4, Table 1). The total amount of phytoplankton production in the grazing vessel consumed by the grazing process (G_{fi}) is then simply calculated as the product of k_{gi} , the exponential mean biomass (V_{it^*}), and the vessel volume, V_0 (eq. 12, Table 1). Summation across all particle size classes yields the total amount of phytoplankton production ingested by all the grazers in the flask per day. It is important to note that G_{fi} is equal to 24 hour net grazing effect (i.e., difference between 24 hour corrected final grazed and control, eq. 5, Table 1) only if k_{ci} equals zero. We have explicitly calculated G_{fi} because it is a direct measure of the amount of primary production being consumed by grazers. It should therefore be very useful in the field in estimating the degree of control exerted by zooplankton grazing on primary production (Donaghay, in prep.). In the laboratory, estimation of G_{fi} is useful in experiments in which one wants to keep particle biomass in the grazed vessel constant by additions of cells.

The ingestion rate on a per copepod basis, I_i is calculated simply as G_{fi}/A (eq. 13, Table 1). Size class specific ingestion rate index, I_i is one of the most widely used indices to describe where in the particle spectrum an animal obtains its ration (Richman, et al., 1977). A plot of I_i vs. particle size class, when both are plotted on a linear volume scale, not only represents a graphic display of where in the

particle spectrum the grazer gets its food: the area under the curve is directly proportional to the total amount of food ingested per animal. This is not true when I_i is plotted as a function of particle size computed as the logarithm of the particle diameter. The mathematical summation of I_i over all size classes is the total particle ingestion rate for the copepod.

4. Filtering rate indices

Another often used index of grazing is the filtering rate. Actually, the filtering rate that is calculated from grazing data is only an apparent filtering rate (eq. 14, Table 1). The true filtering rate, defined as the number of milliliters of water passed through the copepod's filter (maxillae) per unit of time, cannot be directly calculated from particle ingestion experiments. It can, however, be estimated from beat frequency and filter area information (Strickler and Rosenberg, 1977; Starkweather, 1978). These techniques are still difficult for copepods, but have proved very valuable for larger aquatic herbivores (Durbin and Durbin, 1976; Seale and Wassersug, in press). We have adopted the term "apparent filtering rate" (F_{ai}) to distinguish particle size calculated rates from true flow rates. These two rates can be related if the efficiency of the filter is known for any given particle size class and if all particles captured by the filter are ingested.

The apparent filtering rate (F_{ai}) can be calculated from the ingestion rate (I_i) by dividing the ingestion rate by the exponential mean biomass in that size class (V_{it^*}) (eq. 14, Table 1). Apparent filtering rate is expressed in units of volume filtered per animal per unit time. In the algorithm it is calculated in terms of μl filtered per copepod

per minute.

There are a variety of reported methods for calculating apparent filtering rate; however, some of these methods are not directly equivalent and some involve questionable assumptions. Gauld (1951), for example, calculated apparent filtering rate per animal as (in our notation):

$$F_{ai} = \left(\frac{V_o}{A}\right) \frac{\ln G_{it} - \ln G_{io}}{t} \quad \text{eq. d}$$

where G_{io} and G_{it} are the initial and final concentrations in the grazed flask and V_o equals the volume of the grazing vessel, A equals animal numbers, and t equals the length of the grazing period. Gauld did not use a control vessel in his experiments; instead, he assumed that phytoplankton growth (in the dark) was equal to zero. To test this assumption, we conducted a small experiment. Two replicate cultures of each of five phytoplankton species were transferred while still in exponential phase from high light (under which they were grown) to darkness. These cultures were counted and sized at the time of transfer and 24 hours later. The relative changes in biomass over the 24-hour dark period are shown in Fig. 2. It is clear that particle volume tended to decrease for all non-diatoms, but increase for diatoms (Fig. 2a); particle number increased in all cultures save one Amphidinium cartarae replicate (Fig. 2b). The assumption of no growth in the dark should be accepted with great caution.

Recently, an equation very similar in form to the Gauld (1951) equation, but without the assumption of zero phytoplankton growth has been used (Richman, et al., 1977). This form will be widely used because it does not require any measurement of initial concentrations.

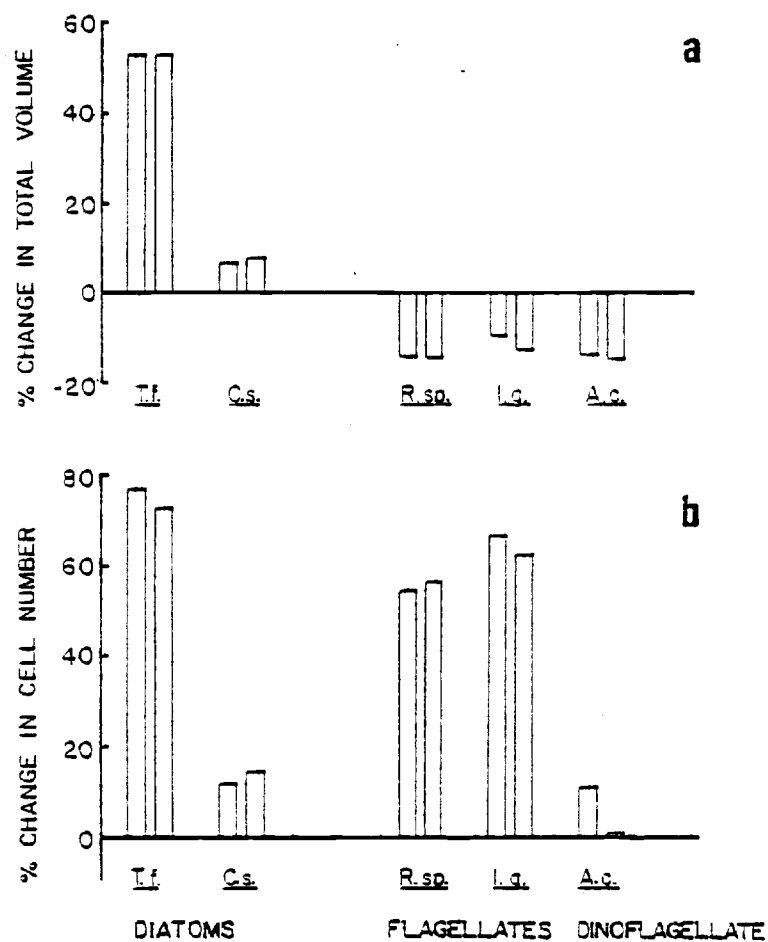


Fig. 2. Dark growth. Percentage change in (a) total cell volume and (b) total cell number for 5 species of algae transferred from high light to darkness for 24 hours. The species are two diatoms: Thalassiosira fluviatilis (T.f.) and Chaetoceros septemtralis (C.s.); two naked flagellates: Rhodomonas ap. (R. sp.) and Isochrysis galbana (I.g.); and the dinoflagellate Amphiodinium carteri. Bars are the results from replicate experiments.

The form used by Richman, et al. (1977) can be derived from equation 9 in Table 1:

$$k_{gi} = k_{ci} - k_{ai}$$

by substituting for k_{ci} and k_{ai} from equation 7 and 8 (Table 1):

$$k_{gi} = \frac{\ln\left(\frac{C_{it}}{C_{io}}\right)}{t_c} - \frac{\ln\left(\frac{G_{it}}{G_{io}}\right)}{t_g} \quad \text{eq. e}$$

where t_c = time interval in control, t_g = time interval in grazed and where the initial and final concentration in the grazed are G_{io} and G_{it} and in the control are C_{io} and C_{it} . If $t_c = t_g = t$ then:

$$k_{gi} = \frac{\ln\left(\frac{C_{it}}{C_{io}}\right) - \ln\left(\frac{G_{it}}{G_{io}}\right)}{t} \quad \text{eq. f}$$

or

$$k_{gi} = \frac{\ln C_{it} - \ln C_{io} - \ln G_{it} + \ln G_{io}}{t} \quad \text{eq. g}$$

If and only if, the initial control and grazed particle concentrations are identical (i.e., $C_{io} = G_{io}$) then

$$k_{gi} = \frac{\ln C_{it} - \ln G_{it}}{t} \quad \text{eq. h}$$

and thus

$$F_{ai} = \left(\frac{V_o}{A}\right) \frac{\ln C_{it} - \ln G_{it}}{t} \quad \text{eq. i}$$

which is the equation of Richman, et al. (1977) using our symbols. Thus the equation used by Richman, et al. (1977) only requires that the final samples be taken simultaneously and that the initial particle concentrations in the two flasks be equal. Both of these conditions are very practical to meet experimentally if one has two particle counters.

Although fewer samples are needed to calculate filtering rate using the above equation (eq. i), we have chosen equation 14 (Table 1) for two reasons. First, eq. 14 is a more general formulation without restrictions on experimental design. Second, if one measures only final control and grazed distributions to calculate filtering rates as in eq. i, ingestion rates can be calculated from the resulting filtering rates only if no growth has occurred in the grazing vessel, i.e., $k_{ai} = 0$. If $k_{ai} \neq 0$, then it will not be possible to estimate the exponential mean biomass (i.e., V_{it^*}) required for calculating ingestion rate from filtering rate. Use of final control or final grazed values as an approximation of V_{it^*} will result in systematic errors in the calculation of ingestion rates.

Apparent filtering rate curves have recently gained wide use in examining patterns of grazing selectivity from a zooplankton viewpoint. Apparent filtering rates have been used (1) for qualitative description of patterns of selectivity (Richman, et al., 1977; Poulet, 1973, 1974; Poulet and Chaunet, 1975; Donaghay, 1979); (2) for development of inter-comparisons of feeding behavior of different life history stages of one species (Allan, et al., 1977) or of different species under a variety of conditions (Richman, et al., 1977); and (3) for rejection of theoretical models based on deviations of selectivity patterns from those expected from existing models (Richman, et al., 1977; Allan, et al., 1978; Poulet, 1978; Donaghay, 1979). In the past theoretical models have been sufficiently simple that the deviations between expected results and observed filtering rates have been sufficiently large to allow rejection of these models for some copepods without resort to rigorous quantitative methods.

However, as models become more realistic and complex, rigorous quantitative testing of those models will become necessary. This will become particularly true as models attempt to separate patterns of feeding behavior into those resulting from purely passive properties of the filtering mechanism (i.e., passive selection) and those resulting from active rejection of unwanted particles by altering the way the filter is used or by rejecting particles after capture. Theoretical models are now under development that attempt to make these separations (Donaghay, in prep.).

Expected filtering behavior in theoretical models is often defined in terms of curves of filtering efficiency versus particle size as measured by the natural log of particle diameter. Filtering efficiency, F_{ei} , is nothing more than filtering rate normalized to the observed filtering rate, F_{ai} , in some standard size class. Filtering efficiency curves are used in theoretical models because observed apparent filtering rates have patterns of selectivity confounded with concentration effects on maximum apparent filtration rate (Frost, 1972): the observed apparent filtration rate is not only a function of particle size but also of concentration. Apparent filtration rate, F_{ai} , increases with increasing size, but tends to decrease as total particle concentration increases (Frost, 1972) above some critical low concentration.

Theoretically derived filtering efficiency curves increase log linearly with particle diameter from some minimal particle size, d' (equivalent to the smallest particle that can be retained by the filter) up to some larger particle size equivalent to the largest pore size of the filter, d^* (Fig. 3a). This largest pore size may be equivalent to

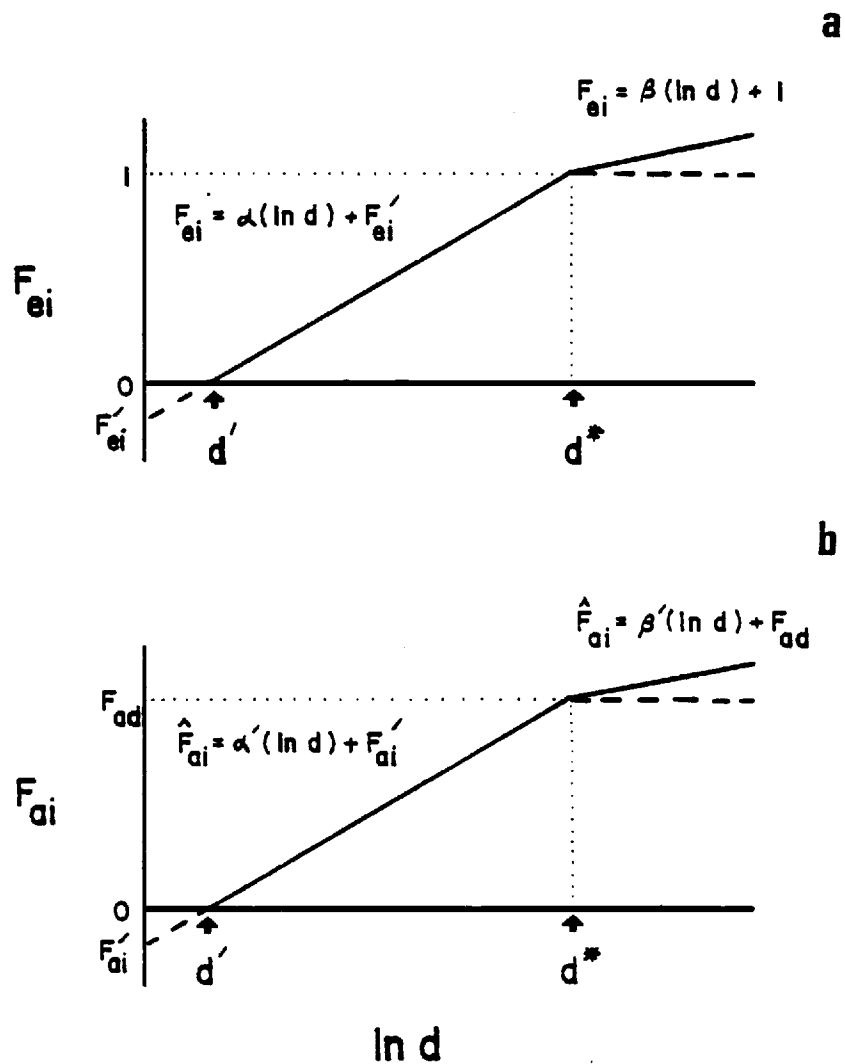


Fig. 3. Theoretical relationship between (a) filtering efficiency (F_{ei}) and (b) apparent filtering rate (F_{ai}) and particle size expressed as the natural log of the equivalent particle diameter $[\ln(d)]$. Solid lines represent expected curves below the inflection point of the curve (d^*). Solid line above d^* is the expected curve if intersetal capture occurs; the dashed line above d^* is the expected curve if no intersetal capture occurs. Terms defined in text.

or less than the largest setule spacing on the filter (Donaghay, in prep.). At d^* the slope of the expected filtering rate curve will change (inflect). If intersetal capture is significant, F_{ei} will continue to increase at some rate, β ; if intersetal capture is not significant, then F_{ei} will be constant above d^* . The values of α , β , d' and d^* are critical in testing the alternate theoretical filtering models (Donaghay, in prep.); therefore their precise estimation from observed filtering rate data is essential.

Measured filtering rate (F_{ai}) curves when plotted versus the natural logarithm of particle diameter are similar in shape to F_{ei} vs. particle diameter curves, but are not equivalent (Fig. 3b). [F_{ai} curves accumulated versus linear particle volume based size classes can be transformed to natural log of particle volume by equation 15 (Table 1).] Apparent filtration rate plots are functions of both size and concentration; filtration efficiency curves are functions only of particle size. To remove the confounding of particle concentration it is necessary to normalize F_{ai} curves to some maximum filtering rate value. If all F_{ai} curves were rectilinear, i.e., $\beta = 0$, then normalization could be achieved by averaging all values of F_{ai} above d^* , then dividing all values of F_{ai} by this maximum value. However, because β is not always zero, and because F_{ai} values greater than d^* are not always defined in experiments, normalization to some other value is better. In order for all F_{ei} curves for a given copepod species to be intercomparable, it is necessary to always use a common point of normalization. We have chosen to normalize to the F_{ai} values observed at the particle size class equivalent to the size of the maximum setule based pore size. This size

(d_s) is fixed by the physical properties of the copepod filter, and should remain fixed for a given population of a copepod species independent of changes in the shape of observed filtering curves. The value of apparent filtering rate in size class d_s , F_{ad} , can be determined by two methods: regression analysis and direct measurement. Regression analysis of apparent filtering rates on the natural logarithm of particle diameter can be used to accurately estimate F_{ad} . However, it is critical to use only those size classes where no particle rejection is occurring and the data are not confounded by particle modification (O'Connors, et al., 1976) or excretion effects (Donaghay, et al., in prep.). This regression calculated value can be very precisely determined if separate regressions are used to estimate F_{ad} based on data collected above and below d_s . Such a regression method is better than using the measured value of F_{ai} at d_s because of the reduction in error achieved through regression analysis. The estimates of slope and intercept derived from this regression analysis will be used below in calculating encounter rates. Once the value of F_{ad} has been calculated, apparent filtering rates can be normalized to that value to calculate filtering efficiency as $F_{ei} = F_{ai}/F_{ad}$ (eq. 17, Table 1). Regression analysis of F_{ei} thus calculated on natural log of particle diameter will give estimates of α , β , d' and d^* . These values are the critical terms needed to test the alternative filtering models described by Donaghay (in prep.). The above procedure of normalizing F_{ai} curves to the apparent filtering rate at the particle size equivalent to maximum setule pore size (rather than observed d^*) will tend to accentuate any differences between d_s and d^* . Detection of such differences is critical to

testing some of the alternative models. but is difficult with raw appar-
ent filtering rate data since it requires detection of the inflection
point in the apparent filtering rate curve.

Although the above procedure for calculating F_{ei} is the most gener-
al and rigorous, in many situations it is not practical. In some cases
the particle spectra is very narrow so that extreme extrapolations are
required to estimate F_{ad} . This is often the case when only a single
species of phytoplankton is used in a grazing experiment and the result-
ing data are obtained with a linear based counting system. In other
cases, F_{ai} may be defined over a broad particle spectra, but the curve
may not have any clearly log-linear sections that are free of particle
rejection effects. In either case it is possible to calculate a pseudo
filtering efficiency curve (F_{nai}) by normalizing the F_{ai} values to the
maximum filtering rates measured in F_{ai} curve (Eq. 18, Table 1). It is
best if the maximum filtering rate, F_{max} , is estimated over several size
classes where F_{ai} has ceased increasing with particle size. If such
size classes are less than or equal to the maximum intersetule pore
size, F_{nai} will tend to be less than or equal to F_{ei} . F_{nai} cannot be
used to evaluate theoretical models.

Capture rate indices

Three indices used by animal behaviorists bear some exploration
relative to zooplankton grazing (Holling, 1959; Schoener, 1971). These
indices are encounter rate, capture rate and rejection rate. It should
be noted that these rates are always defined on a particle number basis
rather than on a particle volume basis. These indices are expressed in
units of the number of particles encountered, captured, or rejected per

unit time per animal. These indices are calculated on a particle number basis because any decisions to accept or reject particles after encounter must be made on a particle number rather than a particle volume basis. These indices are specifically designed to examine the time constraints placed on the copepod if each particle were handled particle by particle. The use of these particle number based indices does not require that copepods handle particles individually but rather allows testing of whether such individual handling of particles is reasonable. The difference between handling particles by number or volume is a very important conceptual distinction. The encounter rate is usually defined as the number of particles the animal encounters per unit of time while searching or filtering. On encounter, the animal presumably has to decide whether or not to eat a given particle. For a copepod, the encounter rate can be defined as the number of particles trapped by the maxillae as they are moved through the water or water is passed over then. As we will use the term here, a particle is not encountered by the maxillary filter if it goes through the spacings between setae and/or setules. Other definitions are also possible. If we accept the above definition, the capture rate can then be defined as the number of particles in a size class that, once encountered by the filter, are removed from the filter and ingested. If a particle is encountered, but is not captured (ingested), then it must by definition be rejected.

Encounter rates can be calculated from apparent filtering rate data if an estimate of expected filtering rate can be obtained for those size classes where particle rejection may be occurring. This can be possible if we assume that no rejection is occurring in those particles size

classes that contain only food particles to which the animals are pre-conditioned. The regression analysis of F_{ai} on the natural logarithm of particle diameter developed earlier to estimate F_{ad} provides the best estimates of expected filtering rate, \hat{F}_{ai} . For all values of d less than d_s

$$\hat{F}_{ai} = \alpha'(\ln d) + F_{ai}' \quad \text{eq. 19, Table 1}$$

and for all values of d greater than d_s

$$\hat{F}_{ai} = \beta'(\ln d) + F_{ads}. \quad \text{eq. 20, Table 1}$$

These equations predict expected filtering rate in all size classes regardless of whether particle rejection is occurring in those size classes as long as the conditions and assumptions necessary for the calculation of the regression are met (see example in Fig. 3c). If these assumptions cannot be met (for reasons discussed in relation to the estimation of F_{nai}), then some other method of estimating \hat{F}_{ai} must be used. Since the value of \hat{F}_{ai} in any size class must be greater than or equal to that in any smaller size class, then \hat{F}_{ai} for all size classes $>F_{max}$ must be F_{max} (eq. 22, Table 1). Likewise for all smaller particle size classes, \hat{F}_{ai} must be at least equal to F_{ai} (eq. 21, Table 1). Because of these conditions, this second method of estimating \hat{F}_{ai} will always provide a minimum estimate of \hat{F}_{ai} . If we know the expected filtering rate in a given size class, we can estimate the rate at which particles are encountered in that size class (regardless of whether they are subsequently rejected or ingested) as the product of expected filtering rate and the exponential mean particle number in that size class: $E_{ri} = \hat{F}_{ai}(N_{it}^*)$ (eq. 24, Table 1). The particle number in each size class (N_{it}^*) is easily calculated from the exponential particle volume

data (V_{it^*}) used in the calculation of the volume based indices as the exponential mean particle volume in the i^{th} size class (V_{it^*}) divided by the mean particle volume of a particle in the i^{th} size class (\bar{v}_i) (eq. 23, Table 1).

Capture rate as we have defined it is nothing more than ingestion rate on a particle number rather than volume basis. Capture rate, C_{ri} , may thus be calculated from ingestion rate by dividing ingestion rate in the i^{th} size class by the mean particle volume in the i^{th} size class, \bar{v}_i , and by 1440 to make C_{ri} (eq. 25, Table 1) be in the same units as encounter rate. If using these definitions, a particle is separated from the water by filtration (i.e., encountered) but not later captured (i.e., ingested), then it must be rejected after encounter and the rejection rate can be calculated by difference (eq. 26, Table 1).

The above method of calculating encounter, capture and rejection rates is widely applicable to grazing data for filter feeding copepods regardless of which alternative theoretical filter feeding model (Donaghay, in prep.) is used. Calculation of these indices allows explicit presentation of those elements so critical to understanding active selection by copepods. In addition, these indices express these events in the same terms that can be measured using cinematographic or other optical techniques. As a result, the capture rate indices offer a critical crosslink to the major alternative method of examining grazing behavior. It must be noted however, that these rates will only be as good as the estimates of encounter rate which in turn are only as good as our estimates of \hat{F}_{ai} . As noted earlier, the data used in the calculation of \hat{F}_{ai} must be free of rejection events and free of confounding

from particle modification and NH_4 effects. Such conditions can be met by using size classes of a single species or closely related species separated by test particles that may be rejected. Detailed understanding of preconditioning, particle modification, and ammonium effects must be used to insure that the parts of a particle spectra used to calculate \hat{F}_{ai} measure only the effects of passive selection. In addition, as with any regression analysis, one must be careful not to extrapolate too far beyond the data set to estimate \hat{F}_{ai} or F_{ad} or errors may result.

As more becomes known about filtering efficiency curves and how they vary, it may become possible to use F_{ei} curves with a limited number of F_{ai} values to calculate encounter rate. For example, if F_{ei} is found to be fixed for a given copepod species (α , β , d' , d^* are fixed), then measured values of F_{ad} can be used directly to compute \hat{F}_{ai} as

$$\hat{F}_{ai} = F_{ei}(F_{ad}) \quad \text{eq. j}$$

and encounter rates can be calculated from these \hat{F}_{ai} values. However, such a step is very premature at this point.

Electivity indices

Although we have attempted above to show that such indices as apparent filtering rates, capture rates, and encounter rates are useful indices to study particle selectivity, selectivity in the past has most often been reported and interpreted solely in terms of the Ivlev electivity index (Ivlev, 1961). Problems with this index arise from the assumptions required for its adaptation to grazing by copepods. The original equation of Ivlev (1961),

$$E = \frac{(r_i - p_i)}{(r_i + p_i)}, \quad \text{eq. k}$$

was designed for comparing gut content measurements with field analysis of food availability. Thus originally r_i , the percentage of a particular food in the total foodstuff in the animal's gut, was derived from gut content analysis, and p_i , the percentage of the particular food in the total food supply in the field, was derived from field estimates of food standing stocks. In the case of fish gut analysis, for example, both r_i and p_i can be independently measured, and it is assumed that during the period required for measurements to be made, the ingestion process has not affected the prey density (availability). When the index is applied to copepod grazing experiments using electronic counting methods, both terms are interdependent and the assumptions are not satisfied. The term r_i is easily calculated as the percentage distribution of the ingestion rate, or rather the capture rate since the electivity index is based on particle number:

$$r_i = \frac{C_{ri}}{\sum C_{ri}} \quad \text{eq. l}$$

Some choice must be made as to when (or how) to calculate p_i . We can use an exponential-mean-grazed base:

$$p_i^* = \frac{N_{it^*}}{\sum N_{it^*}}; \quad \text{eq. m}$$

a final-grazed base:

$$p_i' = \frac{N'_i}{\sum N'_i}; \quad \text{eq. n}$$

a final-control base:

$$p_i = \frac{N'_{ci}}{\sum N'_{ci}}; \quad \text{eq. o}$$

or a base utilizing an average of final-grazed and final-control values:

$$\bar{p}_i = \frac{\frac{N'_{ci}}{\sum N'_{ci}} + \frac{N'_i}{\sum N'_i}}{2}. \quad \text{eq. p}$$

Regardless of the choice of p_i , the terms N_{it^*} , N'_i , N'_{ci} are all in units of particle numbers per ml.

The electivity index can now be calculated, utilizing N_{it^*} as an example:

$$E = \frac{\frac{C_{ri}}{\sum C_{ri}} - \frac{N_{it^*}}{\sum N_{it^*}}}{\frac{C_{ri}}{\sum C_{ri}} + \frac{N_{it^*}}{\sum N_{it^*}}} = \frac{C_{ri} \sum N_{it^*} - N_{it^*} \sum C_{ri}}{C_{ri} \sum N_{it^*} + N_{it^*} \sum C_{ri}}. \quad \text{eq. 27 Table 1}$$

The relationship of electivity to ingestion (as capture rate) and apparent filtering rates (F_{ai}) can also be shown if we use N_{it^*} . By substituting for C_{ri} using equation 25, Table 1:

$$E = \frac{\frac{I_i}{\bar{v}_i 1440} \sum N_{it^*} - N_{it^*} \sum \frac{I_i}{\bar{v}_i 1440}}{\frac{I_i}{\bar{v}_i 1440} \sum N_{it^*} + N_{it^*} \sum \frac{I_i}{\bar{v}_i 1440}} \quad \text{eq. q}$$

Since, from equation 14 and 23 (Table 1),

$$I_i = F_{ai} (1440 V_{it^*}) = F_{ai} (1440 N_{it^*} \bar{v}_i),$$

we can substitute for I_i in eq. q:

$$E = \frac{[F_{ai} N_{it^*} \sum N_{it^*}] - [N_{it^*} \sum (F_{ai} N_{it^*})]}{[F_{ai} N_{it^*} \sum N_{it^*}] + [N_{it^*} \sum (F_{ai} N_{it^*})]} \quad \text{eq. r}$$

It is apparent that the mathematical equivalency between electivity, ingestion rate and filtering rate is very complex. The relationship of electivity to k_{gi} is somewhat simpler, but more difficult to derive. By substituting in eq. 27 for C_{ri} using the relationship

$$C_{ri} = k_{gi} (N_{it^*})^c$$

where c equals a constant ($c = \frac{v_o}{1440 A}$), then

$$E = \frac{[(k_{gi} N_{it^*})^c (\sum N_{it^*})] - [N_{it^*} \sum (k_{gi} N_{it^*})^c]}{[(k_{gi} N_{it^*})^c (\sum N_{it^*})] - [N_{it^*} \sum (k_{gi} N_{it^*})^c]} \quad \text{eq. s}$$

However, since c is a constant,

$$E = \frac{c N_{it^*} [k_{gi} \sum N_{it^*} - \sum k_{gi} N_{it^*}]}{c N_{it^*} [k_{gi} \sum N_{it^*} + \sum k_{gi} N_{it^*}]} \quad \text{eq. t}$$

which reduces to

$$E = \frac{k_{gi} \sum N_{it^*} - \sum k_{gi} N_{it^*}}{k_{gi} \sum N_{it^*} + \sum k_{gi} N_{it^*}} \quad \text{eq. u}$$

The equivalencies between R and C_{ri} , F_{ai} , and k_{gi} can only be derived if the exponential mean particle number (N_{it^*}) is used.

An additional set of problems, common to other percentage based indices, also affect the Ivlev electivity index. Jacobs (1974) has pointed out that E is sensitive not only to selectivity, but also to relative abundance of food types in the environment. The critical problem with percentage-based indices is that removal of particles from one size class (excluding cases of particle modification) always will increase the percentage composition (relative frequency) in other size classes. This can lead to serious errors. These errors can perhaps best be visualized if we compare overlays of actual number or volume

distributions with percentage distributions of grazed, control, and ration from which E is calculated (Figs. 4a,b,c). The results shown in Fig. 4 are from a hypothetical grazing experiment in which particle removal occurred only in size classes equal to or greater than the mode. Overlay of actual number or volume distributions from grazed and controls clearly show grazing only on the larger size classes (stippled area, Fig. 4a); however, percentage distributions calculated for these same data show a reduced area of particle removal occurring only above the modal size class, and a net increase in percent occurrence at the mode and at all smaller size classes. As will be discussed below, these percentage plots, when used to analyze data show features of apparent increase in small size classes that can easily be misinterpreted as particle production. It can also be seen that r_i is affected differently than p_i (Fig. 4c). These problems make E sensitive to particle abundance as well as to selectivity. Jacobs (1974) was able to show mathematically that the above problems could be solved by redefining the electivity index as:

$$D = \frac{r_i - p_i}{r_i + p_i - 2r_i p_i} \quad \text{eq. v}$$

Using the equivalences for r_i and p_i defined in equations l and m, respectively, Jacob's electivity can be defined in terms of C_{ri} and N_{it^*} as:

$$D = \frac{\frac{C_{ri}}{\sum C_{ri}} - \frac{N_{it^*}}{\sum N_{it^*}}}{\frac{C_{ri}}{\sum C_{ri}} + \frac{N_{it^*}}{\sum N_{it^*}} - 2\left(\frac{C_{ri}}{\sum C_{ri}}\right)\left(\frac{N_{it^*}}{\sum N_{it^*}}\right)} \quad \text{eq. 28, Table 1}$$

Although both formulations of Jacob's electivity index (eq. v and eq.

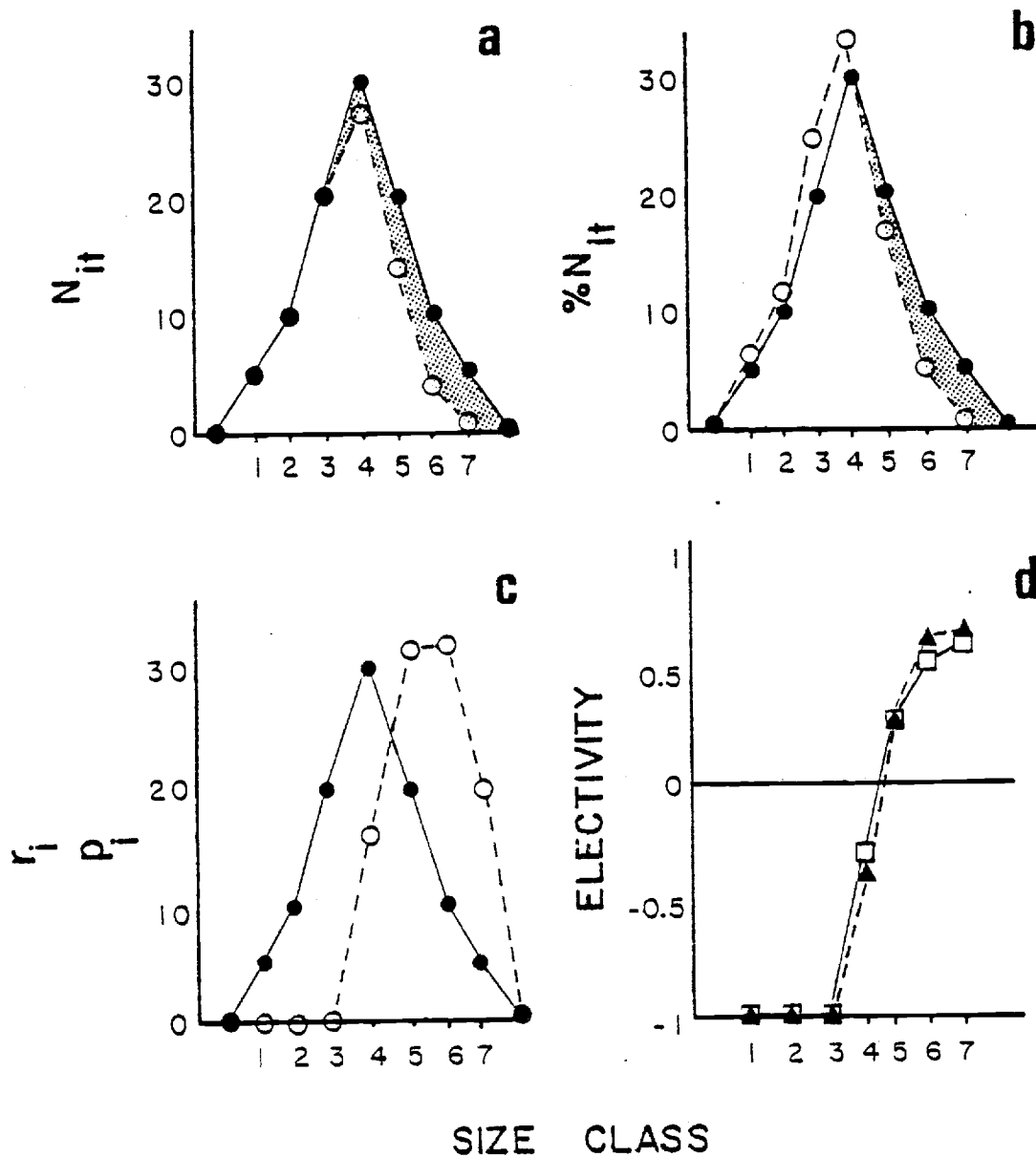


Fig. 4. Percentage based indices. Comparison of overlays of grazed (o) and control (●) (a) absolute number distributions (b) relative frequency distributions and (c) relative frequency distributions from control (●) and ration (o). Electivity indices are shown as overlays for Ivlev's formulation (□) and Jacobs' formulation (▲). Data are from a hypothetical experiment.

24) are free of the percentage problems illustrated in Fig. 4, the absolute values of Jacob's index are somewhat affected by the relative abundance of prey items as pointed out by Paloheimo (1979).

In an effort to solve these problems, Jacobs (1974) redefined electivity in terms of relative prey mortality rates. In contrast to gut content data where relative mortality rates can only be estimated (Jacobs, 1974), particle "mortality rates" in copepod grazing experiments are directly measured by k_{gi} . Thus, in mortality rate terms, electivity for grazing experiments can be expressed as mortality in a given size class relative to the mortality in all size classes:

$$E' = \frac{nk_{gi} - \sum k_{gi}}{nk_{gi} + \sum k_{gi}} = \frac{k_{gi} - \frac{\sum k_{gi}}{n}}{k_{gi} + \frac{\sum k_{gi}}{n}} \quad \text{eq. w}$$

where n equals the number of size classes. This definition of electivity differs from that derived in equation 27 in that it does not have a weighting factor for particle number. Although E' is much simpler in form and derivation than E , there is still a problem of frequency interference illustrated in Fig. 4 above. Using a logic similar to Jacobs' (1974) this problem can be removed by subtracting out the contribution of the given size class from the summation term and using the average rather than the total mortality for those size classes as:

$$D' = \frac{k_{gi} - \frac{(\sum_{i=1}^n k_{gi}) - k_{gi}}{n-1}}{k_{gi} + \frac{(\sum_{i=1}^n k_{gi}) - k_{gi}}{n-1}} \quad \text{eq. x}$$

which reduces to

$$D' = \frac{nk_{gi} - \sum_{i=1}^n k_{gi}}{nk_{gi} + \sum_{i=1}^n k_{gi} - 2k_{gi}} = \frac{nk_{gi} - \sum_{i=1}^n k_{gi}}{[(n-2)k_{gi}] + [\sum_{i=1}^n k_{gi}]} \quad \text{eq. y}$$

D' is very analogous in form to Jacobs' electivity D. As with Jacobs' electivity, this formulation removes the effect of enhancing frequencies of other size classes by removal of particles from a given size class. It is also free from any effects of abundance objected to by Palaheimo (1979). From a comparison of overlap of electivity indices D and E (Fig. 4d), it can be seen that the basic effect of Jacobs' electivity is to make intermediate sized values more negative or positive. The difference between E and D will become important when a few size classes dominate ingestion. E will approach the results of D whenever ingestion occurs over many size classes; i.e., when n becomes very large. D' can be used to compare selectivity on prey of different relative abundances. However, because of the complexity of the D' equation, it is even more difficult to relate electivity to ingestion, apparent filtering rate and capture rate indices. In addition, because the variance associated with individual estimates of k_{gi} is statistically dependent on the abundance of the i^{th} size class, errors in $\sum k_{gi}$ can be expected to be large unless care is taken to control variance in k_{gi} . These errors will further confound the ambiguities involved in assigning relevance to dimensionless numbers such as E' and D'. As a result, indices such as filtering rate and k_{gi} are probably better measures of selection.

Experimental Intercomparison of Grazing Indices

The final evaluation of any grazing index must rest with its performance with data from real grazing experiments. In an effort to

evaluate the indices, the algorithm has been run on over 250 sets of grazing experiments. From this body of data, four very different grazing situations have been chosen to illustrate properties of the various indices. The four cases are (1) weakly-selective grazing by juvenile Neomysis sp. on the single celled diatom Thalassiosira fluviatilis, (2) selective grazing by the copepod Acartia clausi on the same T. fluviatilis; (3) grazing by A. clausi on a two peaked mix of food and plastic spheres in which sphere rejection occurs; and (4) grazing by A. clausi on the chain-forming diatom Thalassiosira aestivalis, in which particle modification occurs. It is the intent here to evaluate the indices under conditions eliciting increasingly complex grazing behavior starting from weakly-selective feeding and progressing to "passive" selection (Donaghay, 1979), active selection involving post capture rejection (Donaghay and Small, 1979b; Donaghay, 1979) and finally particle modification (O'Connors, et al., 1975).

Cases (1) and (2) (the mysid and single food A. clausi data) are from 24 hour grazing experiments on Thalassiosira fluviatilis grown and grazed in high light ($200 \mu\text{e m}^{-2} \text{sec}^{-1}$). In these experiments, all animals were preconditioned on T. fluviatilis for at least two days prior to the start of the experiment. These experiments were performed in specially built 2 l flasks that were gently stirred by a vertically falling plunger-stirrer once every five minutes. The rejection data (Case 3) are from two replicate 24-hour grazing experiments with 50 Acartia clausi females fed a particle mix of 11 μm T. fluviatilis and 19 μm inert plastic spheres (Donaghay and Small, 1979b). Animals were preconditioned first on 11 μm T. fluviatilis for five days prior to the

experiment, then on 11 μm T. fluviatilis plus 19 μm spheres for 12 hours. The particle modification data (Case 4) is from an experiment where A. clausi grazed for 24 hours on the chain forming diatom T. aestivalis. These copepods were starved in filtered sea water for 12 hours prior to the experiment.

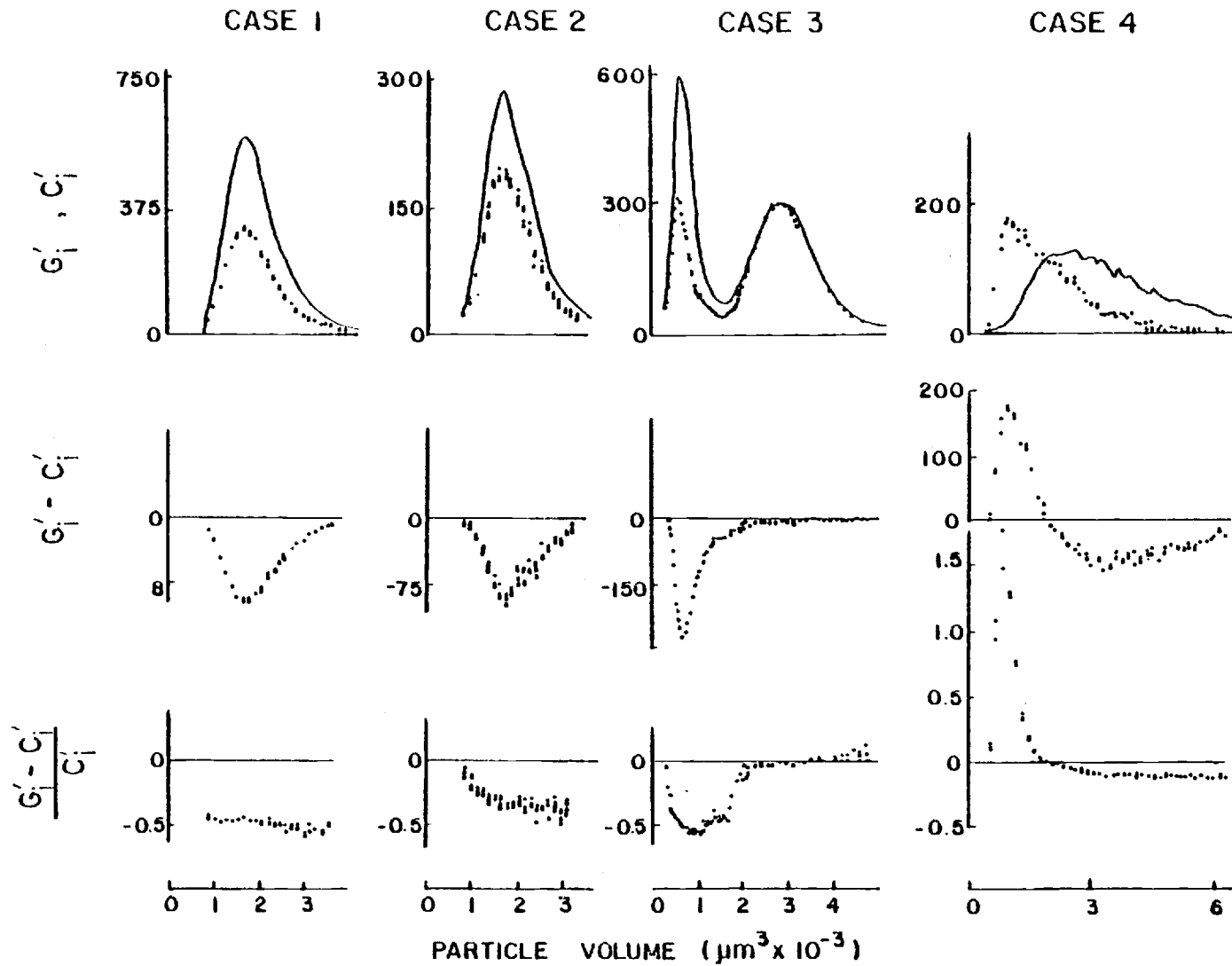
The grazing indices will be evaluated in 6 groups of similar indices: (1) 24 hour net effect indices (equations 3, 4, 5, 6); (2) growth rate indices (equations 7, 8, 9); (3) ingestion rate indices (equations 10, 11); (4) filtering indices (equations 16, 17, 18, 19, 20, 21, 22); (5) capture indices (equations 23, 24, 25, 26); and (6) electivity indices (equations 27, 28). The filtering rate indices will be further subdivided to examine the effects of method of calculation and data plotting format on the indices.

(1) Twenty-four hour net effect indices (Equations 3, 4, 5, 6)

In the case of the slightly-selective grazer (Case 1), grazed and control distributions are similar in shape and differ mainly in magnitude (Fig. 5). This results in a net effect index ($G'-C'$) that is an inverted mimic of the particle size distribution. The net removal pressure index ($\frac{G'-C'}{C'}$) is strongly negative at all size classes. It increases slowly and apparently linearly with particle size.

The above pattern is in contrast to that formed when Acartia clausi feeds on a similar food suspension (Fig. 5, Case 2). With A. clausi as the grazer, the grazed distribution is displaced to the left (toward smaller particle sizes) relative to the control. The net effect index ($G'-C'$) is displaced to the right (toward larger particle sizes), re-

Fig. 5. The net effect indices are shown for the four cases as overlays of (a) 24 hour grazed (●) and controls (—), (b) net grazing effect, and (c) removal pressure index. The four cases are (1) Neomysis sp. feeding on Thalassiosira fluviatilis (2 replicates); (2) Acartia clausi feeding on T. fluviatilis (4 replicates); (3) A. clausi feeding on 15 μm T. fluviatilis plus 19 μm plastic spheres (2 replicates) and (4) A. clausi feeding on the chain forming diatom Thalassiosira aestivalis (2 replicates).



flecting higher grazing rates on the larger cells. The net removal pressure index ($\frac{G'-C'}{C'}$) becomes increasingly negative starting at zero at the smallest particle size class. This index rapidly increases to a maximum negative value at the mode of the particle size distribution, then remains constant at larger particle size classes. In Case 2 grazing pressure can be formulated as a hyperbolic (or rectilinearly) decreasing function of mean particle size. These patterns are typically observed when A. clausi are fed uni-algal single-celled diatom food suspensions.

When post capture rejection of particles is elicited from a selective grazer such as A. clausi (Fig. 5, Case 3), the distribution of food particles is reduced, but the non-food (spheres) peaks often are not reduced. Reduction in non-food peaks occurs only when those peaks overlap food peaks. The distributions tend to be qualitatively similar in the grazed (G'_1) and control (C'_1) for the food peak, with less shifting of the peak than was observed in the single-food case (Case 2). The ($G'-C'$) index tends to mirror the C' food peak, but rapidly falls to zero in the size classes dominated by spheres. The net grazing effect is very small (near zero) in the sphere dominated size classes. The removal pressure index is U shaped rather than hyperbolic as in Case 2.

In each of the first three cases, the net removal pressure index can be interpreted in terms of feeding mechanisms (Donaghay, 1979; Donaghay, in prep.). However, when a chain-forming diatom is the food (Case 4), this is no longer true (Fig. 5, Case 4). The grazed distribution is displaced sharply to the left (smaller side) of the control distribution. Whenever such a displacement occurs, particle modifica-

tion must be occurring. As discussed in O'Connors et al. (1975), such distributions are the result of removal of particles from large size classes by both breakage and ingestion of chains, and the addition of particles to smaller size classes by breakage of the large particles. The $G'-C'$ index and $\frac{G'-C'}{C'}$ index reflect this effect by negative values in large particle size classes and very large positive values in small size classes. This often results in the indices having a sinusoidal form. Experiments in which particle modification occurs cannot be interpreted in terms of selective behavior (Donaghay and Small, 1979a).

Growth rate indices (Equations 7, 8, 9)

The shape and statistical variability of the particle growth rate indices control the nature and quality of the other indices. The control growth rates (k_{ci}) for both the mysid and Acartia single-food cases (Cases 1 and 2) show one of several typical k_{ci} patterns: high values at the smallest size classes, then decreasing toward larger particle sizes (Fig. 6). These shapes are typical of rapidly growing cultures under laboratory conditions. However, a variety of other shapes are also observed depending on environmental conditions. The k_{ci} values can be interpreted as the size class specific growth rates of cells in each size class unless plastic spheres or any other non-growing particles are present in a size class (Case 3), or when chain formers are used (Case 4). In Case 3, the k_{ci} curve is of similar form to Cases 1 and 2 in the smaller size classes, but as the sphere peak is approached, an increasing contribution of spheres results in an apparent dilution of actual cell growth. In all particle size classes where spheres alone are

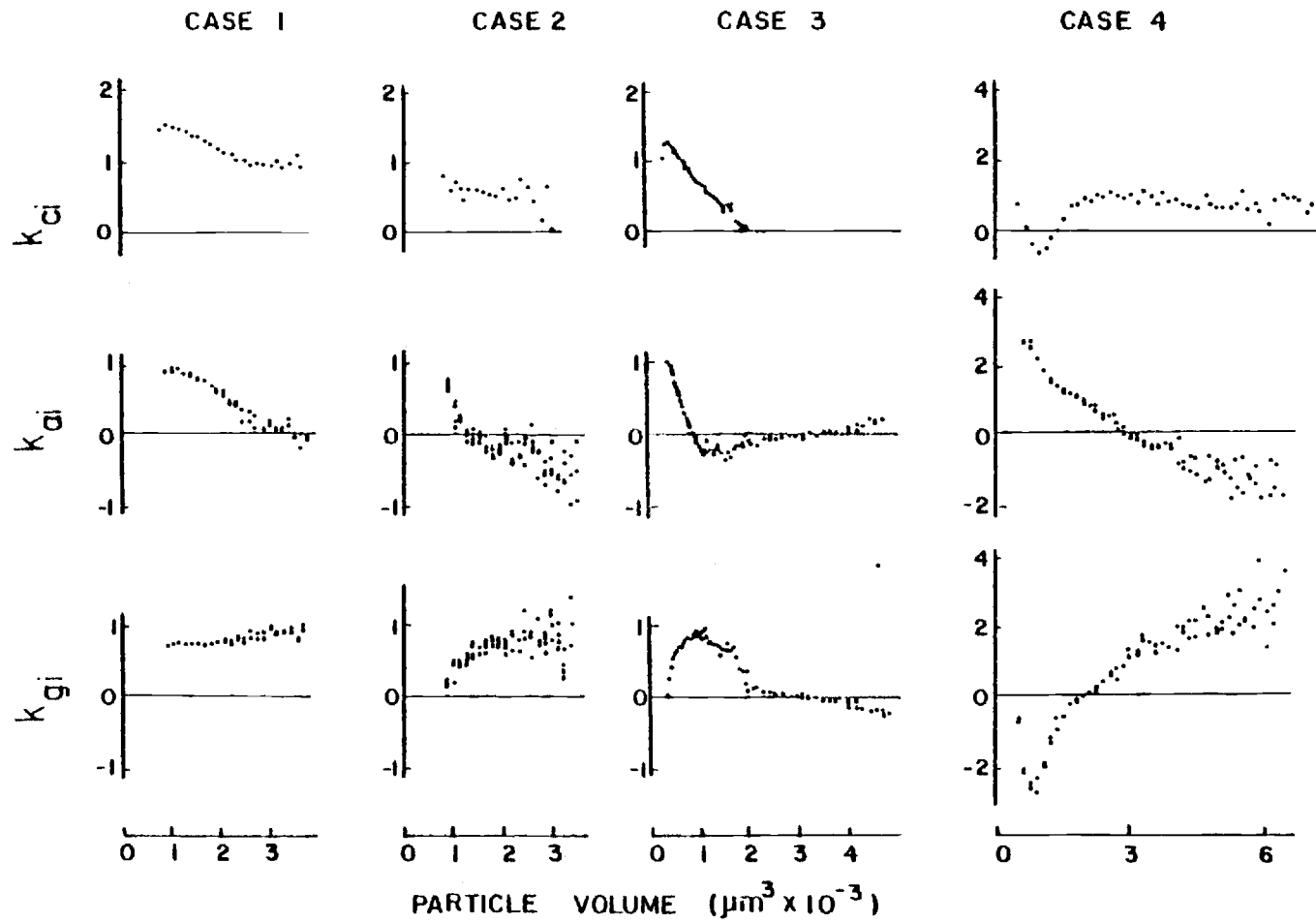


Fig. 6. The growth rate indices k_{ci} (a), k_{ai} (b) and k_{gi} (c) are plotted for the same four cases as in Fig. 5.

present, k_{ci} values are zero. Any non-zero k_{ci} values in the sphere size classes are clear evidence of particle counting problems such as coincidence, counting interference or sphere clumping. When k_{ci} values of chain-formers are examined (Case 4) a variety of distributions may be observed. Often there will be negative values at small size classes, which reflect a tendency for increasing chain length with time in control vessels (see Donaghay and Small, 1979a). Otherwise the distribution often appear similar in shape to the k_{ci} distribution of non-chain formers.

In contrast to the normally positive values of k_{ci} , k_{ai} values can be, and often are, negative (Fig. 6). With a weakly-selective grazer (Case 1), k_{ai} distributions will have nearly identical shapes to those of k_{ci} , but will have a much lower mean value. The k_{ai} distributions can have a slightly steeper negative slope with increasing particle size. These features will be reflected in large positive k_{gi} that might increase with increasing particle size. With a simple selective grazer (Case 2), the shape of k_{ai} will be skewed to the left (toward smaller particle sizes) relative to k_{ci} . The k_{gi} term increases with particle size, but the increase might be linear, or curvilinear as shown in Fig. 6.

When multiple particle peaks are present, more complex features are often observed in k_{ai} and k_{gi} . In Case 3, k_{ai} for the food peak decreases much more rapidly than k_{ci} and then, also in contrast to k_{ci} , goes slightly negative then returns to zero. The values of k_{ai} greater than zero in the largest size classes are probably not really greater than zero due to low counts in those size classes. The k_{gi} distribution

in Case 3 shows a clearly parabolic form throughout the food peak, then remains more or less near zero throughout the sphere-dominated size range. Since in both Cases 2 and 3 the food peak is composed of the same Thalassiosira fluviatilis, the differences in the shapes of the k_{gi} distributions between these two cases illustrates the way in which non-food particles can alter the grazing pressure in given particle size ranges.

In each of the first three cases k_{ci} can be used to predict changes in the control distributions, k_{ai} can be used to predict changes in the grazed distributions, and k_{gi} can be used as a measure of the size-class-specific grazing pressure. Further, in size classes without spheres, k_{ci} is an estimate of cell-size-specific growth rates as indicated before, and k_{gi} is an estimate of grazer-induced-particle mortality rates. However, for size classes containing mixtures of spheres and cells, these interpretations are no longer strictly valid. Although k_{gi} is still an accurate estimator of cell-size-specific grazer induced particle mortality rate (as long as spheres are not ingested), k_{ci} is an underestimation of the true cellular growth rate.

In the case of particle modification (Case 4), no inferences about cell growth rates or grazing pressure (k_{gi}) can be made from plots of k_{ci} , k_{ai} and k_{gi} . Curves of apparent growth rate are almost always sharply sloping curves with very large positive values at small particle sizes and very large negative values at large particle sizes. Values of k_{ai} often approach zero at the largest particle size classes. The k_{gi} curve is always a very sharply increasing function of particle size, and almost always has a strongly negative component at small particle sizes.

The degree of negativity in the small particle size range depends upon how much the injection of particles into small size classes by chain breakage overwhelms ingestion in those same size classes.

Ingestion indices. (Equations 10, 11)

Ingestion rate and grazer flux loss indices are plotted as overlays in Fig. 7. Ingestion rate will normally have the same shape as grazer flux loss, although the magnitude of the two curves will differ greatly. Ingestion rate and grazer flux loss will differ between replicates only when animal numbers vary between vessels or when animal numbers are poorly estimated due to mortality. In Cases 1, 2 and 3, the ingestion rate indices show where in the food spectrum the copepod gets its ration. When particle modification occurs (Case 4), the ingestion indices cannot be interpreted in terms of ration location. With particle modification, ingestion will be negative at small sizes. However, in all four cases, the integrated area under the ingestion curve (algebraic sum of both positive and negative sections) is an accurate estimate of the total amount of ingestion.

Filtering rate indices (Equations 15 to 22)

The filtering rate indices will be considered in two subgroups:

(1) F_{ai} and those indices based on F_{max} calculations (Equations 16, 18, 21, 22), and (2) F_{ai} and those indices based on logarithmic regression calculations (Equations 15, 16, 17, 19, 20). The F_{max} based indices will be considered for all four cases, but the log-regression based calculations will only be considered for those cases where the necessary

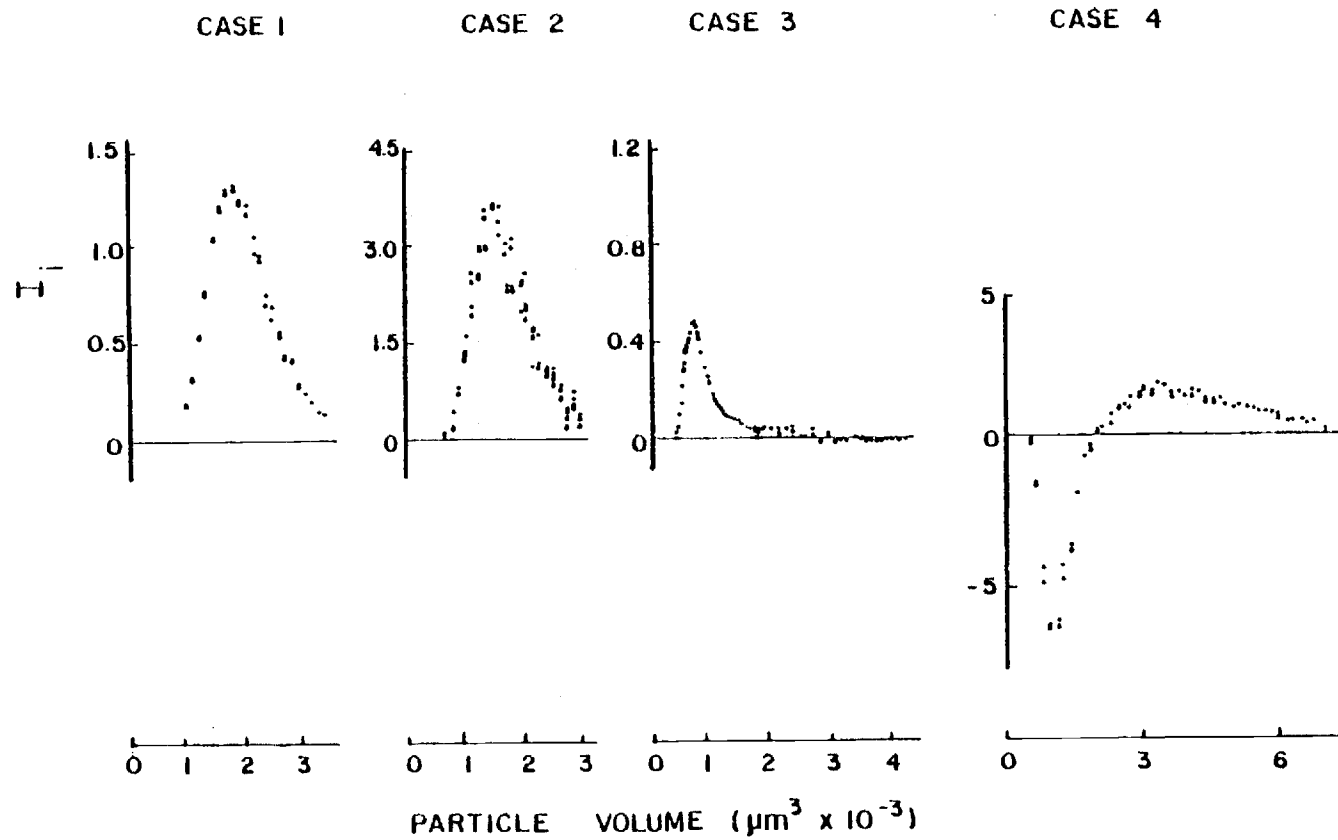


Fig. 7. Ingestion rate indices (I_i) are plotted for the same four cases as in Fig. 5.

assumptions are met (Cases 2 and 3).

Within the particle size range measured, the mysid apparent filtering rate curve (F_{ai} , Case 1, Fig. 8) is basically flat up to the particle size class mode, then slowly increases with particle size. Because the maximum intersetule pore size for the mysid is probably much smaller than the smallest size class, F_{max} has been arbitrarily based on the flat segment of the F_{ai} curve. For Acartia clausi feeding on the same Thalossiosira fluviatilis (Case 2) F_{ai} is non-linear over most particle size classes. From the smallest size classes up through the modal size class, F_{ai} rapidly increases with size. At particle sizes much larger than the mode, F_{ai} levels off and allows a reasonably straightforward estimation of F_{max} .

The filtering curves observed in rejection experiments (Case 3) usually have well developed F_{max} regions and, compared to Case 2, a much steeper region of increasing filtering rate with increasing particle size. In Case 3, F_{max} is easily and very precisely definable over a number of particle sizes. As a result, calculation of the other filtering indices and the rejection indices can be made with considerable precision. In more complex rejection experiments (such as the three-peak experiments described by Donaghay and Small (1979b), apparent filtration rate curves can be very complex functions of particle size.

Apparent filtering rates in experiments in which particle modification occurs (Case 4) are nearly meaningless or at least uninterpretable in terms of filtering mechanisms (Fig. 8). Under such conditions, F_{ai} curves have sharply increasing segments, very high F_{max} values, and, sometimes, strongly negative values at small size classes. The positive

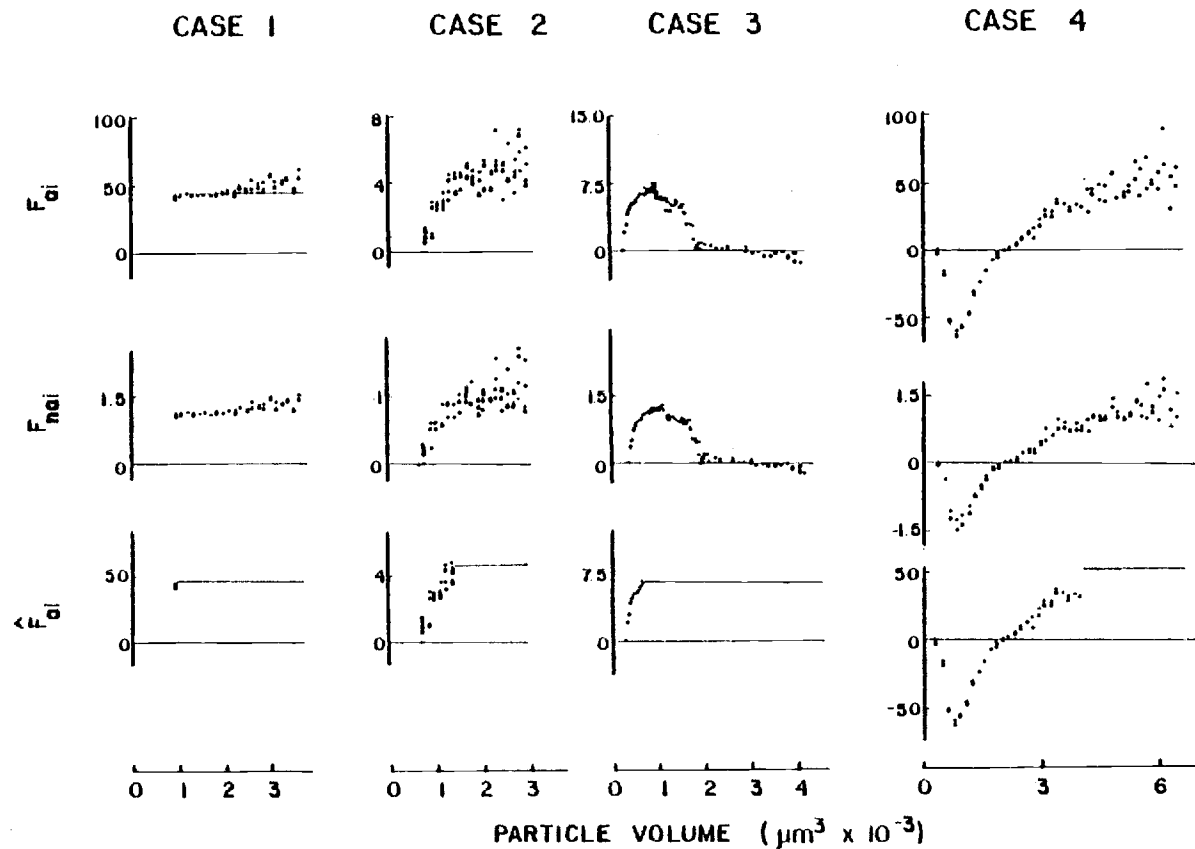


Fig. 8. The F_{\max} based filtration rate indices are plotted for the same four cases as in Fig. 5 as (a) apparent filtration rate (F_{ai}) with F_{\max} defined by a thin line and arrows denoting w_1 and w_2 , (b) normalized apparent filtering rate ($F_{nai} = F_{ai}/F_{\max}$) and (c) expected apparent filtering rate based on F_{\max} (\hat{F}_{ai} [F_{\max} based]).

segment of the F_{ai} curve in Case 4 is very similar in shape to Case 2; however, the F_{max} values are much larger in Case 4 than normally observed for Acartia. Regardless of whether such negative values are observed, filtering curves with particle modification present have no functional relationship to the animals filter structure.

In all four cases, apparent filtering rate and normalized apparent filtering rate (F_{nai}) are very similar in shape and response to each other and to both k_{gi} and the grazing pressure index ($[G'-C']/C'$). As careful examination of Fig. 8 will indicate, the F_{max} normalized filtering curves all have about the same magnitude. As discussed earlier, this facilitates intercomparison of filter curve shapes over a variety of conditions.

For Cases 2 and 3, it is possible to calculate regression based filtering rate indices since the necessary assumptions are met. When F_{ai} values are plotted vs. the natural logarithm of particle diameter (rather than vs. particle volume), the shape of the F_{ai} curve changes somewhat. In Case 2, F_{ai} rapidly increases from zero value at about 10 μm to a maximum value at 14 μm . Above 14 μm variability increases dramatically, but F_{ai} on the average is constant. The region between 10 and 14 μm is sufficiently log-linear so that log-regression analysis could be used to estimate α' , d' , α and F_{a14} based on that segment. The values of F_{ad} where $d = 14 \mu\text{m}$ (the maximum intersetule pore size) were not significantly different from the average of F_{ai} values above 14 μm . The inflection point of the F_{ai} curve, d^* , is thus consistent with that expected from the morphology of the filtering appendages. However, the value of d' estimated from the regression analysis (10.4 μm) is much

larger than the minimum interstetule pore size, 3 μm (Table 2). Such alteration of d' but not d^* , is in agreement with the drop filter model (Donaghay, in prep.).

In Case 3, the compression of the large size classes by the conversion of particle volume to $\ln(d)$ is much more obvious. The F_{ai} curve also shows a clear bending over at approximately 12 μm . As a result, only the segment below 12 μm was used in the regression analysis. When the resulting regression based values of \hat{F}_{ai} are plotted over the F_{ai} curve (Fig. 9, Case 3), there is a slight bend noticeable in the F_{ai} curve at the modal particle size class of T. fluviatilis. The origin of this slight curvilinearity, if real, is unknown. Based on the deviations above 12 μm of F_{ai} from \hat{F}_{ai} it is clear that the presence of spheres in the larger size classes resulted in considerable reduction in F_{ai} in all particle size classes above the modal size of T. fluviatilis. Such a reduction is not present in the F_{max} based estimate of \hat{F}_{ai} discussed in Fig. 8 (Case 3). The use of F_{a14} in the calculation of filtering efficiency results in an F_{ei} curve that has a maximum at values considerably less than 1. In order for these maximum values to approach 1, maximum interstetule pore size would have to be reduced from 14 μm to 12 μm . This is in sharp contrast to the F_{ei} calculated in Case 2 where the maximum values of F_{ei} varied around a mean of 1. The depression of maximum F_{ei} below 1 in Case 3 clearly demonstrates that the observed d^* is different from that expected based on maximum interstetule pore size and different from that measured in Case 2. The values of d' and α , however, are not significantly different in the two cases. The observed difference in d^* , but not d' and α are strong evidence for the combing

Fig. 9. Regression based filtration rate indices for Cases 2 and 3 are plotted as (a) apparent filtering rate (F_{ai}) overlaid by \hat{F}_{ai} (regression based) and (b) apparent filtering efficiency (F_{ei}). Note that F_{ai} , \hat{F}_{ai} and F_{ei} are plotted versus the natural logarithm of equivalent particle diameter ($\ln d$) rather than versus particle volume as in Figures 5, 6, 7, 8, 10, 11. Values of \hat{F}_{ai} are indicated by the line in part (a). The solid segment represents the area of the F_{ai} data used in the regression; the dashed line represents the extrapolated segments of \hat{F}_{ai} .

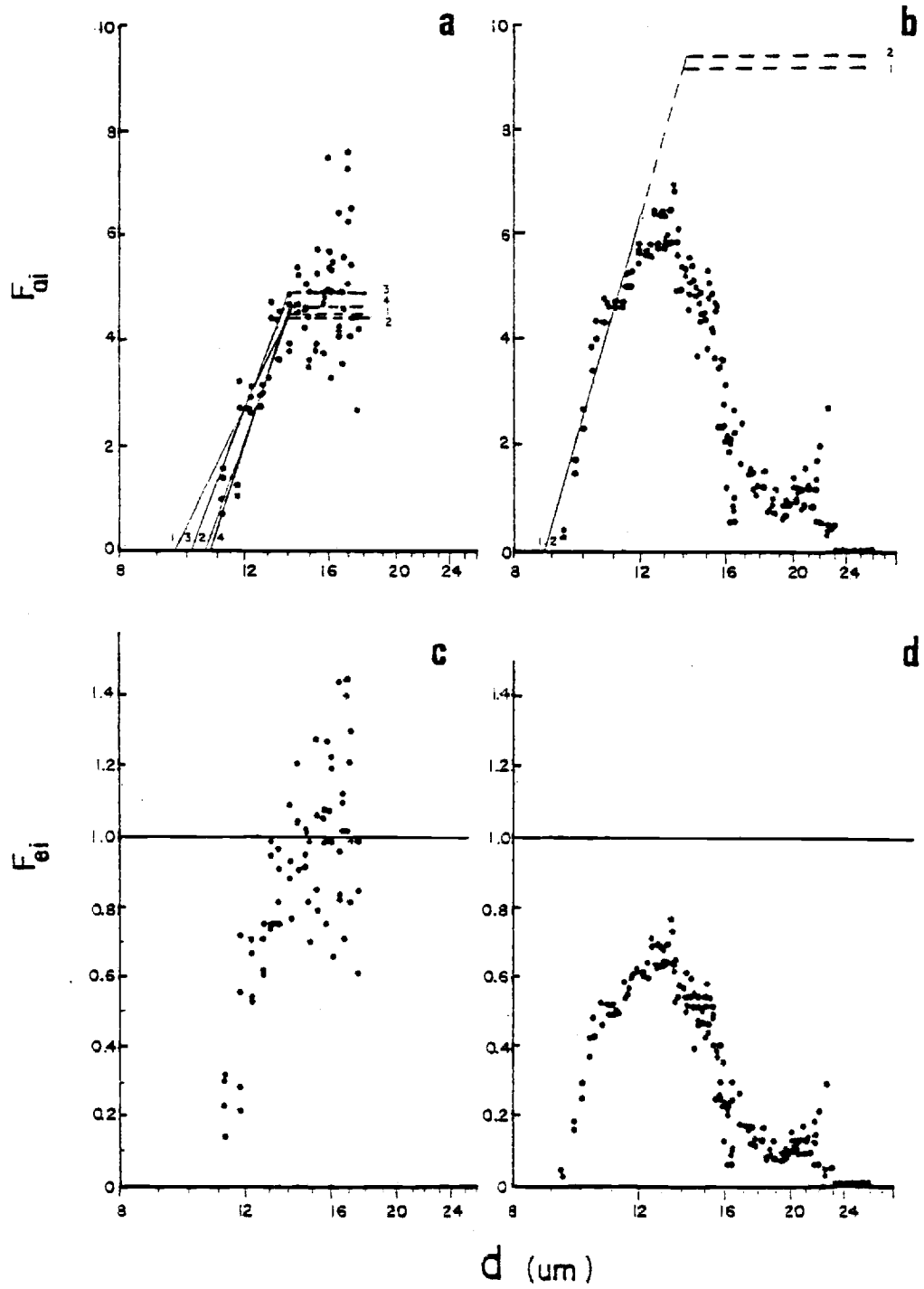


TABLE 2. REGRESSION ANALYSIS OF F_{ai} VALUES FOR CASE 2 AND CASE 3.

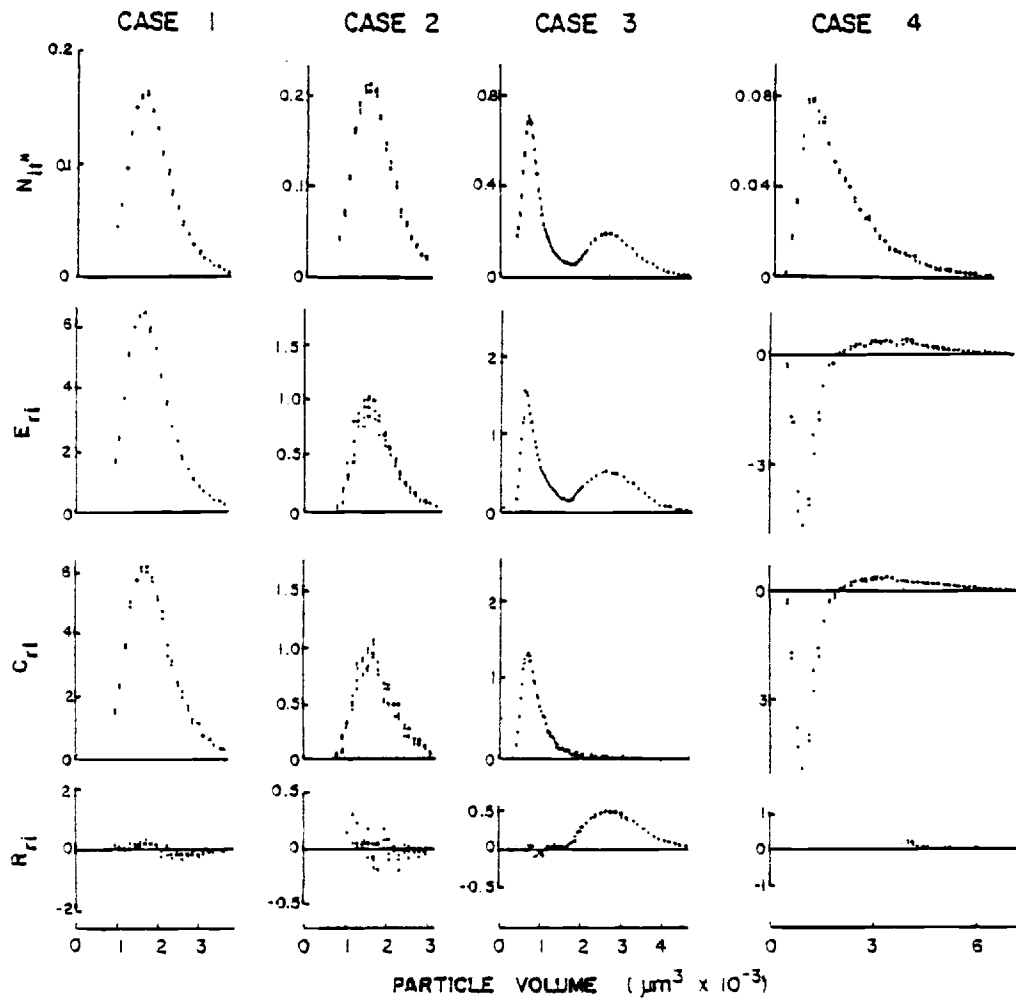
CASE	REP	REGRESSION VALUES			CALCULATED VALUES			
		α'	F'_{ai}	r^2	F_{a14}	mean \pm 1 sd $i > 14\mu\text{m}$	d'	α
Case 2	1	16.85	-40.04	.9060	4.10	5.32 \pm 1.19	10.76	3.17
	2	11.75	-26.59	.6817	4.41	4.65 \pm 0.96	9.61	2.53
	3	15.70	-36.52	.8591	4.90	4.78 \pm 0.47	10.24	3.28
	4	18.54	-44.32	.8851	4.61	4.29 \pm 1.48	10.92	4.32
	mean	15.71	-36.87	-	4.50	4.76	10.38	3.33
Case 3	1	19.13	-41.34	.8360	9.14	-	8.67	2.09
	2	20.49	-44.69	.9540	9.39	-	8.86	2.18
	mean	19.81	-43.02	-	9.27	-	8.77	2.14

rejection of the spheres and thus for the combing model (Donaghay, in prep.). The ability to clearly detect changes in d^* is a major advantage to using the regression based \hat{F}_{ai} method over the F_{max} based method. However, such distinctions will be only as good as measurements of minimum and maximum interstule pore size. In addition, the confidence with which one calculates \hat{F}_{ai} is critically dependent on having a clearly log-linear F_{ai} curve over a reasonable number of particle size classes.

Capture Rate Indices (Equations 23, 24, 25; 26)

Using the two different estimates of \hat{F}_{ai} calculated above, the capture indices can now be calculated. As with the filtration rate indices, we shall first consider the use of F_{max} based calculations of the capture indices for all cases, then we shall consider the regression based calculations for Cases 2 and 3. Since encounter, capture and rejection all occur on a particle number rather than a particle volume basis, particle number distributions (N_{it^*}) have been plotted above the rejection indices (Fig. 10). With a non-selective grazer (Case 1) encounter rate and capture rate curves are identical in shape, but the magnitude of each the peaks is slightly different (Fig. 10). The magnitude is dependent (here and in the other cases as well) on total particle concentration, because of the well established dependence of apparent filtering rate at any given particle size on total particle concentration (Frost 1972, 1977; Donaghay, 1978). Both E_{ri} and C_{ri} peaks are slightly shifted in position relative to the particle size distribution. The rejection rate curve in Case 1 is a reasonably flat line with a mean

Fig. 10. F_{\max} based capture indices are plotted for the same four cases shown in Fig. 5 as (a) exponential mean particle number (N_{it^*}), (b) encounter rate (E_{ri}), (c) capture rate (C_{ri}), and (d) rejection rate (R_{ri}). These are all plotted versus linear particle volume size class. As a result, areas under the curves are proportional to particle number (a) or the rate measured (b, c, d); summation of areas under the curves are equal to total encounter rate (ΣE_{ri}), total capture rate (ΣC_{ri}), and total rejection rate (ΣR_{ri}).



of zero and small variance. For a selective grazer (Case 2) the encounter rate and capture rate curves are similar in shape to the particle number distribution except for the fact that (1) they are skewed toward larger sizes, and 2) there is an increase in the modal particle sizes of the C_{ri} and E_{ri} curves, relative to the modal particle size of the N_{it^*} curve. The amount of skewness and the shift to larger particle sizes are direct functions of the steepness of the increasing segment of the F_{ai} curve. Again, as in Case 1, rejection rate is variable but on the average near zero.

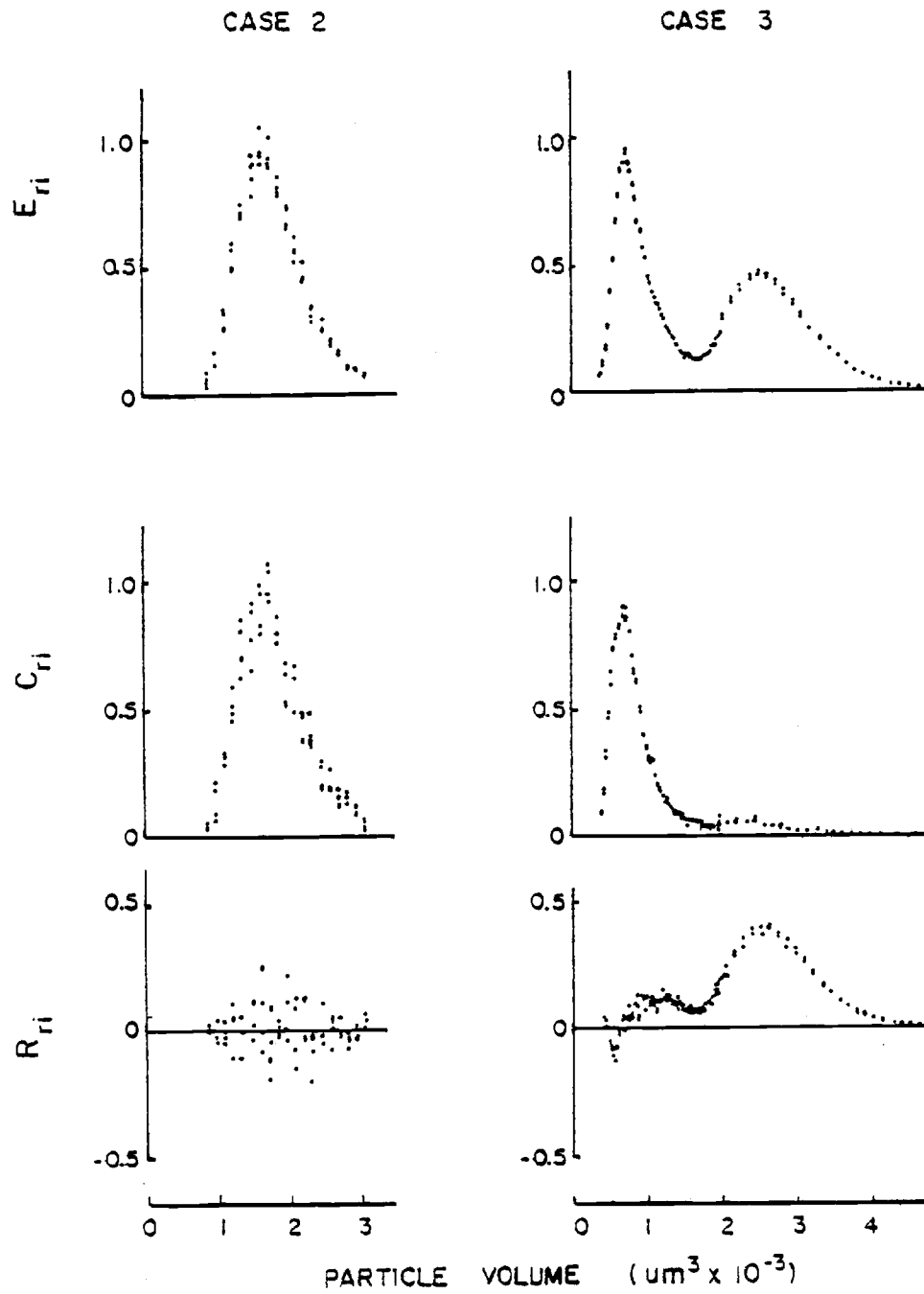
In Case 3, the patterns of the capture indices are unique (Fig. 10). The encounter rate shows a higher relative proportion of plastic spheres (relative to Thalassiosira fluviatilis cells) than would be expected from the cell and sphere number distributions. This is the result of the higher expected filtering rates on the spheres. The T. fluviatilis encounter rate peak is somewhat skewed to larger sizes, as was observed in Case 2; however, the shift is smaller in Case 3 because of the increased width of the F_{max} section of the filtering curve in Case 3 versus Case 2. The capture rate is radically depressed for spheres in Case 3 (Fig. 10). If the rate at which a copepod makes an error (ingests a plastic sphere) is as low as reported by Donaghay (1979) (1 in 200 events) then the number of spheres ingested compared to food particles should be so low that the measured capture rate in the large size classes should not be significantly different from zero (within our limits of detection). The rejection rate plot, in contrast to the near zero values observed in Cases 1 and 2, now shows a peak in the sphere-dominated size classes as expected. This peak is very simi-

lar in shape to the original sphere number distribution and the encounter rate peak. Some rejection may also occur in the large size classes of the T. fluviatilis peak where there is size overlap of spheres and T. fluviatilis. The mode of the sphere rejection peak is not skewed or shifted because it is calculated based on a constant apparent filtering rate in those large size classes.

A slightly different pattern of rejection emerges when the indices are based on regression determined values of \hat{F}_{ai} (Fig. 11). These differences are almost imperceptible when no rejection is occurring (Case 2, Fig. 11). The only difference is that the scatter around the zero line for R_{ri} extends below the modal particle size class (w_i) to include all particle sizes in Fig. 11, but not in Fig. 10. However, in Case 3, the changes are much more dramatic. Because \hat{F}_{ai} continues to increase at particle size classes larger than the T. fluviatilis mode, the encounter rate for these particles, particularly the plastic spheres, is much higher. Since the estimate of capture rate is unaffected by changes in \hat{F}_{ai} , the rejection rate is also much higher in the sphere dominated size classes (compare R_{ri} for Case 3 in Fig. 10 and 11). This higher R_{ri} is completely a function of the difference between F_{max} (used in calculating E_{ri} in Fig. 10) and F_{ai4} (used in calculating E_{ri} in Fig. 11). A second interesting difference between the two methods is that the regression based R_{ri} shows some rejection occurring on the upper side of the T. fluviatilis peak. Such rejection is not apparent in the F_{max} based R_{ri} .

There is a small secondary feature of the regression based calculation that does not appear in the F_{max} calculations and needs to be

Fig. 11. Regression based capture indices plotted for Case 2 and 3 as (a) exponential mean particle number (N_{it^*}), (b) encounter rate (E_{ri}) (c) capture rate (C_{ri}) and (d) rejection rate (R_{ri}). Although the \hat{F}_{ai} calculations are based on the log regression analysis shown in Fig. 9, N_{it^*} , E_{ri} , C_{ri} and R_{ri} are all plotted versus mean particle volume on a linear scale. Plots are in the same units as in Fig. 10 and are directly comparable.



considered. The small peak of negative R_{ri} observed at small particle sizes is the result of the small inflection in the F_{ai} curve at these sizes mentioned earlier. Any such non-linearity will appear in regression based R_{ri} curves, but will not be present in F_{max} based R_{ri} curves. The error involved here is small and, based on \hat{F}_{ai} data from a variety of other experiments, is probably not real.

Electivity indices (Equations 27, 28)

The electivity indices show different patterns for each of the four cases (Fig. 12). However, the differences between Ivlev's and Jacobs electivity are very small for any one case. Such small differences between E and D are the result of the large numbers of size classes in the particle counting data and the fact that selectivity patterns are spread over a large number of size classes.

In the first three cases, the electivity indices (Fig. 12) have shapes very similar to the filtering rate indices (F_{ai} and F_{ei} , Fig. 9). However, unlike F_{ai} or R_{ei} , the electivity indices are now dimensionless and the zero line has been shifted upward. The electivity indices thus present no information not already available from the filtration rate indices. A careful comparison of the electivity with the rejection indices indicates that the electivity indices can actually cause a misrepresentation of patterns of selectivity. Positive values of electivity are usually considered to be evidence of preference while negative values are evidence of rejection. A careful comparison of electivity (Fig. 12) and rejection rate (Fig. 11) for Case 3 shows that positive values in electivity occur in size classes where rejection is

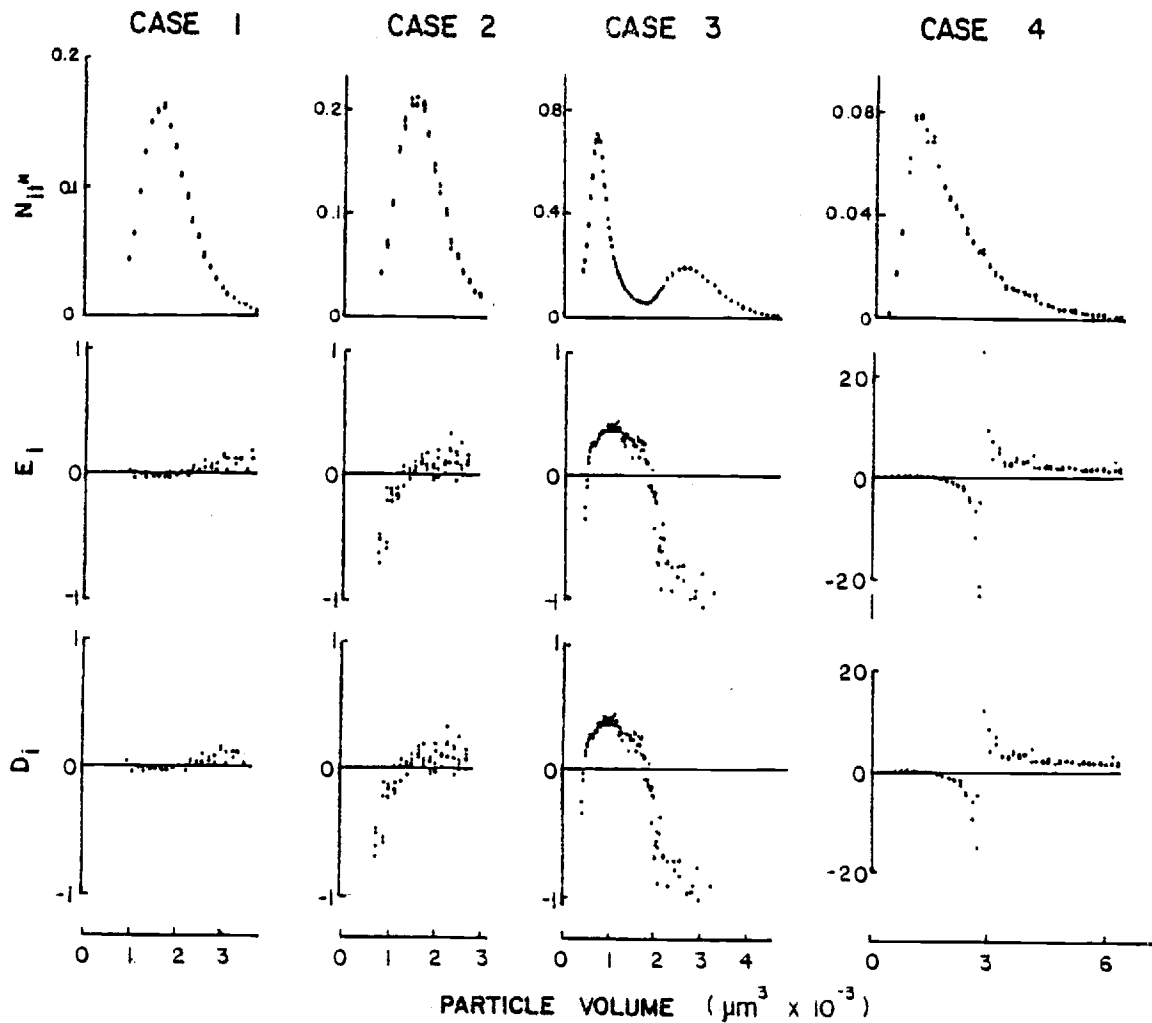


Fig. 12. Electivity indices are plotted below (a) exponential mean particle numbers ($N_{i,t}^m$) as (b) Ivlev electivity (E_i) and (c) Jacobs' electivity (D_i). These indices are also plotted for all four cases shown in Fig. 5. The indices are plotted versus mean particle volume on linear scale.

actually occurring.

When particle modification occurs (Case 4, Fig. 12), a very unusual distortion of the electivity indices results. With particle modification, both electivity indices show a pattern of decreasing electivity with increasing particle size up to a point where the index goes from a maximum negative value to a maximum positive value, then steadily decreases back to zero. This flip has nothing to do with selectivity patterns. Rather, it is the direct result of the fact that, because of particle modification, C_{ri} values are negative at small size classes and positive at large size classes. When C_{ri} is negative, equation 27 (Table 1) is effectively converted to

$$E = \frac{-\frac{C_{ri}}{\Sigma C_{ri}} - \frac{N_{it^*}}{\Sigma N_{it^*}}}{-\frac{C_{ri}}{\Sigma C_{ri}} + \frac{N_{it^*}}{\Sigma N_{it^*}}} = -1 \frac{\frac{C_{ri}}{\Sigma C_{ri}} + \frac{N_{it^*}}{\Sigma N_{it^*}}}{\frac{C_{ri}}{\Sigma C_{ri}} - \frac{N_{it^*}}{\Sigma N_{it^*}}} \quad \text{eq. z}$$

This not only causes the index to flip when C_{ri} goes from negative to positive, but can also cause the index to exceed maximum and minimum limits of ± 1 (Case 4, Fig. 12). In addition if particle modification results in total particle production balancing particle ingestion, then ΣC_{ri} will be zero, and the index will be totally undefined. The electivity indices are clearly unusable in any data set where particle modification occurs. Because of these and the other problems described above with the electivity indices, it would appear advisable in the future not to use this index.

Acknowledgements: This work was supported by NSF grant OCE 76-10347. The original algorithm was formulated by P. L. Donaghay and programmed by J. M. DeManche, R. D. Leatham and D. W. Menzies. The interface between the channelizer and computer was designed and constructed by D. W. Menzies, B. Moon and R. Bartz. Modifications of FOCAL 1969 were made by R. Bartz, D. W. Menzies and S. Johnson. We wish to express our appreciation to B. L. Dexter, S. Richman and D. R. Heinle for their comments and assistance.

REFERENCES

- Allan, J.D., S. Richman, D.R. Heinle, and R. Huft. 1977. Grazing in juvenile stages of some estuarine calanoid copepods. *Mar. Biol.* 43:317-331.
- Donaghay, P.L. 1979. Grazing interactions in the marine environment. Proceedings of the International Symposium on Zooplankton Community Structure. Dartmouth College, Hanover, N.H. August 20-25, 1978.
- Donaghay, P.L. in prep. Conceptual and experimental approaches to understanding grazing behavior.
- Donaghay, P.L. and L.F. Small. 1979a. Long-term food modification by Acartia clausi: a preliminary view. *Mar. Biol.* 52:129-136.
- _____ and _____. 1979b. Food selection capabilities of the estuarine copepod Acartia clausi. *Mar. Biol.* 52:137-146.
- _____, _____ and R.D. Leathm. In prep. Effects of ammonium regeneration on algal-grazer interactions: Part I. Eurytemora affinis.
- Durbin, A.E. and B.G. Durbin. 1975. Grazing rates of the Atlantic naenhaden Brevoortia tyrannus. *Mar. Biol.* 33:265-277.
- Frost, B. 1972. Effects of size and concentration of food particles on the feeding behavior of the marine planktonic copepod Calanus pacificus. *Limnol. Oceanogr.* 17:804-815.
- _____. 1977. Feeding behavior of Calanus pacificus in mixtures of food particles. *Limnol. Oceanogr.* 22:472-491.
- Holling, C.S. 1959. Some characteristics of simple types of predation and parasitism. *Canadian Entomol.* 41:385-398.
- Jacobs, J. 1974. Quantitative measurement of food selection. *Oecologia (Berl.)* 14:413-417.
- Kremer, J.N. and S.W. Nixon. 1978. A Coastal Marine Ecosystem Simulation and Analysis. Springer-Verlag, Berlin. 220 pp.
- Lam, R.K., B.W. Frost. 1976. Model of copepod filtering response to change in size and concentration of food. *Limnol. Oceanogr.* 21:490-500.
- Mayzaud, P., R.J. Conover. 1976. Influence of potential food supply on the digestive enzyme activity of neritic copepods. In *Proceed. of the 10th Europ. Mar. Biol. Symp. Astond, Belg.* 2:415-427. Ed. by G. Persoons and E. Jaspers. Watteren, Universa Press.

- _____ and S.A. Poulet. 1978. The importance of the time factor in the response of zooplankton to varying concentrations of naturally occurring particulate matter: *Limnol. Oceanogr.* 23:1144-1154.
- Mcallister, _____. 1970. Zooplankton rations, phytoplankton mortality and the estimation of marine production. In Marine Food Chains. Ed. J.H. Steele. Oliver and Boyd, Edinburg, 419-457.
- Mullin, M.M. 1963. Some factors affecting the feeding of marine copepods of the genus Calanus. *Limnol. Oceanogr.* 8:239-250.
- O'Connors, H.B., L.F. Small, P.L. Donaghay. 1976. Particle-size modification by two size classes of the estuarine copepod Acartia clausi. *Limnol. Oceanogr.* 21:300-308.
- Paleheimo, J.E. 1979. Indices of food type preference by a predator. *J. Fish. Res. Bd. Can.* 36:470-473.
- Parson, T.R. 1969. The use of particle size spectra in determining the structure of a plankton community. *J. Oceanogr. Soc. Japan.* 25:172-181.
- Porter, K.G. and J.R. Strickler. In Prep. The mechanisms of selective feeding in Daphnia.
- Poulet, S.A. 1973. Grazing of Pseudocalanus minutus on naturally occurring particulate matter. *Limnol. Oceanogr.* 18:564-573.
- _____, 1974. Seasonal grazing of Pseudocalanus minutus on particles. *Mar. Biol.* 25:109-123.
- _____, 1976. Feeding of Pseudocalanus in living and non-living particles. *Mar. Biol.* 34:117-125.
- _____, and J.P. Chanut. 1975. Nonselective feeding of Pseudocalanus minutus. *J. Fish Res. Bd. Canada.* 32:706-713.
- Seale, D.B. and R.J. Wassersug. In press. Suspension feeding dynamics of Anuran larvae related to their functional morphology.
- Starkweather, P.L. 1978. Diel variation in feeding behavior of Daphnia pulex. Influences of food density and nutritional history on mandibular activity. *Limnol. Oceanogr.* 23:307-317.
- Steele, J.H. and B.W. Frost. 1977. The structure of plankton communities. *Phil. Trans. Royal Soc. London.* 280:485-534.
- Strickler, R.S. and G. Rosenberg. 1977. Visual observation of filter-feeding by copepods. 40th annual meeting. A.S.L.O. E. Lansing.
- Richman, S., D.R. Henile, and R. Huff. 1977. Grazing by adult estuarine copepods of the Chesapeake Bay. *Mar. Biol.* 42:69-84.

Storm, S. 1974. Selective feeding, ingestion and assimilation rates and the distribution of the copepod Acartia in Chesapeake Bay. Ph.D. dissertation, Johns Hopkins Univ. 162 pp.

no page 99

CHAPTER 4

Conceptual Approaches to the Control of
Feeding Behavior in Copepods

Percy L. Donaghay
School of Oceanography
Oregon State University
Corvallis, Oregon 97331

To be submitted to Limnology and Oceanography

Running head: Copepod feeding behavior

ABSTRACT

An objective of the study of grazing processes is to be able to predict both quantitatively and qualitatively what a copepod (species and life history stage) will ingest in any given situation, and subsequently to predict how that ingestion will affect copepod growth and reproduction. This objective can best be met by addressing the questions of how do the animals select and why do they select one food over another. A series of alternative sub-models are proposed to define the ways selective choices are made. The mechanisms whereby particles are captured (raptorial or filter feeding), sensed, and handled after capture all influence how choices are made. For raptorial feeding, the mechanisms of sensing prey prior to capture and the one-by-one method of handling prey are most significant in controlling the expected results. For filter feeding, the morphology of the filter (setal spacing, length of setae, variance in setule pore sizes, patterns of setule spacing on the filter), the hydrodynamics of the filter (the rate and pattern of water flow relative to the filter) and the process of transfer of particles to the mouth after capture all interact to control expected feeding behavior. These factors are considered in developing a general theory of copepod feeding that consists of a series of alternative sub-models each with specific predictions as to how the sub-models will affect feeding behavior. Techniques for testing these sub-models for a given species include (1) examination of the morphology of the feeding appendages for patterns of pore spacing, (2) comparison of predicted shapes of filtering curves with observed data, (3) experiments to define the selective capabilities of a copepod, and (4) high speed cinematography. Examina-

tion of existing data for a single species is used to show that a given copepod may switch between alternative modes of feeding depending on environmental conditions. In considering why copepods make selective choices, it is argued that when food is very scarce, capture processes will limit selective behavior; however, when food is plentiful, the nutritional needs of the copepod will strongly influence selective choice. A general model is proposed that makes specific predictions as to the relationship between ingestion rate, past feeding history, and digestive enzyme levels. In a final section, it is argued that the feeding behavior of a particular copepod species may depend on the nature of the environment in which that species has evolved. Differences in the evolutionary history of copepods should lead both to differences in feeding mechanisms between species, and to flexibility in feeding behavior for some species but not for others.

INTRODUCTION

An objective of the study of grazing processes is to be able to predict both quantitatively and qualitatively what a copepod (species and life history stage) will ingest in any given situation, and subsequently to predict how that ingestion will affect copepod growth and reproduction. This objective can best be met by addressing the questions of how do the animals select and why do they select one food over another. Filter feeding copepods in marine environments are presented with the task of ingestion, from a wide variety of particle types, those particles that will be most valuable for growth and reproduction. Natural particle spectra contain not only food items (diatoms, naked flagellates, dinoflagellates, and small animals that may vary in food value) but also items of no food value (inorganic materials such as minerals or inorganic particles, refractory biogenic materials such as wood fiber) and items that are detrimental to ingest (toxic cells of some phytoplankton species, and the copepods' own progeny). The relative fraction of each of these items in the environment may vary radically both in time and space and between estuarine, coastal and oceanic environments. The penalties for inappropriate choices may range from very small (for example, ingestion of a single small inert particle) to very large (ingestion of a toxic cell). Because of the variability of penalties and relative fractions of particle types in both time and space, one might expect: (1) that no one behavior would be universally optimal (i.e., diversity in responses would be observed); (2) that behavioral plasticity would be observed in species facing rapidly changing particle spectra; and (3) that radically different selective pres-

prey) first perceived at a distance. These prey may be either zooplankton or phytoplankton. Filter feeding, on the other hand, is defined as movements of the feeding appendages in such a way as to capture groups of prey on the feeding appendages or to concentrate such particles from the water in such a way that they may be transferred to the mouth and ingested. With filter feeding, particles are only perceived once captured on the filter or transferred to the mouth. Particles captured by filter feeding may be either plant or animal. As defined here, the important distinction between raptorial and filter feeding involves both the time (location) at which particles are first sensed and the numbers of particles handled at one time. The importance of these differences should become apparent below.

In raptorial feeding, prey are first sensed at a distance. The decision to go after (select) a given prey is made before any physical contact has been made with the item by the copepod. Three mechanisms have been suggested for sensing at a distance: mechanical vibration, chemical stimuli, and electrical signals. Mechanical vibrations of animal prey have clearly been shown to be sensed by some copepods and to stimulate and orient attack (Strickler, 1977, 1978 for large predatory copepods). How well this works with basically omnivorous copepods feeding on small prey is unknown. It clearly should not work with phytoplankton cells as prey. Chemical stimuli may be involved since copepods clearly have some chemosensory structures on the mouth and on the maxillary setae (Friedman and Strickler, 1975). Although there is some evidence that chemosensory selection may occur in close proximity to the mouth (Porter and Strickler, in press) or to the maxillae

tures would have operated on copepod feeding behavior in environments that are highly temporally variable versus those that are temporally constant. In light of the above considerations, a series of alternative filtration and ingestion models have been developed. The text of this paper is divided into 3 parts: (1) control of feeding by capture processes, (2) control of feeding behavior by the assimilation process, and (3) consideration of the ecological and evolutionary implications of the alternative models. Throughout, an effort has been made to insure that each model has a series of alternative submodels each with its own unique predictions and testable hypotheses.

PART I: CAPTURE PROCESS CONTROL OF FEEDING BEHAVIOR

Feeding Mechanisms: An Overview

A variety of different methods of feeding have been described for marine copepods (see reviews by Marshall, 1973; Conover, 1978). These different methods and the steps involved in each are summarized in Fig. 1 and Table 1. The following section is meant to provide an overview and to clearly define terms and processes discussed in detail in later sections.

Types of feeding

Copepod feeding has often been separated into raptorial feeding and filter feeding. However, the differences between these terms have often been blurred in the literature. For our purposes here raptorial feeding will be defined as movements of the body and feeding appendages in such a way as to capture and ingest a single prey (or small group of like

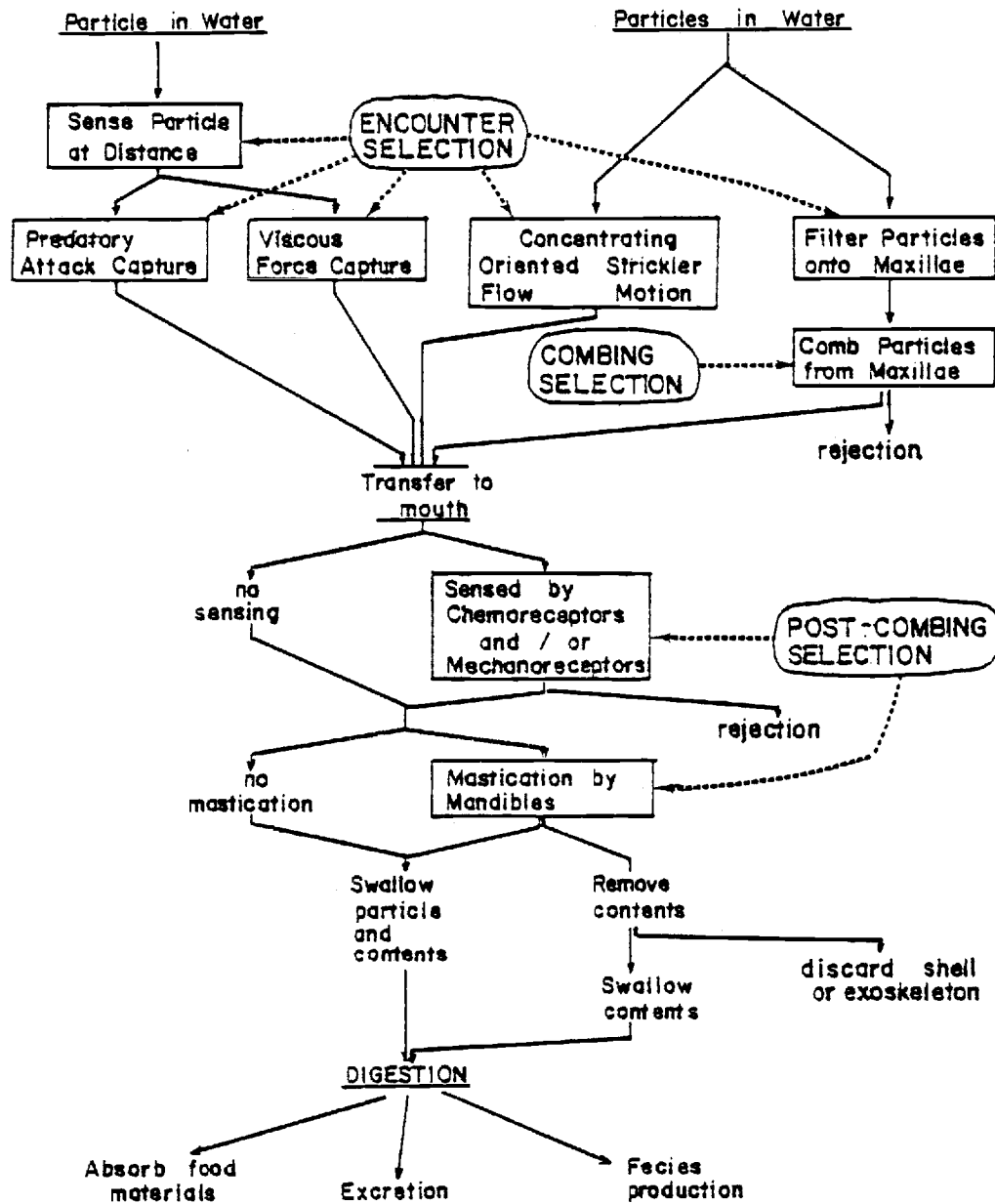
RAPTORIAL FEEDINGFILTER FEEDING

Fig. 1. Feeding mechanisms in herbivorous and omnivorous copepods.

Terms defined in text and in Table 1. Steps enclosed in boxes are steps where selection can occur; the type of selection is indicated by term enclosed by an oval.

Table 1. Alternate encounter and capture mechanisms.

BEHAVIORAL CATEGORY	DEFINITION (MOVEMENTS)	ADVANTAGES	LIMITATIONS	EXAMPLES
RAPTORIAL	movement of feeding appendages to capture a single prey after first sensing it at a distance	large, rare prey: nauplii, rotifers, etc. large phyto.	requires large handling time	
Predatory attack capture	move entire body to intercept and capture prey	use for small animal prey that can escape	" " " " high energy cost	predatory feeding by some omnivores
Viscous force capture	move feeding appendages in such a way to draw prey to mouth via use of viscous forces at low Reynolds numbers	use for large slow moving prey (large phytoplankton)	not work for motile prey; may not work for small alga	Calanus feeding on <i>Lauderia</i> (Strickler and Paffenhofer, 1978)
FILTERING	movement of feeding appendages through the water, or water over them to capture large numbers of prey without distance sensing	reduces total encounter rate, enhances relative encounter rate for large particles	no prey sensing prior to capture, not work for motile prey	
Concentrating	movement of feeding appendages so as to separate (drain) water from particles without trapping particles on filter	handles large numbers of particles of variant sizes; E_{T1} not significant	active selection	
Oriented flow	movement of secondary feeding appendages to create a feeding swirl or other flow pattern designed to accelerate particles to mouth and drain off water	best with good food; permits very high E_{T1}	limited selection; mostly passive	<i>Calanus</i> feeding swirl (Cannon, 1928; Gauld, 1951, 1956)
"Strickler motion"	repeated movements of maxillae and swimming legs to concentrate particles from water; particles may be (but probably are not) combed from filter	best for separating large good food from small sticky materials	intermediate selection; for large only	<i>Acartia</i> feeding movies of Strickler (1977)
Filter particles onto maxillae	movements of feeding appendages to cause particles to be deposited on the maxillae prior to combing transfer to the mouth	allows both encounter selection and combing selection	filter may be clogged by sticky materials	<i>Acartia</i> feeding (Conover, 1956)
Combing \neq 90°	removal of particles from maxillae by secondary structure with transfer to mouth	most refined method of selection; both high E_{T1} and selectivity	selection must be sized based	<i>Acartia</i> feeding (Donaghay, 1979a; Donaghay and Small, 1979b)

(Strickler and Paffenhöfer, 1979), no experiments have yet demonstrated its use for detection of prey at greater distance (Friedman and Strickler, 1975). There is, however, some evidence that once in pursuit of a prey, some copepods can follow a "chemical scent" trail left by the fleeing prey organism (Strickler, 1978). Electrical signals have been recently suggested (Smayda, personal communication) as a possible mechanism. Many marine animals (see review by Kalmijn, 1979) have impressive electrical sensing abilities in seawater and use it for detection of prey. As yet, no experiments have demonstrated the use of electrical sensing by copepods in detecting prey at a distance. If it exists it should work well for both plant and animal prey.

After a prey is sensed by a raptorial feeder, it must then be captured and brought to the mouth. Two methods have been described: capture by predatory attack, and viscous-force capture. With capture by predatory attack the copepod moves its entire body so as to intercept and capture the prey. This type of feeding probably is very similar to predatory feeding by large, purely carnivorous copepods. Predatory attack should work well for prey that are fast enough to avoid capture by other methods, but it has the disadvantage of being more time and energy consuming than other methods. Viscous force capture involves moving the feeding appendages in such a way as to draw a prey slowly to the mouth by taking advantage of the high viscous forces operating at low Reynolds numbers. With this mechanism the animal appears to move its appendages in such a way as to draw segments of water, with associated prey, down toward the mouth in a ratcheting motion. This mechanism was first demonstrated by Strickler and Paffenhöfer (1979) in their high

speed movies of Eucalanus feeding on Lauderia. Viscous force capture, in contrast to capture by predatory attack, should work well for large, slow moving prey, and have very low energetic costs. Although both raptorial mechanisms may involve use of the maxillae, it is quite clear from the movies of Strickler and Paffenhöfer (1979) that the maxillae are not used as a filter. Rather, the maxillae and other feeding appendages are used to manipulate the particle toward the mouth, often without direct contact with the particle. After capture by either of the raptorial methods, prey are transferred to the mouth where they may be sensed, masticated and swallowed much as prey captured by filtering.

In contrast to raptorial feeding, filter feeding involves removing large numbers of small particles from large volumes of water. Two methods have been described. First, the maxillae can be used as a direct filter wherein the filter is moved relative to the water in such a way as to collect particles on the filter. After capture on the filter, particles must be combed from the maxillae by a second appendage and transferred to the mouth. Second, the feeding appendages can be moved so as to separate (drain) water from the free-floating particles without necessarily trapping the particles on the filter. With this type of "concentrating" mechanism, no combing step is required to transfer particles to the mouth. Two different methods have been observed for concentrating particles near the mouth: oriented flow and "Strickler motion." With oriented flow, secondary feeding appendages are moved so as to create a feeding swirl (Cannon, 1928) or other flow pattern designed to accelerate particles to the mouth and drain off water. With the Strickler motion, repeated movements of the maxillae and swimming

legs are used to form a basket to concentrate particles from the water (Strickler and Rosenberg, 1977). After particles are combed from the filter or concentrated near the mouth (using any of the above filtering methods), they are transferred to the mouth.

Once particles are transferred to the mouth, they may be sensed by chemoreceptors and/or mechanoreceptors located on the labrum and other mouthparts (Friedman and Strickler, 1975). It is not at all clear whether such sensing occurs under all conditions for all copepods (Donaghay, 1979). Next, particles may be masticated by the mandibles. This appears to be true for large particles, but seems not to occur (based on whole cells in gut contents) for all small particles (Schnack, 1975). With some types of particles, particularly very large or irregularly shaped ones (Conover, 1956; Schnack, 1975 and personal communication) the particle may be punctured by the mandibles and the contents sucked out and swallowed. The remainder of the particle may then be discarded. Based on gut content work (Schnack, 1975) it appears that normally all parts of the masticated particles are swallowed.

Types of selection

With this overview of the feeding process in mind, it can be seen that the ingestion of a particular particle is the net (cumulative) result of selective processes occurring at several levels: encounter selection, combing selection and post-combing selection.

Encounter selection is the most energetically efficient mode of selection and one of the most widely recognized in the ecological literature on feeding (see Schoener, 1971, for review). The chief

advantage of encounter selection is that by actively or passively making choices before capture, handling time costs are greatly reduced. For raptorially feeding copepods, encounter selection is a function both of the characteristics of the mechanism for sensing prey at a distance and the physical properties of the capture mechanism. Because of our extremely limited understanding of the sensing mechanism and of the ways in which the feeding appendages are used in raptorial feeding, it is difficult to make predictions as to the types of selection expected. In all likelihood, however, the selection observed will be much more size and shape independent than in filter feeding. In filter feeding copepods, encounter selection will be highly dependent upon the filter design and the patterns of movement of water relative to the filter (i.e., the hydrodynamic properties of the filter). Since filter design and patterns of water movement can be quantified, predictions of expected feeding behavior are possible (see conceptual filtering model below).

After particles are captured on the filter, selection can occur during removal of the particles from the filter. Selective removal of particles from the filter has been termed combing selection (Donaghay and Small, 1979b). The expected results of combing selection are highly dependent on filter design, the way in which particles are distributed along the filter, and the way they are removed. Since these are all quantifiable, the expected results can be theoretically examined (see theory below).

After transfer to the mouth, an additional level of selection is possible (termed post-combing selection). Whenever particles are sensed by the chemoreceptors and/or mechanoreceptors on the mouthparts, rejec-

tion can occur. There is evidence that these sensors can be employed (Poulet and Marsot, 1978; Poulet, 1979; Donaghay, 1979), but there is also evidence that they are not always operative (Donaghay, 1979). Rejection should also be possible if during mastication a particle cannot be crushed. However, there is little evidence for this since Wilson (1973) has shown that large plastic spheres (70 μ) that would normally be masticated may be swallowed whole. Some very large diatoms also can be swallowed whole (Schnack, personal communication). At the end of the filter theory section, some consideration will be given to the requirements for, and expected effects of, post-combing selection.

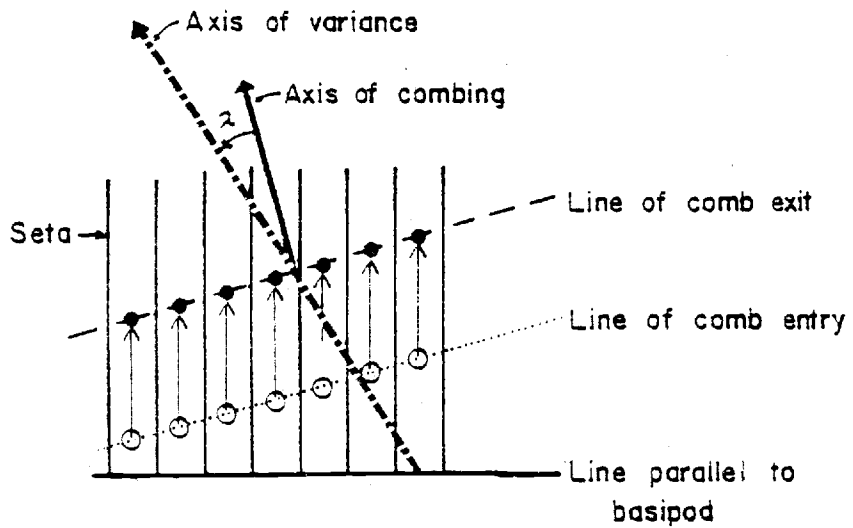
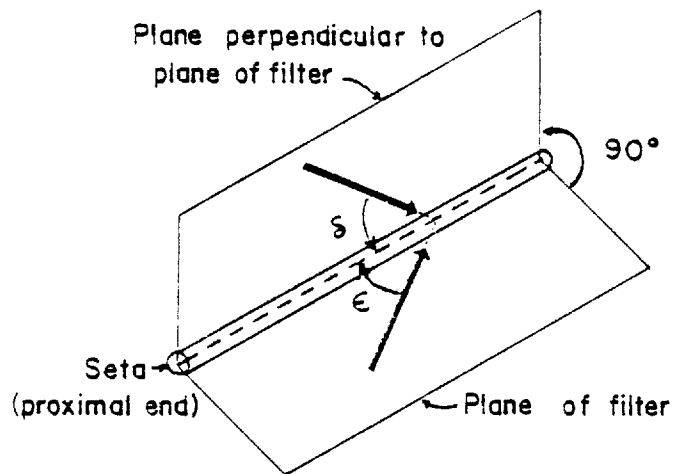
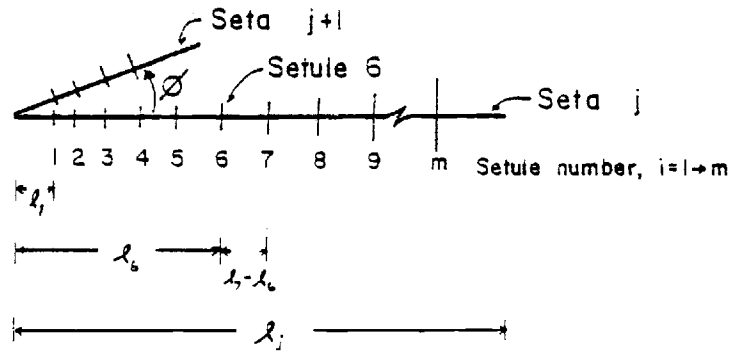
Filter Model: Factors Affecting Encounter and Combing Selection

Theoretical statement of model of filter feeding

Let us consider a hypothetical copepod filter with the following configuration (Fig. 2).

- (1) Let the filter be composed of j setae of length l with some variance in $l \geq 0$.
- (2) Let \emptyset be the angle between any two adjacent setae with some variance in $\emptyset \geq 0$. The variance in \emptyset may result either from alteration of \emptyset between any one pair of setae over time, or from the differences in \emptyset between different pairs of setae at one time, or both. The setae can be fixed (i.e., $\emptyset =$ a constant with or without variance in \emptyset), or \emptyset can be varied either actively through muscle controlled spreading of the setae, or indirectly through alteration of filter speed in the water, or possibly by growth induced changes through life history stages.

Fig. 2. Design of hypothetical filter. (a) Properties of two adjacent setae (\emptyset), length of seta j (λ_j), distance down seta to first setule (λ_1), distance down seta to last setule (λ_m), distance down seta to some given setule i (for example, setule 6: $\lambda_i = \lambda_6$), and the spacing between two setules (for example, setule spacing between setules 6 and 7, or $\lambda_7 - \lambda_6$). Pattern illustrated is a pattern of increasing setule pore spacing and setule length with increasing distance down the seta. Other patterns are possible. (b) Patterns of water flow (defined by large arrows) relative to an individual seta. Lines of flow are defined lying in the plane of the filter (ϵ) and in a plane perpendicular to the plane of the filter (δ). δ and ϵ are the vector components of flow relative to the setal axis (setal axis defined by dashed line at center of seta). (c) Properties of entry into and movement of combing appendage relative to second maxillae. Only a small segment of setae of the maxillae is shown. Combing appendage setae enter between maxillae setae at open circles, move along between the maxillary setae to solid circles where comb exits. Axis of combing (large solid arrow) is defined as a line perpendicular to the points of entry or exit of the comb. λ defines the angle between the combing axis and the axis of variance (heavy dashed arrow).



- (3) Let all the setae lie along a planar surface termed the plane of the filter. The plane of the filter need not be flat, but at least initially it will be so considered.
- (4) Let setal axes be defined parallel to each seta in the plane of the filter.
- (5) Let each seta have m setules spaced along its length, with the number, spacing and length of setules being either constant or variable (Fig. 2a).
- (6) Let the spacing between adjacent setules form a pore whose size is determined by the distance between setules (or setule length, or a combination of both). Pores may also be formed by the spacing between setae.
- (7) Let the pores (defined in 6) be randomly distributed down the length of each seta or be ordered in some linear or curvilinear fashion. If ordered along each seta, let the order of setule pore sizes on adjacent setae be either similar or different. If setule spacing is ordered along each seta in a similar fashion, a pattern of pore sizes will exist on the filter surface. Let an axis of setule variance be defined on the filter surface such that variance in setule spacing will be minimized at right angles to that axis of variance. This axis may be linear or curvilinear. If setule variance is random along each seta, or differently ordered on adjacent setae, the axis of variance will be termed undefined.
- (8) Let the pattern of water flow be straight through the filter or at some angle to the filter. Let this flow be defined in terms of the two component angles δ and ϵ (Fig. 2b). Let δ

define the angle of flow relative to a given seta along a plane that is parallel to the setal axis but at right angles to the plane of the filter. Let ϵ be the angle of flow relative to the setae along the plane of the filter. (In terms of the whole filter, δ describes the angle at which water strikes the filter from above and ϵ describes the angle at which water flows across the filter. These two angles define the vector components of all flow relative to the filter).

- (9) Let particles be trapped on the filter at setule and/or setal based pore sizes less than the effective diameter of the particles but only as constrained by the hydrodynamic properties of the filter (see below).
- (10) Let A_D equal the area of the filter where, given (8) above, particles of size D will be trapped.
- (11) Let the relative efficiency of capture of a particular particle of size D be defined as the ratio of the area in which it can be captured to the total area of the filter.
- (12) Let the copepod remove particles trapped on the setae and/or setules by combing with a secondary appendage. Let the point of entry and exit of the comb be either the same or different for each setal pair. Let an axis of combing be defined as a line perpendicular to an imaginary line passing through the comb as it moves down the setae of the filter (Fig. 2c). If the combing axis is perpendicular to the setal basipod, and the comb enters and starts combing at the basipod and extends to the end of the filter, all particles trapped on the filter

will be removed. This is termed full combing. Entry of the comb at any other point will result in leaving some particles on the filter, and will result in some form of partial (selective) combing.

- (13) Let the filtering behavior of the filter be defined by both its structure and by the hydrodynamic properties of that structure as it is moved relative to the water.
- (14) Let the structure be defined by the setal number and length, the setule number, spacing and length, and the angle between setae (curvilinearity of setae will also be considered).
- (15) Let the hydrodynamic properties be defined by (a) filter structure, (b) angle of water flow relative to the filter and (c) velocity and acceleration of movement of water relative to the filter.

Effect of critical elements of model on feeding behavior

The above model allows consideration of a variety of potentially important variables in addition to those considered in previous models. Previous models (Lam and Frost, 1976; Lehman, 1976; Boyd, 1976; Steele and Frost, 1977) have considered only ϕ , ℓ , variance in setule spacing, and number of beats per minute of the filter as variables with all other factors held constant or ignored. Hydrodynamics has been considered only as it might affect drag calculations and thus energetics of filtration. These past models have generally considered (1) pore size to be random, i.e., without pattern on the filter surface; (2) δ to be 90° , (3) ϵ to be 0; (4) combing, if it occurs, to be full, i.e., to go from

λ_1 to λ_m ; and (5) hydrodynamics to be unimportant in affecting selectivity. Each of these factors and their possible interactions are considered below.

(1) Effect of pattern of pore spacing:

The pattern of pore sizes on the filter is extremely important to the selective properties of the filter. Regardless of pattern, the relative frequency of pore sizes will define the relative passive filtration efficiency curve (after Nival and Nival, 1973, 1976). If, however, the pore sizes are patterned on the filter (particularly if pore sizes increase across and/or down the filter), the potential exists for sorting of particles by size on the filter. Partial combing will then result in selective removal of particles of a given size from a segment of the filter. There is a large potential interaction with the other factors considered below.

(2) Effect of δ :

If $\delta = 90^\circ$, water will flow through the filter leaving behind particles of sizes greater than the pore size. These particles will be randomly distributed along λ at all pore sizes less than the particle size, D . Large particles may also be captured across the setae as well as in the pores defined by the setules. The lack of strong sorting of particles along the setal length will strongly limit the combing selectivity possible. As the water passes through the filter a large eddy will probably develop behind the setae, causing a continuously expanding drag until a maximum is reached. This filter should be directly analogous in behavior to a simple screen of similar pore sizes. This leaky sieve model is the one most often used in the past (Lam and Frost, 1976;

Lehman, 1976; Boyd, 1976).

If δ is less than 90° , then flow will be proximal to distal along the setae as well as through the filter. Under such conditions particles may be trapped at pore sizes just slightly less than the particle diameter. This can occur in one of two ways. First, if setules are level with or slightly below the plane of the filter (as the filter is being moved through the water), a particle striking the filter at setal pore sizes less than D will move along the setae until its diameter is less than the intersetal distance, at which point it will fall between the setae and be trapped by the setules. Second, the movement of water along the filter's surface might also cause small eddies to develop along the filter's surface and these eddies may in turn act as an important trapping mechanism. With this type of flow particles should be carried outwards along the filter until the scales of turbulence caused by water passing over and through the filter are of the same scale as the particle size, at which point the particles should be trapped by the setules. In either case, particles will be sorted according to size along the length of the setae. To the degree to which setule spacing is ordered both down and across the filter, particles will be spatially sorted on the filter surface. As a result, subsequent selective combing of the filter can result in selection of particles with both upper and lower size controlled (see effect of combing below). The position where a given sized particle should be captured should be a function of (but not necessarily equal to) setule spacing. The efficiency of capture will be unchanged from when $\delta = 90^\circ$. Setal spacing should have a much smaller role in trapping particles when $\delta < 90^\circ$ than when $\delta = 90^\circ$. If

the small eddies develop along both sides of the filter when $\delta < 90^\circ$ move down the filter, they can be dissipated off the tips of the setae, thus resulting in much lower drag than with $\delta = 90^\circ$. This type of filter ($\delta < 90^\circ$) is analogous to a drop filter used in industrial ore sorters and in some newly developed, high-speed, low-resistance filters (operating on particles 0.1 to 100 μm in size).

If δ is greater than 90° , then the flow will be from distal to proximal along the filter as well as through the filter. With this type of flow particles should be carried inwards along the filter until the scales of turbulence caused by the water passing over and through the filter are of the same scales as the particle size. At this point the particles should be captured. This mechanism will also result in sorting of particles by size along the filter much as with δ less than 90° . However, this sorting may not be precisely as would be expected from the size of the pores since the sorting is based solely on turbulence properties rather than pore size directly. This sorting mechanism is also a type of drop filter.

If the setae are curved, then δ may change along the length of the filter. As a result the filter may act as a hybrid, with sorting along the proximal parts and non-sorting in the distal section. For curved setae, the operation of the filter with $\delta > 90^\circ$ (but not for $\delta \leq 90^\circ$) may deviate from the pattern described above for straight setae. The hybrid type filter has the advantage that while small abundant particles are well sorted, large rare ones are all grouped together toward the distal part of the filter.

If δ is very small, very few particles may be trapped on the filter surface. However, the filter may still act to drain water away from the particles very efficiently. The particles leaving the end of the filter will be very concentrated and will have a significant velocity. If the tips of the feeding appendage are pointed toward the mouth, particles might be concentrated close enough to the mouth to be ingested. This is one type of oriented flow already discussed (Fig. 1 and Table 1). If δ is slightly larger so that particles are trapped according to pore size on the filter, yet large particles are concentrated near the mouth (assuming the same orientation of the setae toward the mouth as above), it is possible to get a feeding behavior that is a combination of drop filter for particles smaller than the maximum pore size and oriented flow for all particles larger than the maximum pore size.

(3) Effect of cross filter flow, ϵ

Cross filter flow may result in somewhat different sorting patterns from that expected from simple setal/setule spacing, because such flow may change the hydrodynamic characteristics of the filter. The extent to which this occurs is uncertain. The degree to which cross-filter flow alters the location of particle capture on the filter may be used by the copepod to alter its selective capabilities. Since the net effect of increasing cross-filter flow would be to increase scales of turbulence, it should also enhance the capture of larger particles. Alteration of ϵ can be achieved by rotation of the basipod of the filter, a relatively simple task.

(4) Effect of combing

The effects of combing are highly interdependent on both the pat-

terns of pore size on the filter and on the way in which flow across the filter causes particles to be trapped by the setae and setules. If the pore sizes are randomly distributed, then partial combing of the filter only results in a reduced encounter rate and a reduced capture efficiency for all sized particles, neither of which are of much benefit. If pore sizes are ordered but $\delta = 90^\circ$, then selective combing of the distal half of the filter can result in selection against small particles, but at the price of reduced capture efficiency for large cells that may be trapped on the small pore areas of the filter. If pore sizes are ordered and if $\delta < 90^\circ$, then particles will be size sorted along the axis of variance of the filter and partial combing can result in very strong patterns of combing selection (Fig. 2c). If the combing axis is parallel to the axis of variance, then partial combing will result in minimum variance in the upper and lower size limits of the combed particles. This minimum variance will be determined by the variance in pore size at right angles to the variance axis. Increase in the angle (λ) between the combing axis and the variance axis will result in an increase in the variance of the upper and lower size limits of the combed particles. In contrast to the reduced efficiency of selective combing with $\delta = 90^\circ$, selective combing with $\delta < 90^\circ$ leads to discrimination against particles of unwanted size without any loss of efficiency for other sizes. It is important to note that the orientation of the filter while combing is taking place may be quite different (i.e., θ may be different) from the orientation of the filter during particle capture. In addition, all that is needed for some selective combing to occur is for the copepod to be able to control the orientation of the comb rela-

tive to the filters, a presumably easy task.

(5) Effect of hydrodynamics

Hydrodynamics of water flow around the copepod filter clearly plays an important, though controversial, role in determining feeding behavior. For example, the reader may object to the above drop filter argument because of hydrodynamic considerations. Although a variety of hydrodynamic models have been proposed for copepod filters (Table 2) (Lam and Frost, 1976; Lehman, 1976; Rubenstein and Koehl, 1977), our knowledge of the correct hydrodynamic model to apply at scales of less than 100 μm is limited by our inability to make measurements of flow at those scales. For example, flow 100 μm above the filter might be laminar while flow near the setules might be turbulent. However, the existence of very low resistance commercial drop filters that operate in precisely these size ranges (retention of particles of 0.1 to 100 μm) suggests that such a model may not be inappropriate for some copepods.

Although there may be a strong tendency to make simple Reynolds number calculations and conclude that flow must be purely viscous or inertial, great care must be taken in doing so for several reasons. First, it does not appear to be clear at all as to what dimension to use in the Reynolds number calculation: length of setule, length of seta, or the area of the filter. The filter is a very complex structure composed of many component parts: the size of the smallest part compared to the size of the total filter covers over two orders of magnitude, a range clearly important to a Reynolds number calculation. Second, with some animals the movements are relatively slow and discrete, conditions which permit calculation of Reynolds numbers and cinematic proof of viscous

TABLE 2. Hydrodynamics explicitly evoked or implied by past models or descriptions. Bar in hydrodynamics category indicates relative range over which model works.

AUTHOR	TYPE OF FEEDING	HYDRODYNAMICS	
		100% VISCOUS	100% INERTIAL
<u>DESCRIPTIONS</u>			
Cannon, 1928	feeding swirl or vortex; move water past a fixed filter		_____
Conover, 1956	seine (capture on a moving filter)		_____
Strickler and Rosenberg, 1977	Strickler motion	_____	
Donaghay, this paper	drop filter		_____
Strickler and Paffenhöfer, 1979	viscous force capture	_____	
<u>MODELS</u>			
Lehman, 1976	general filter capture	both viscous and inertial flow considered in math model	
Boyd, 1976	leaky seive; capture on a filter		_____
Lam and Frost, 1976	same as Cannon, 1928		_____
Rubenstein and Koehl, 1977	direct interception		_____
"	inertial impaction		_____
"	gravitational deposition		_____
"	diffusion or motile-particle deposition		_____

flow (Strickler and Paffenhöfer [1979] movies of Eucalanus). However, for other copepods, movements are very fast and smooth, and visual observation of particle rejection suggests a more intermediate value for the Reynolds number. Third, with some copepods, such as Acartia clausi, movements are not only very fast (more than 60 cycles per second), but the feeding appendages appear to stop and reverse direction twice each beat cycle. This results in average velocities that are high, but also requires both very high rates of acceleration and much higher peak velocities. Such conditions would appear to invalidate some of the assumptions required for making Reynolds number calculations (see Bachelder, 1967). It is clear that much more work needs to be done. It seems reasonable that further work may demonstrate that in feeding as well as swimming some copepods have evolved behaviors to take advantage of the hydrodynamic properties of their environment. For example, movies of escape swimming by copepods (Strickler, 1978) have shown that at low speeds (while accelerating) the animals swim in a fashion appropriate to viscous flow but once they reach maximum velocity, they swim in a fashion appropriate to inertial flow. In a similar fashion it may eventually be shown that by altering the speed of water flow relative to the filter copepods may alter the hydrodynamic properties of that filter.

Factors Affecting Post Combing Selection

Thus far we have considered how the mechanisms (both raptorial and filtering) used to capture particles and bring them to the mouth can lead to selective behavior. Selection can also occur once particles are brought to the mouth. Selection based on chemosensory and/or mechano-

sensory reception by the mouth parts has a series of requirements (or limitations). First, because the sensed particle must be individually analysed, capture rate must be slow enough to allow for the sensing step to occur. The time required for such selection is the sum of the time required (1) to bring the sensory organ(s) in contact with the particle and allow sensory organ response, (2) for neuro-transmission between the sensory organ, the neural ganglion (where a "decision" is made) and the effector muscles, and (3) for rejection or ingestion to be effected by the mouth parts. Although the precise total time required will have to be established using cinematographic techniques to observe rejection events as has been done for Daphnia by Porter and Strickler (in press) (and will clearly be different with different copepods and different types of prey), it seems reasonable to assume that the time required is not trivial. Personal observation of single particle rejection by Eurytemora affinis indicates that the time is long enough to cause complete cessation of the filter current before rejection occurs. The total time required was on the order of 0.5 second. This time requirement puts limits on the capture rate permitted and thus might limit the utility of such single particle rejection to larger prey encountered at low densities. Second, there are significant morphological requirements for post combing selection. The copepod must have the required chemosensory and/or mechanosensory receptors. Existence of such receptors (chemosensory ones in particular) have been established in a variety of copepods based (1) on the existence of morphological structures identical to chemosensors in insects (Friedman and Strickler, 1975) and (2) on experimental evidence showing discrimination between particles based on

amino acid content (Poulet, 1979). However, our knowledge of what kinds of substance copepod chemosensors react to and how they work is as yet extremely limited. Because of the great complexity of the chemical composition of particles in sea water, chemosensing is most likely used in conjunction with other mechanisms of selection rather than by itself. We shall consider this problem in more detail in the last section. The action of chemosensory selection will have very different results from any of the filter-based selection mechanisms: chemosensory selection will be totally size independent. Those copepods with chemosensory selective capabilities can make choices between two particles of identical size but different chemical composition (Donaghay, 1979).

Steps in evaluating feeding mechanisms

In the preceding theoretical discussion a series of alternative feeding mechanisms were proposed that need to be evaluated for any given copepod as conceptual and/or explicit descriptions of feeding behavior. It must be realized that while some species may use only one mechanism, other species may be able to switch mechanisms depending upon changing environmental conditions. Our own observations and those of D. R. Heinle (personal communication) clearly indicate switching must be considered at least for coastal species. This apparent flexibility on the part of some copepod species places certain critical constraints on the approach used to examine the mechanisms. Such flexibility invalidates the assumption that the mechanism is fixed for any one species for all conditions, or that all species use the same mechanism in response to any one set of conditions. Careful observations of feeding behavior

by themselves, regardless of how sophisticated the observational techniques, are not sufficient to reject a particular hypothesized mechanism, because such observations can only define the existence of a specific movement pattern, not its generality or its behavioral result. Analyses of (1) feeding appendage morphology, (2) predicted shapes of filtering curves, (3) experimentally defined selective capabilities, and (4) the codevelopment of structure and behavior with ontogeny, are important steps in both evaluating theoretical models and in evaluating which alternative tactics are used by a given copepod and under what conditions. Each of these steps will be considered in detail below. Each of these steps allows some evaluation of the conceptual validity of the model (or proposed mechanisms). However, the final determination of whether a submodel is mechanistically correct can only be made by coupling experimental techniques to elicit a particular response with cinematographic techniques sufficiently refined to not only show movements of feeding appendages but also the hydrodynamic patterns of water flow and particle movement along the filter surface.

(1) Analysis of feeding appendage morphology

The structure of feeding appendages places a series of constraints on how those appendages are used. The use of combing selection by a given copepod species was considered to be dependent upon the existence of patterned setule spacing leading to the definition of an axis of variance. The presence of such patterns not only permits combing as a possible selection mechanism, but, if selective combing is not used, the presence of such patterns must be explained on other grounds.

Patterns of setule spacing were derived for Acartia clausi adult females using the method of Schnack (1975). Briefly, the second maxillae (Fig. 3) were removed from the copepod, mounted in polyvinyl-lactophenol, and examined under a microscope. Setule spacings were measured with an ocular micrometer for all the setae of 6 animals, and setule lengths were determined for 1 animal. The spaces between setules were then plotted versus distances between the setule pair and the base of the seta. Two examples are shown in Fig. 4a,b. Setule spacing increased curvilinearly with distance from the basipod for all setae. There was some variability around the means for all copepods, but it should be remembered that a large fraction of that variability could be attributed to measurement errors arising from estimating setule spacing to the nearest micron. This measurement error is probably responsible for the stair step pattern of increase in setule spacing in Fig. 4a,b. Greater precision of measurement (to 0.1 μm) can reduce this error in the future. Considerable variability was noted in the length of a given seta on different animals (Table 3). Some of the variability in setule spacing between animals could come from this source. In order to remove this component of variance, the data were normalized by dividing through by the length of an individual seta (Fig. 4c,d). This resulted in some reduction in variability between animals. Such a reduction in variability for Acartia suggests that setule spacing is relative to the length of the seta. Since there was also some variation in the size of individual animals used, this could also contribute to the variance. When the setule spacing data were normalized to the size of the filter (as measured by the sum of the lengths of all the setae for a given animal),

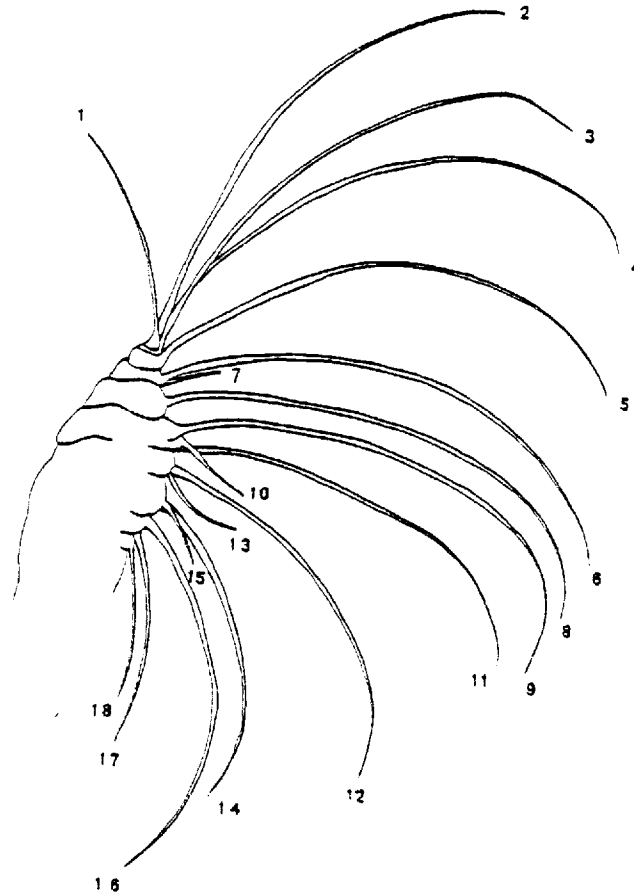


Fig. 3. Second maxillae of Acartia clausi adult female (from down bay population of O'Connors et al., 1975). Setae of maxillae are shown in fully distended position. Numbers at tips of setae are setal numbers. Setae number 7, 10, 13, 15 have no setules and lie at approximately right angles to the plane of the filter. They clearly have a different function from the rest of the setae and are not included in Fig. 5. Drawing was made using a camera lucida by S. Schnack.

Fig. 4. Variability in setule spacing as affected by different normalization procedures: (a,b) raw setule spacing versus distance down setae; (c,d) raw setule spacing normalized to the length of the individual setae on each animal; (e,f) raw setule spacing normalized to the relative size of the individual copepod's filter as measured by the sum of the lengths of all setae for that animal; (g,h) raw setule spacing normalized by the ratio of the length of a given seta on a particular individual copepod to the lengths of that setae on the average animal. Examples for each normalization are shown for (a,c,e,g) setae 5 (where setule spacing has a large range and variability is small) and for (b,d,f,h) seta 16 (where setule spacing has a small range and variability is large). Symbols are for the individual copepods used.

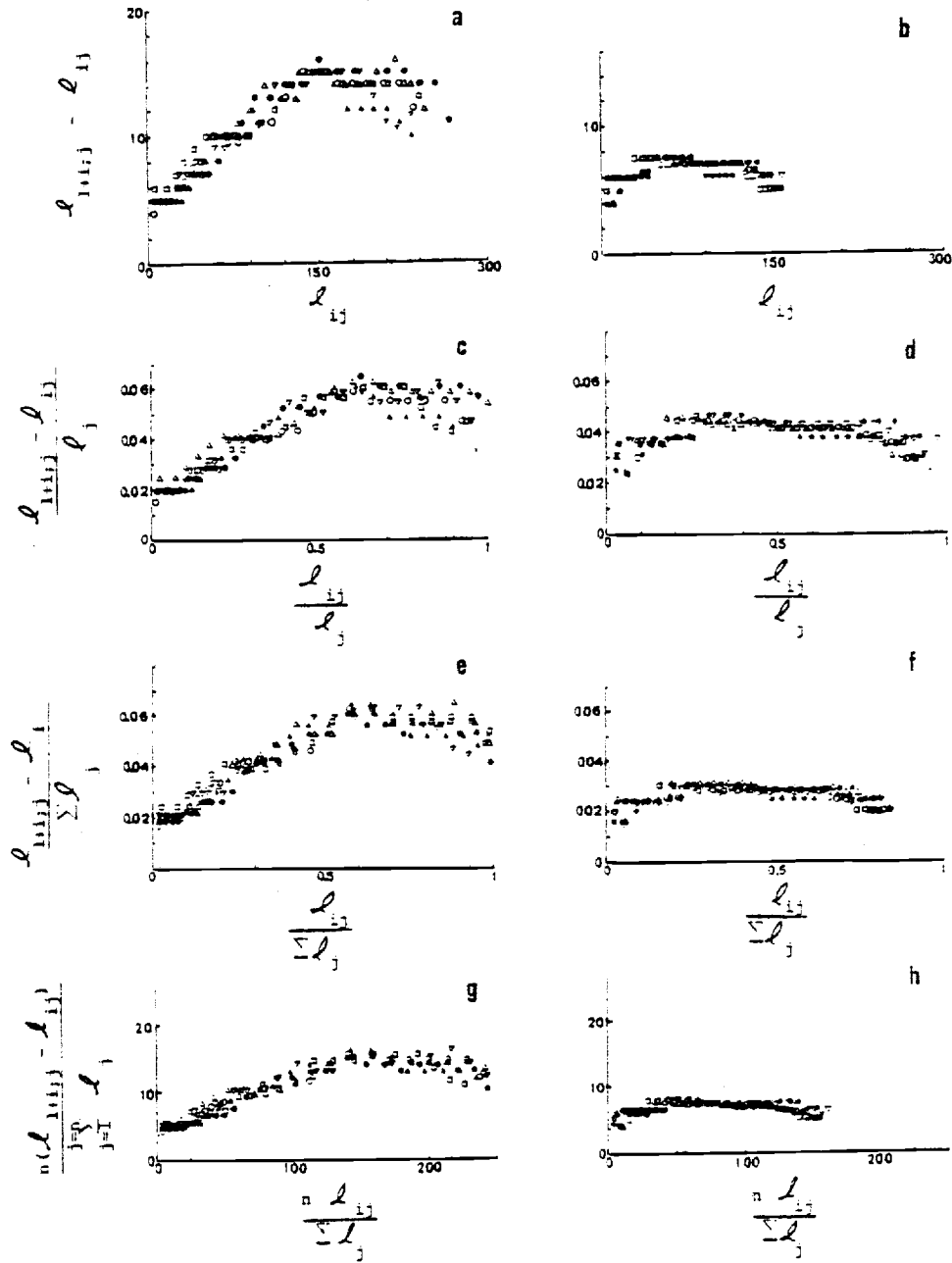


Table 3. Comparison of the properties of the setae of the second maxillae of Acartia clausi females. Means and standard deviations are based on the measurements of these properties for all setae of six individuals.

SETAE NUMBER	LENGTH OF SETAE		SETULE NUMBER		DISTANCE FROM LAST SETULE TO END OF SETAE	
	mean \pm lsd		mean \pm lsd		mean \pm lsd	
1	95.83	7.05	5.17	1.17	52.67	5.16
2	190.50	24.79	26.17	2.93	17.83	2.64
3	227.17	9.96	24.33	0.82	9.33	1.86
4	238.08	24.65	24.83	1.94	1.67	0.52
5	244.17	12.29	23.17	0.89	4.50	3.08
6	211.02	19.50	24.67	1.03	18.93	5.31
7	27.95	3.70	-	-	-	-
8	200.92	17.01	24.50	1.38	14.33	3.61
9	228.58	20.11	29.50	0.84	10.17	1.60
10	36.98	2.42	-	-	-	-
11	210.33	14.33	30.00	2.00	11.83	3.19
12	172.67	10.93	26.17	2.14	13.83	2.23
13	41.87	2.86	-	-	-	-
14	141.17	2.93	27.17	1.17	3.67	0.52
15	31.37	2.19	-	-	-	-
16	166.25	4.63	23.67	0.52	13.33	4.46
17	95.17	5.98	18.00	0.89	3.00	2.28
18	72.00	2.37	16.00	0.63	3.17	0.98

again the variance was reduced over the raw data (Fig. 4e,f compared to 4a,b), but no more so than by normalizing by the individual setal length. The reduction in variance by normalizing by either of these methods suggests that the pattern of setule spacing, rather than the absolute pore sizes, is more important to the animal and has been under stronger evolutionary (selective) pressure. Preliminary work on other species indicates that this is true for some other species, but not for all (personal observations; Schnack, 1975).

The above normalizations result in plots of setule spacing in relative units. As a result, it is not possible to directly intercompare them to develop patterns on the feeding appendage. This problem can be solved by multiplying the setal length normalized data by the average length of each seta (Fig. 4g,h). The axes of the plots of the normalized values are now in absolute units (μm). A smooth curve drawn through the data is an estimate of the relationship between average setule spacing and distance from the base of the seta. Data points for individual setule spacings represent deviations from that average relationship. These average relationships have been plotted for all setae except setae 7, 10, 13, 15 which are out of the filter plane and have no setules (Fig. 5). From Fig. 5 it is clear that all the relationships have the same basic shape (although setal length from seta 1 through 5 increases then generally decreases from seta 9 through 19). It is also clear that the patterns smoothly change as one moves across the filter. Moving inward along the basipod (i.e., from seta 5 to seta 18) the setae shorten, maximum setule spacing decreases, and the pattern becomes slightly more curvilinear. These plots demonstrate that setule spacing

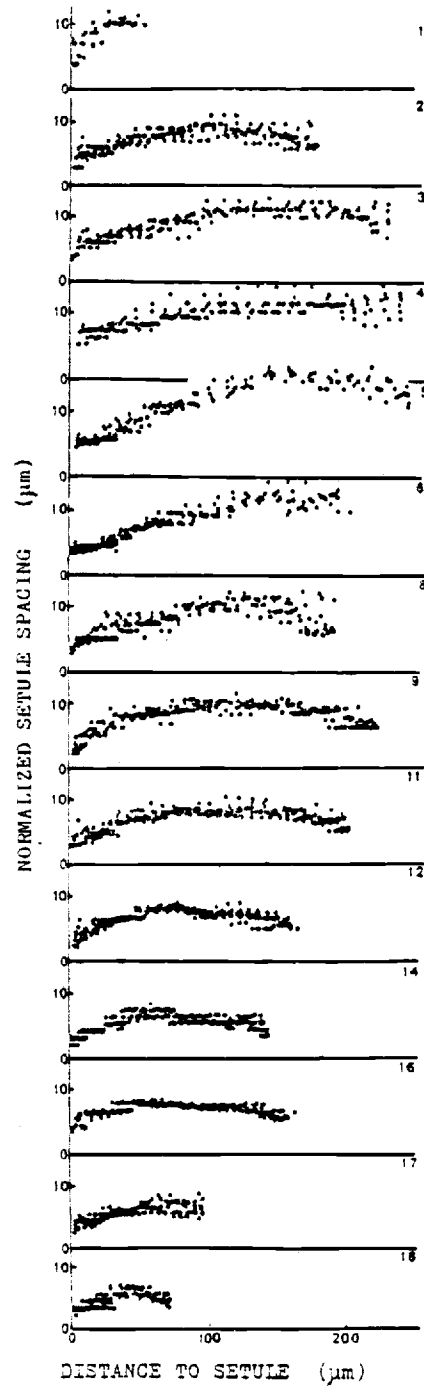


Fig. 5. Comparison of patterns of setule spacing for all setae for all animals. Data is normalized to the average setal length as in Fig. 4d. Symbols (o) are the individual value of setule spacing for each animal.

patterns for Acartia clausi meet the criteria necessary for combing selection: spacing increases smoothly along individual setae and in similar patterns along adjacent setae. These two facts require that an axis of variance be defined on the surface of the filter. The length of the setules (as well as spacing between setules) increases down the length of each seta. If the length of the setules as well as the spacing between setules is important in determining pore size, then the definition of the axis of variance may be strongly enhanced if both factors are considered.

In summary, patterns of setule spacing strongly support a combing selection model for Acartia clausi. On the other hand, the apparent absence of such patterns on some other species (Schnack, 1975) may make such a model inappropriate for all species.

(2) Analysis of the predicted shapes of filtering curves.

The theoretical feeding model can be used to make explicit predictions about the shape of filtering curves and how that shape can change in response to the nature of particle spectra offered in feeding experiments. These predictions take the form of curves of expected filtering efficiency (\hat{F}_{ei}) versus the natural logarithm of particle size. Observed curves of filtering efficiency (F_{ei}) versus particle size can be computed from apparent filtering rate data (F_{ai}) obtained from standard copepod grazing experiments. The computational procedures have been described in detail by Donaghay, et al. (in prep. a). Insofar as many of the variable factors (\emptyset , δ , partial combing, axis of variance, λ) considered in the theory have unique effects on the observed relative

efficiency of capture of particles, changes in filtering efficiency curves (resulting from such efficiency changes) can be used to evaluate the model and can be used as evidence for proposed mechanisms.

As discussed above, the expected filtering efficiency for a particle is a function of the area of the filter with pore sizes less than the diameter of that particle. The shape of the filtering efficiency curve is a function of the contribution of both setule and setal spacing to pore size. Setule spacing alone results in a rectilinear filtering efficiency curve (solid line, Fig. 6a) which can be completely specified by the size of the smallest particle captured, d' , and the size of the smallest particle captured at maximum rate (efficiency) by intersetule capture, d^* . If only setule retention is involved in particle capture, then d' and d^* will correspond to the minimum and maximum effective pore sizes on the filter respectively. Because the effective pore size is equivalent to the measured pore size as modified by hydrodynamics, d' and d^* may differ from actual measured intersetule pore size. The shape of the filtering curve between d' and d^* is controlled by the statistical distribution of pore sizes (not ordering or pattern) and can generally be approximated as log linear (Nival and Nival, 1973, 1976; Boyd, 1976). The rate of increase of expected filtering efficiency with particle size in this segment, α is fixed by the distance between d' and d^* . If setal spacing is also involved in controlling pore sizes, the expected filtering curves will be strongly influenced by the degree of overlap in setule-generated and setal-generated pore sizes. Two cases will be considered. In case 1 (Fig. 6a) the minimal intersetal distance is greater than the maximum intersetule spacing, then setal capture will

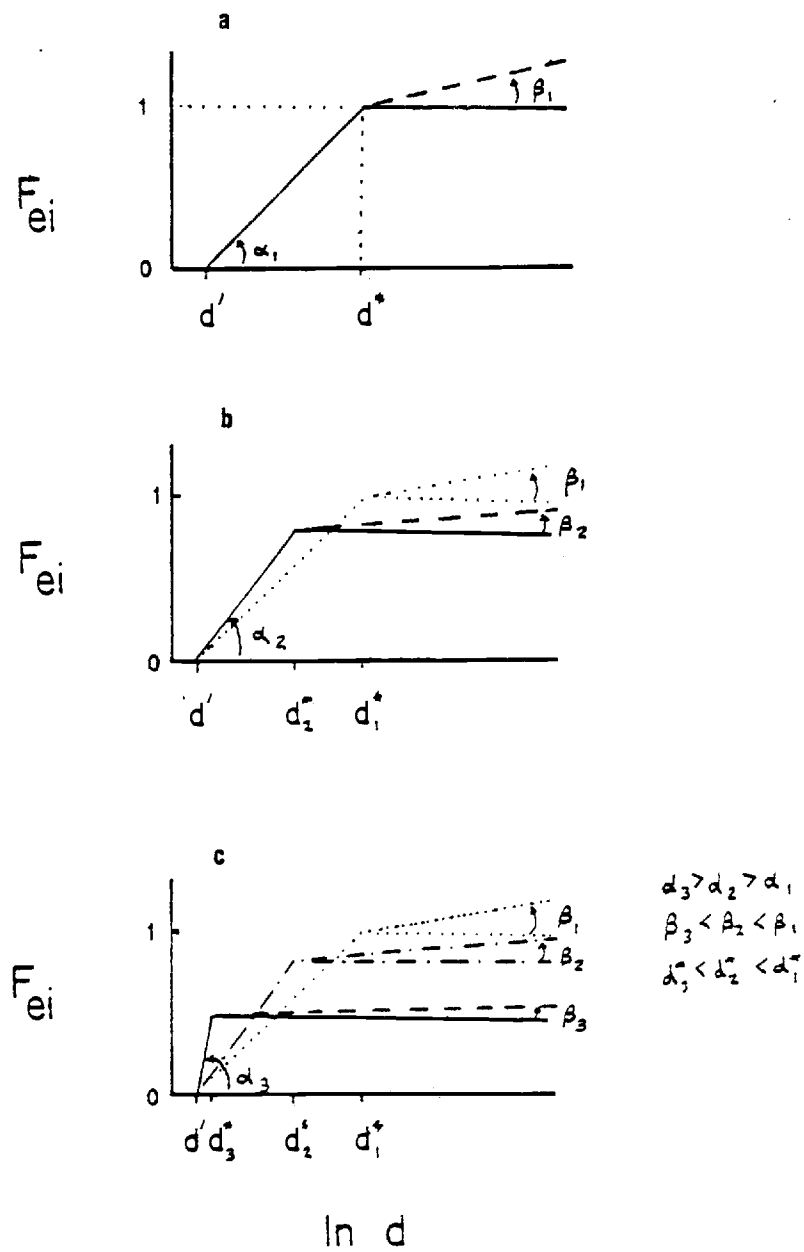


Fig. 6. Properties of theoretical filtering efficiency curves. Terms defined in text.

occur only for particles greater than the maximum setule based pore size, d_1^* . This will result in an increasing capture rate at particle sizes greater than d^* . The rate, defined by the slope β will increase as intersetal spacing (\emptyset) increases. In case 2 (Fig. 6b and 6c), in which intersetal and intersetule spacings overlap, the picture is more complex. Consider two subcases. If the minimum intersetal spacing is approximately equal to the minimum intersetule spacing, then intersetal capture will occur at all particle sizes. Since there is an overlap of setule- and setal-based pore sizes, there will be an enhanced efficiency of capture for small particles (compare dashed and solid lines in Fig. 6b at particle sizes $<d_2$). This enhanced capture efficiency for small particles will be reflected in an increased value of α_2 . However, because of the increase in overlap of setae and setule spacing, there will probably be some setule overlap and the total area of the filter will be slightly reduced. The smaller filter area will result in a smaller maximum efficiency ($F_{\max 2}$) at any given filtering rate (absolute, not apparent, filtering rate--see Donaghay et al., in prep.). The concomitant reduction in \emptyset necessary for such setule overlap will result in a reduction in the effectiveness of intersetal capture of very large particles; as a result, β_1 will also decrease to β_2 (Fig. 6b). If setal spacing is variable, as overlap further increases (via reduction in \emptyset), α will further increase from α_2 to α_3 and $F_{\max 2}$ and β_2 will further decrease to $F_{\max 3}$ and β_3 (Fig. 6c). Under conditions of increasing overlap of setal and setule pore sizes, there will be three very significant changes in feeding response. First, in contrast to Case 1, d^* will no longer be equal to the effective maximum setule defined pore

size: as the setae close down, the largest setule pore size will probably be reduced by overlap of setules, reducing d_1^* to d_2^* or d_3^* in Case 2. Secondly, α will no longer be fixed as in Case 1, but will increase as \emptyset decreases to α_2 or α_3 ; thus, the slope of the rapidly increasing segment of the filtering curve will no longer be determined by setule spacing alone. Thirdly, alteration of \emptyset in Case 2 has a strong effect on the relative efficiency of capture of small relative to large particles while in Case 1 it has no effect.

With these two cases in mind, the effects of \emptyset , δ , combing, axis of variance and λ can be considered on the expected filtering efficiency curve. The possible responses of a copepod to two different selection demanding situations will be considered using first the constraints of Case 1, then of Case 2. The twelve possible relevant combinations of \emptyset , δ , combing, axis of variance and λ are shown in Fig. 7. Relevant combinations are those combinations where the results of one factor do not negate the combination of any subsequent factors, i.e., full combing negates the possible effects of axis of variance and λ . The expected filtering efficiency curves were derived for a copepod using a given relevant combination and trying to best handle two situations: (A) to enhance ingestion of a large cell and reject a small cell and (B) to enhance ingestion of a small cell and reject a large cell (Fig. 8). It is assumed that the penalty for not altering feeding behavior is large enough to insure the maximum response possible.

The simplest combination involves a fixed \emptyset , $\delta = 90^\circ$, full or partial combing and an undefined axis of variance. This is essentially the leaky sieve model of Boyd (1976). When \emptyset is fixed, no selection is

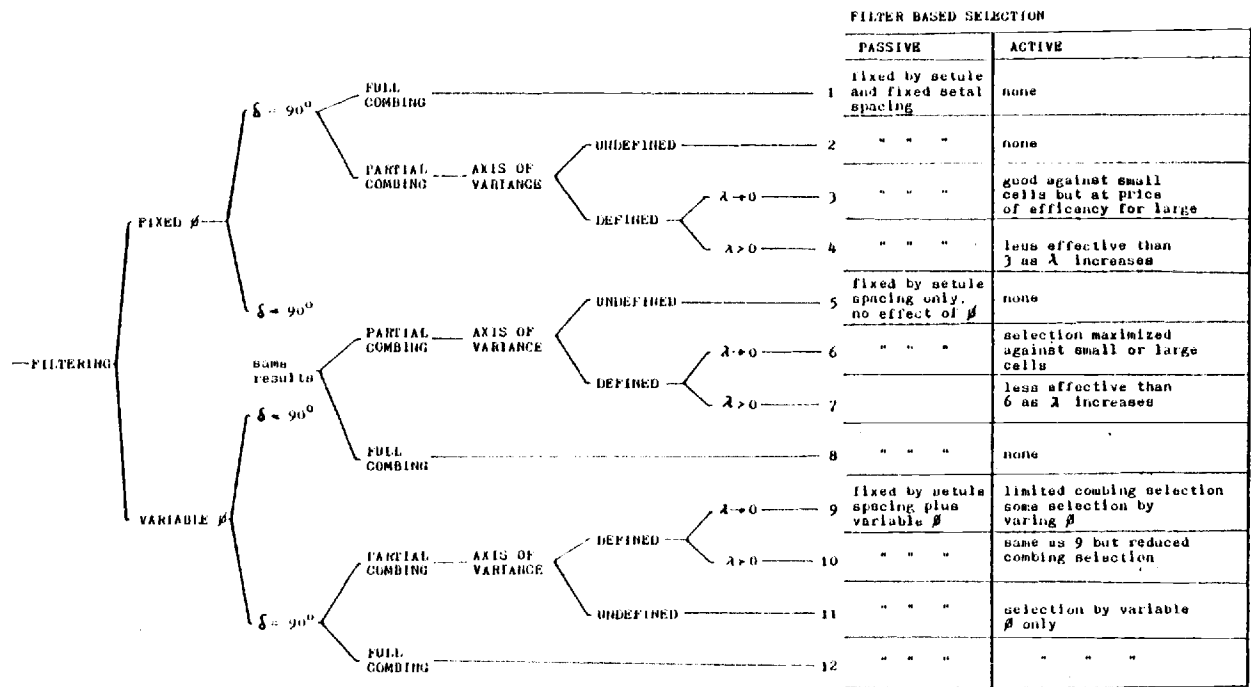
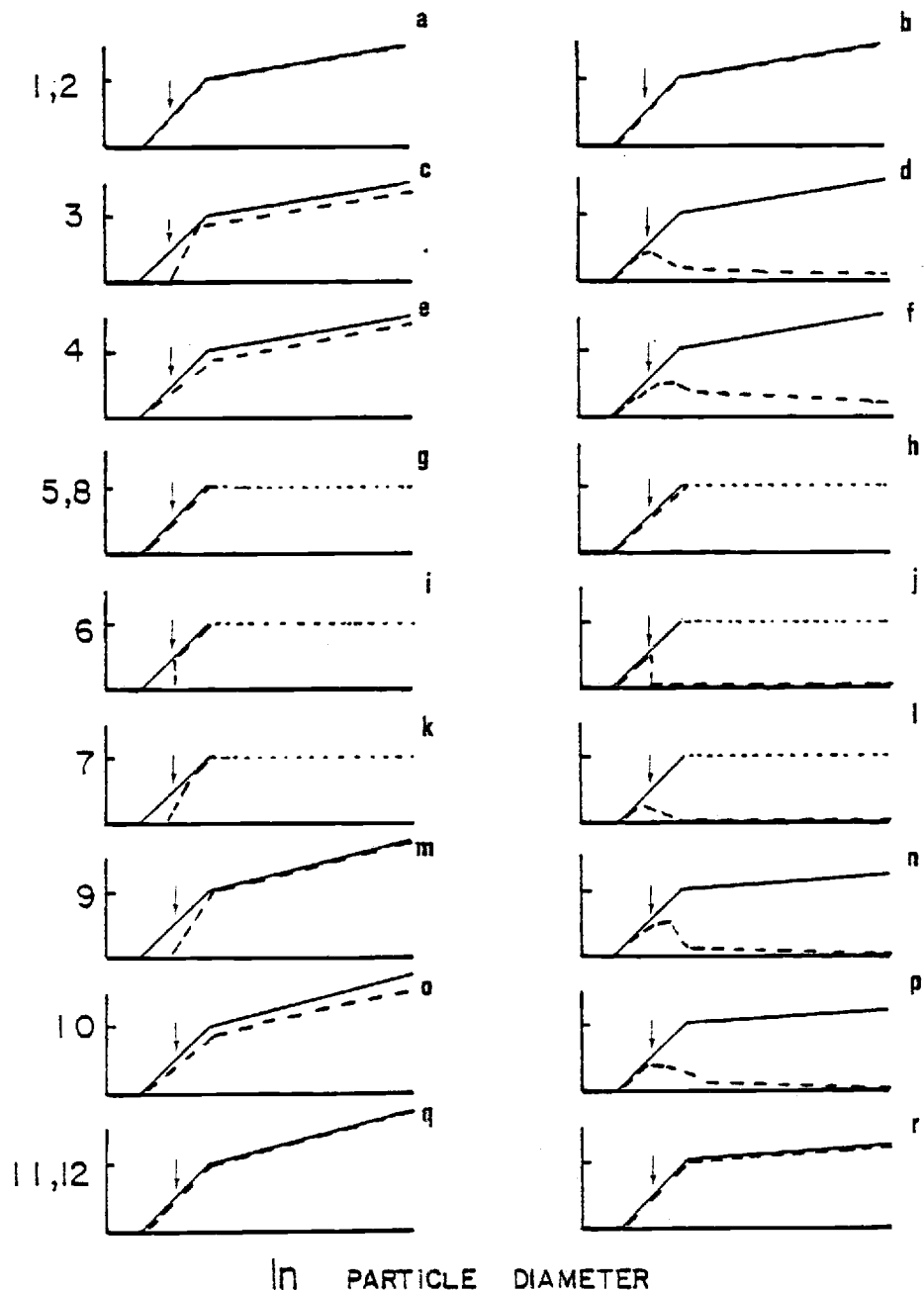


Fig. 7. Possible relevant combinations of θ , δ , combing, axis of variance and λ . Combination number refer to the combination of options connected by lines to the left of the combination number. The results of active and passive filter based selection are listed to the right of the combination numbers. The expected filtering curve resulting from these combinations are shown in Fig. 8.

Fig. 8. Expected filtering curves if minimum intersetal distance is greater than maximum interstetule distance (Case 1, Fig. 6). Combination numbers refer to combinations listed in Fig. 7. Solid line refers to curve resulting from passive properties of filter plus \emptyset change based active selection; dashed line represents effect of active plus passive selection. Dotted line above inflection point in combinations 5, 6, 7, 8 refers to responses defined only if filter is operated as a hybrid. Selection is assumed to be for particles larger than (a) or smaller than (b) a particle of the size indicated by the arrow (\dagger).

ENHANCE LARGE
REJECT SMALL

ENHANCE SMALL
REJECT LARGE



possible against large or small cells and the filtering curves will be identical for both situations (Fig. 8a compared to 8b). Full combing or partial combing with an undefined axis of variance have the same results (combinations 1 and 2, 5 and 8, 11 and 12) regardless of \emptyset or δ (Fig. 8). In these cases partial combing can result only in a reduction of efficiency at all particle sizes since particles are randomly distributed on the filter surface (because of an undefined variance axis). If, however, the axis of variance is defined under fixed \emptyset and $\delta = 90^\circ$, some selection is possible depending on how small λ is (condition 3 and 4, Fig. 8c,d,e,f) (i.e., how close the axis of combing is to the axis of variance). Selection against small cells will be relatively good with complete exclusion of cells smaller than a given size selected against (denoted by arrow in Fig. 8c) if λ is small. However, this selection will be at the price of lowered efficiency for large particles because large particles are trapped at setule pores smaller than the particle size selected against (Fig. 8c). Selection against large cells, however, will be much poorer with complete exclusion impossible, since such particles are trapped at all pore sizes (Fig. 8d). Under these same conditions of fixed \emptyset , $\delta = 90^\circ$, and partial combing, but with increases in λ , the ability to discriminate against a given size will be sharply reduced along with a reduction in capture efficiency for the preferred food (Fig. 8e,f). It would seem that the limited benefits of combinations 3 and 4 would make it unlikely that this combination has evolved.

The results for variable \emptyset with the other factors being the same as above are similar in many respects but with one major difference (combination 9, 10, 11, 12, Fig. 8m,n,o,p,q,r). Again, full combing or

partial combing with an undefined axis of variance give similar results (Fig. 8q,r). However, in this case some selection is made possible by variable \emptyset . When selection is for large cells, \emptyset would be maximized and the slope of the curve above d^* will be steeper (i.e., β is increased). Since the slope of the filtering curve is fixed between d' and d^* , no active selection is possible between two particles occurring within this size range (i.e., as in condition 3, Fig. 8c and d); selection, however, is possible between particles less than d^* and those greater than d^* . Such selection can result in the enhancement of capture of one particle type over another, but cannot result in the exclusion of an unwanted particle type. Selection resulting from a change in \emptyset plus the passive component of setule spacing should be the same for conditions 9 to 12 (Fig. 8m,n,o,p,q,r). The results of active selection with variable \emptyset will be identical in form to those observed in the parallel case with fixed \emptyset : condition 9 will be similar to 3 (Fig. 8m and n to 8c and d) and condition 10 will be similar to 4 (Fig. 8o and p to 8e and f).

The most pronounced selective results are provided when $\delta < 90^\circ$. The same results will be observed regardless of whether \emptyset is fixed or variable, because when $\delta < 90^\circ$ no intersetal capture occurs. Because no intersetal capture occurs, filtering curves are only defined between d' and d^* (minimal and maximal setule pore sizes). Definition of the filter curve at particle diameters exceeding d^* will occur for copepods with hybrid filters or with copepods employing raptorial feeding for such large particles. With full combing or partial combing with an undefined axis of variance (condition 5 and 8), filtering curves will be identical in shape regardless of selective conditions (Fig. 8g and 8h).

However, if the axis of variance is defined and λ is small, then very precise selection can occur against small (Fig. 8i) or large (Fig. 8j) cells. Only with this combination will total exclusion of unwanted food types be possible without a reduction in filtering efficiency for the preferred type. In addition, if multiple entry combing occurs, this is the only combination that can result in selection against an intermediate sized particle with ingestion of particles both smaller and larger in size. The precision of the discrimination against a particular sized particle will decrease as λ increases (Fig. 8k, 8l).

Having considered the expected filtering curves resulting from Case 1 (Fig. 6a) where intersetal and intersetule based pores do not overlap in size, we can now ask how these curves are affected if such overlap occurs. The presence of such overlap (except as already discussed in connection with Fig. 6a) will only have a significant effect on selection when \emptyset is variable and $\delta = 90^\circ$; i.e., filtering curves for combinations 9-12 in Fig. 7 and Fig. 8m,n,o,p,q,r. When $\delta < 90^\circ$ all capture is on the setules so no effect of pore size overlap would be expected on selection (although filtering efficiency might be reduced as total filter area is reduced by reduction of \emptyset). When $\delta = 90^\circ$, and \emptyset is fixed, the presence of overlap will not affect selection, although the existence of such overlap will cause d^* (and possibly d') of the observed filter curve to be different from the d^* and (possibly d') values expected from minimum and maximum setule spacings. However, if \emptyset is variable and $\delta = 90^\circ$, alteration of \emptyset will strongly affect selection (Fig. 9). In the discussion of Fig. 6c, alteration of the filtering curve by alteration of \emptyset has already been considered. These effects are

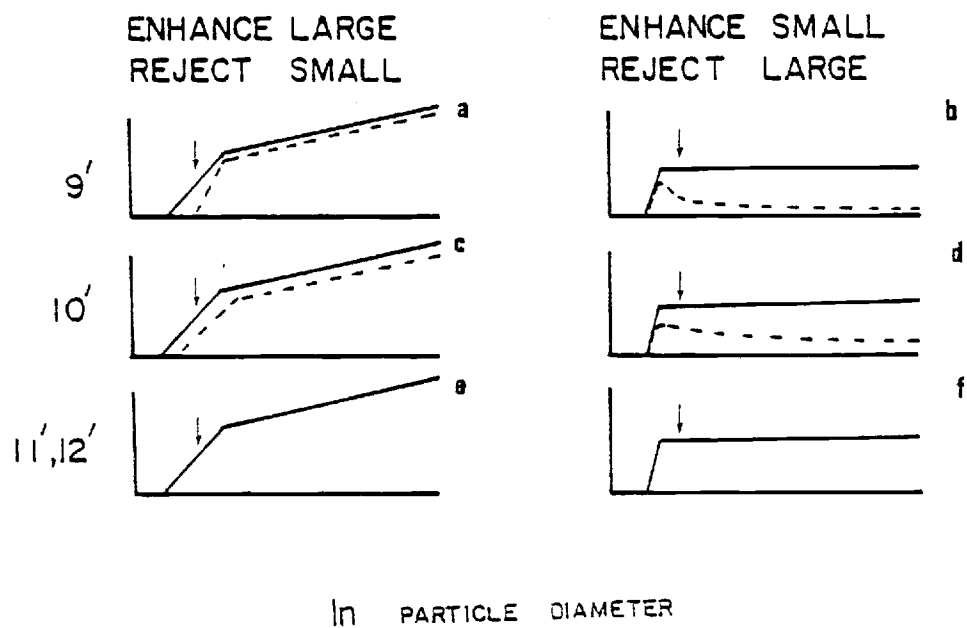


Fig. 9. Expected filtering efficiency curves if minimal intersetal distance is approximately equal to minimal intersetule distance. Only combinations 9, 10, 11 and 12 are shown. See text for explanation. Figure legend otherwise same as Fig. 8.

reflected in Fig. 9 in that variable ϕ under conditions of pore size overlap becomes a powerful tool by itself in selecting for small cells, with a gain (rather than a loss or no change) in efficiency of capture (compare Fig. 9f to Fig. 8r). However, because setal capture occurs at all sizes (in Case 2b, Fig. 6c) combing is less effective in selecting for either small or large cells than it was with no overlap of setal and setule pore sizes (compare condition 9 & 10 of Fig. 8m,n,o,p with 9 & 10 of Fig. 9a,b,c,d).

The filtering curves predicted in Figs. 7, 8 and 9 are based on direct filtering of particles onto the maxillae. Since any feeding mechanism can result in the data required to calculate an experimentally derived filtering curve, the question arises as to how one can differentiate the above filtering curves from those produced by the other feeding mechanisms (raptorial feeding and concentrating type filter feeding). If sufficient numbers of captures occur to experimentally generate an "apparent filtering curve" for raptorial feeding, the curve should have four properties (Fig. 10a,b). First, since encounter is dependent on sensing at a distance rather than on filter design, the "apparent filtering curve" should be totally independent from a curve derived from maxillary pore sizes. Second, over the range of sizes which prey can be detected, the filtering curve should be independent of size insofar as the mechanism for sensing prey at a distance is size independent. Third, the filtering curve should only be defined for fairly large particles because of size limitations of the sensing mechanism and because of capture rate limitations imposed by the sensing and handling processes. Fourth, the selective response to large or small

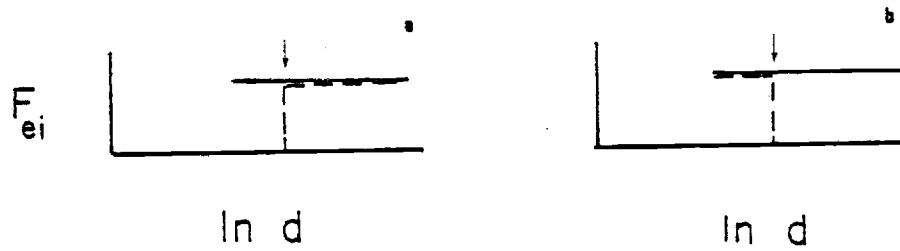


Fig. 10. Expected "filtering curves" for raptorial feeding copepods. Solid line represents range of sizes over which prey are sensed at a distance. It is assumed that such sensing is prey size independent over this size range. Dashed line represents response to selecting for prey smaller than (a) or larger than (b) prey of size designated by arrow (+). The arrow here is located at a larger size than in Figs. 8 and 9.

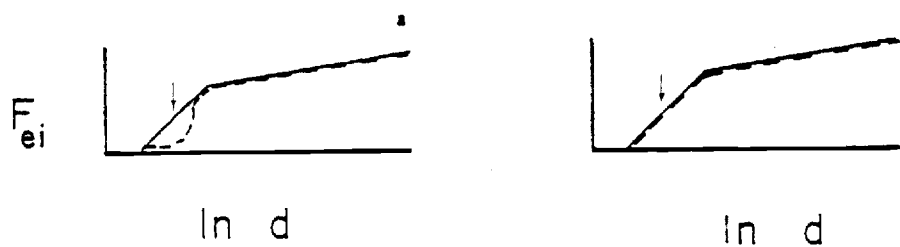


Fig. 11. Expected filtering curve for "Strickler motion." Legend same as in Fig. 8 except dashed line now is the selective effect of not ingesting all concentrated particles at the end of each stroke. See text for details.

prey (within the range of sensing) should be very sharp (with total exclusion of unwanted prey) regardless of the distribution or size overlap of those prey.

Two methods of using the feeding appendages as concentrating devices were discussed in Fig. 1: oriented flow and Strickler motion. Oriented flow will result in "apparent filtering curves" that behave identically to full combing combinations in Fig. 7, 8 and 9. The curves should have identical shape if the other variables are the same (\emptyset , δ , etc.). Combing selection in this case will not exist. For oriented flow, the most useful method of particle selection is alteration of \emptyset under conditions where setal and setule based pore sizes overlap (Case 2, Fig. 6b,c). This mode of feeding can be differentiated from true filtering modes only by observing whether particles are combed from the filter or flow continuously to the mouth.

Use of the appendages as a concentration device as described by Strickler and Rosenberg (1977) (Strickler motion, Fig. 1, Table 1) will result in a unique filtering curve under certain conditions. Recalling that the Strickler motion involves using both the maxillae and the swimming legs to form a basket to concentrate particles from the water (or drain off water from the particles), the shape of the "apparent filtering curve" resulting from removal of all particles from the basket following each stroke (closure) should be a function of the combined setal and setule capture by the maxillae, and to some unknown extent the setae and setules of the swimming legs. The resulting curve may have the same shape as those in Fig. 8, or may be different. If, however, multiple strokes are taken before captured particles are ingested from

the basket, a very different and unique curve will result (Fig. 11a,b). In this case, small particles captured on one stroke will be refiltered on the next stroke and have an additional opportunity to pass through larger pore sizes. This will not occur for particles larger than the maximum pore size. As a result, the filtering curve will have a sigmoid shape that is progressively enhanced (i.e., steepened) by the number of strokes taken before particles are ingested. This multiple sieving mechanism might yield a very efficient method for selecting against small particles, particularly if those particles are such that they might stick to (or clog) the filter if combed from it. This method would not be effective in rejecting large particles.

The theoretically derived mechanisms discussed above differ greatly both in their mechanistic and behavioral complexity and in their resultant selective powers. It seems likely evolution would favor only two different classes of mechanisms: those that are behaviorally complex but have strong selective powers and those that are mechanistically and behaviorally simple. It seems unlikely that behaviorally complex mechanisms would have evolved without some definite benefit attached. Conditions 2, 3, 4, 5, 8, 9, 10, and 11 (Fig. 7, 8, both Cases 1 and 2) provide little selective power considering their complexity. It seems unlikely that these mechanisms will be observed. Condition 1 (fixed θ , $\delta = 90^\circ$, full combing [or oriented flow], Case 1) is basically the leaky sieve model of Boyd (1976); it is mechanistically very simple with no active behavioral selection. Some selective power against small particles is gained by the Strickler concentrating motion without much increase in complexity: the potential advantages against small sticky

Table 4. Expected properties of the five most likely alternative models. Terms as in text and as defined in Fig. 1 and Table 1 except "f" equals fixed and "v" equals variable.

MODEL	FEEDING TYPE	PROPERTIES	DISTINCTIVE FILTERING CURVE	FILTERING CURVE			
				d'	d*	α	β
LEAKY SEIVE	Filtering or Concentrating Oriented flow	β = fixed δ = 90° full combing (if done)	d', d*, α , β , fixed all conditions d* = max. pore size if Case 1 (Fig. 5) d* < max. pore size if Case 2 (Fig. 5)	f	f	f	f
STRICKLER MOTION	Concentrating Strickler Motion	β - variable or fixed combing full (if done)	sigmoid shape of F curve in response to rejection of small sticky particles	f	f	v	f
WILSON FILTER	Filtering or Concentrating Oriented flow	β - variable δ = 90° Case 2 (Fig. 5) full combing (if done)	d' - fixed (min. setule pore size) d* - movable and \neq max. setule pore size α , β both vary with d* α , β , d* vary with β	f	v	v	v
DROP FILTER	Filtering onto maxillae with partial combing	β : not significant δ < 90° axis of variance defined, $\lambda \neq 0$ partial combing	d' - fixed min. setule pore size and d* - fixed at max. setule pore size if all particles equal; in challenge, d', d* moveable β usually 0	v	v	f	f

materials (particularly without combing) are large and make this mechanism likely. Additional selectional power against both large and small particles is gained in combination 12, with $\delta = 90^\circ$ (Fig. 8q,r) by varying \emptyset , particularly if setal and setule spacing overlap (Fig. 9e,f). This is basically the model proposed by Wilson (1973). Since combing provides almost no advantage when setule overlap is large (with variable \emptyset but $\delta = 90^\circ$), it would seem likely that oriented flow or Strickler motion would be employed rather than capture directly on the filter with subsequent combing. However, both may be observed. The greatest selective power, but also the greatest mechanical and behavioral complexity, is found with combination 6 (Fig. 8i,j) - the drop filter model. The complexity of this mechanism makes it likely that it will only be employed (or have evolved) only under conditions where high degrees of selection are required at high encounter rates.

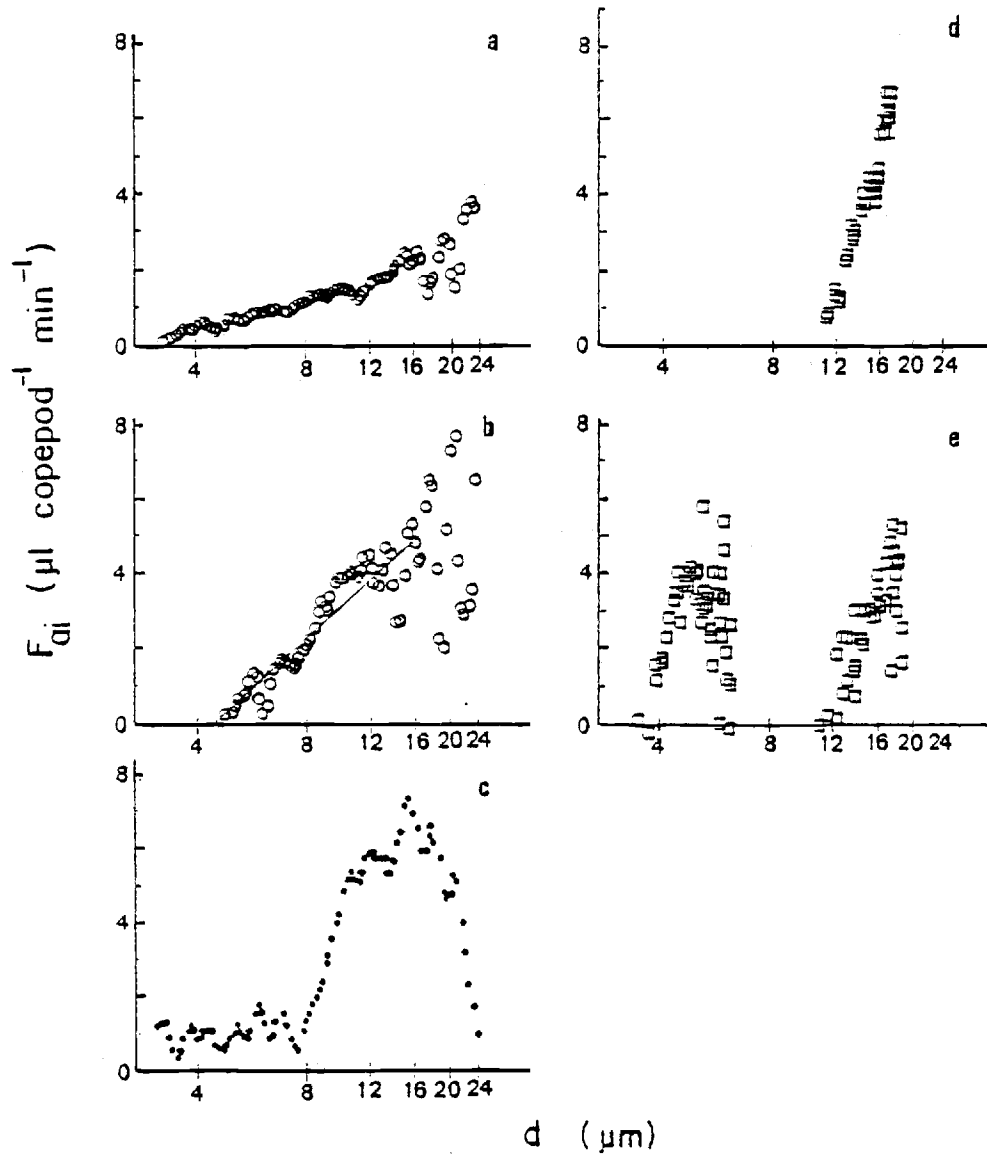
The expected properties of the above four most likely models are summarized in Table 4. Careful analysis of these properties demonstrates that the expected filtering efficiency curve shapes (as defined by d' , d^* , α , β) should be unique. Differences in shape, however, will only be observed when conditions are such that there is a strong advantage for a copepod to be as selective as possible.

Experimentally derived filtering curves are now available for a limited number of copepod species grazing on a wide variety of field and laboratory particle spectra. For rigorous interpretation of the data in terms of filtering theory, only those data free of particle modification effects (O'Connors et al., 1976) or other effects of algal-grazer interactions, can be used. The most extensive set of data of this kind

is for Acartia clausi and includes the field data of Richman et al. (1977) and the laboratory data from Donaghay and Small (1979b) and Donaghay (1979).

The various types of filtering curves reported for Acartia clausi are shown in Fig. 12. The field data illustrate two distinct patterns: rectilinear and sigmoid (Fig. 12a,b,c). Rectilinear filtering curves were always observed when Acartia clausi was fed natural particle spectra dominated by a single broad peak. Sigmoid shaped F_{ai} curves were observed when particle spectra had no clear peak, but rather particle concentration increased monotonically with size. It is apparent from the F_{ai} curves that the particle size at which F_{ai} begins to dramatically increase varies widely from 2 μm (AC10, Fig. 12a) to 4 μm (AC11, Fig. 12b) to 9 μm AC12, Fig. 12c). The slope of the F_{ai} curve, α' , and the value of d' can be estimated by regression analysis of the log-linear sections of the F_{ai} curves (Donaghay et al., in prep. a). The value of α' so determined is an estimate of α confounded by the effects of particle concentration on filtering rate. In order to remove these confounding effects, it is necessary to normalize the F_{ai} curves to the F_{ai} value in the size class equivalent to the maximum intersetule spacing (F_{ad}). The maximum intersetule spacing for Acartia clausi is about 15 μm . Values of F_{ai} at 15 μm (F_{a15}) were estimated from the regression analysis of the log linear section of the F_{ai} curves (Table 5). For the two rectilinear curves (AC10 and AC11, Fig. 12a and b), the regression analyses clearly there is little question as to what particle size classes to include in the logarithmic section: F_{ai} increases logarithmically from 3 μm to 15 μm after which variability in F_{ai} increases

Fig. 12. Shape of experimentally-derived filtering curves for Acartia clausi from grazing experiments on natural field particle suspensions (a,b,c) and from artificial laboratory mixes of single celled diatoms and inert plastic spheres (d,e). Fig. 12a,b,c are redrawn (to a common scale) from data of Richman et al., 1977 for Acartia clausi feeding on particles collected from Chesapeake Bay, Maryland, USA. The nature of the food mixes and animal preconditionings are defined in the text. Symbols are for data consistent with varying models: leaky sieve (o); Strickler motion (●) and drop filter (◻).



dramatically (due to poor counting statistics). However, in AC11, there is some indication that F_{ai} begins bending over at about 12 μm . If α and d' values are calculated from regression of values less than 12 μm , α increases slightly but there is no significant change in d' . Such an increase in α only increases the differences in α between AC10 and AC11. Attempts to estimate β by regression analysis of values above 15 μm show that β is not significantly different from zero. Because of the high data variability above 15 μm , the conclusion that $\beta = 0$ must be considered tentative. However, according to D. H. Heinle (personal communication) none of the field experiments with Acartia clausi have shown β to be greater than zero.

The above field data would appear to be strong evidence for the drop filter model: α and d' vary but $\beta = 0$ and d' equals maximum inter-setule pore size. However, such a conclusion may be premature since the differences in d' are well within the seasonal range of inter-setule pore size reported for Acartia clausi (Conover, 1956). Without measurements of minimal inter-setule pore size, these data must be considered still consistent with all but the Strickler motion model.

The sigmoid shaped apparent filtering rate curve (AC12, Fig. 12c) is clearly not explainable by the leaky sieve or Wilson filter models. Although it appears to be consistent only with the Strickler motion model, it could be argued that the sharp reduction in F_{ai} below 9.5 μm was the result of counting behavior with the drop filter model. Because of this possibility, regression analyses were performed on the three log-linear segments of the F_{ai} curve (Table 5). Since only the segment above 9.5 μ appears free of rejection events, it was used to calculate

TABLE 5. RESULTS OF REGRESSION ANALYSIS

$$F_{ai} = \alpha' \ln(d) + F'_{ai}$$

EXPERIMENT	SEGMENT		REGRESSION			MEAN if $\alpha' = 0$ mean \neq lsd	CALCULATED VALUES			
	min.	max.	F'_{ai}	α'	R^2		d'	α	F_{a15}	F_{a12}
Richman, et al (1977) <u>A.c.</u> 10	3.15	23.4	- 1.36	1.26	.832	-	2.94	0.614	2.05*	-
	3.15	15.1	- 1.16	1.15	.925	-	2.74	0.588	1.95*	-
	15.4	23.4	-	-	-	2.40 \pm 0.74	-	-	-	-
Richman, et al (1977)	4.6	15.1	- 5.70	3.86	.845	-	4.38	0.812	4.75*	-
	4.6	12.0	- 7.46	4.79	.938	-	4.74	1.077	5.52*	4.45
	15.4	23.4	-	-	-	4.69 \pm 1.65	-	-	-	-
	12.1	23.4	-	-	-	4.45 1.47	-	-	-	-
Richman, et al (1977) <u>A.c.</u> 12	3.01	7.56	-	-	-	1.01 0.32	-	-	-	-
	7.40	9.32	- 22.50	11.59	.976	-	6.97	1.304	8.89	-
	9.52	15.10	- 5.90	4.61	.722	-	3.60	0.701	6.57	-
	9.97	15.10	- 4.10	3.91	.627	-	2.86	0.603	6.48	-
<u>A.c.</u> on <u>Thalassiosira</u> <u>fluviatilis</u>	2.45	2.71	- 30.87	12.89	.941	-	10.98	3.203	4.02	-
<u>A.c.</u> on <u>T. pseudonana</u> + spheres + <u>T. fluviatilis</u>	1.30	1.48	- 31.04	23.68	.970	-	3.71	0.716	33.07	-
	2.50	2.71	- 20.08	8.45	.656	-	10.79	2.998	2.82	-

* F_{ad} values not significantly different from mean for particle sizes $> d_s$.

d' and F_{a15} . This assumption appears reasonable since the F_{a15} value so calculated is close to the maximum F_{ai} value observed and the d' value so calculated is intermediate to the d' values for the two rectilinear curves (Table 5). Although the sharp drop in filtering efficiency below 9.5μ can be explained by combing, such combing cannot explain the low but constant F_{ai} values from 3μ to 7.6μ . This field data is therefore in strong agreement only with the Strickler motion model.

Rectilinear patterns similar to those observed in the field can be generated in the laboratory when single foods are offered. However, by carefully controlling the composition of the different size classes in the particle spectra and the preconditioning of the copepods, radically different patterns can be generated (Donaghay and Small, 1979b; Donaghay, 1979). When Acartia clausi was preconditioned on a large single celled diatom, Thalassiosira fluviatilis, the F_{ai} curves generated from grazing experiments showed that both d' shifted to the size of the smallest cell of T. fluviatilis (11μ) and α became much larger (3.2 vs. 0.6 to 0.8 in the field data) (Table 5, Fig. 12d). Part of the same collection of A. clausi (with the same minimum and maximum intersetule pore size) was observed to have d' values of 3.7μ and α of 0.716 when preconditioned on a small single celled diatom, Thalassiosira pseudonana. These laboratory data showing change in both α and d' are thus evidence for the combing model.

The strongest evidence of combing reported by Donaghay and Small (1979) occurred when Acartia clausi was offered a particle mix consisting of a small food, Thalassiosira pseudonana, an intermediate sized inert sphere and a large food, Thalassiosira fluviatilis. When copepods

preconditioned on the small food were offered this mix, a very different F_{ai} curve was observed (Fig. 12e). F_{ai} first increased to a maximum in size classes dominated by the small diatom, then fell to very low values in size classes dominated by spheres only to increase again in the large size classes dominated by the large diatom. The value of d' ($3.7 \mu\text{m}$) was intermediate to those observed in the field data (2.7 to $4.4 \mu\text{m}$). Since there appeared to be some effects of rejecting the spheres on all values of F_{ai} larger than the mode of the T. pseudonana peak, the determination of F_{a15} was based on the regression analysis of the log linear section of the T. pseudonana peak (Table 5). The resulting F_{ad} value was large ($33 \mu\text{l}/\text{copepod}/\text{minute}$). This rate is close to the highest rates observed for A. clausi feeding on particles of $15 \mu\text{m}$ at low concentrations. The value of α calculated from this regression, 0.716 , was intermediate to those observed in the field data (0.6 to 0.8) and is thus very reasonable. However, because the value of F_{a15} was based on an extreme extrapolation of the regression, the values of F_{a15} and α must be considered as very tentative. If the values of α so calculated is correct, then it would imply that α and therefore setal spacing were not altered in response to the presence of spheres, but rather filtering rate was maximized to capture small cells and combing was used to eliminate spheres. Regardless of whether the value of α is correct, the process whereby the spheres were rejected resulted in considerable reduction in F_{ai} values for those particles approaching the size of the spheres, i.e. large cells of T. pseudonana and small cells of T. fluviatilis. Such a reduction in F_{ai} 's for these cell types would not be expected if post-combing rejection were used to reject the spheres.

However, such a reduction would be expected if combing were used (with a drop filter model) for two reasons. First, since spheres and T. fluviatilis overlap at the smaller cell sizes, some rejection of captured small T. fluviatilis will occur in the rejection of like sized spheres. Second, since there is some variability in the pattern of pore spacing on the maxillae of A. clausi, and since λ is probably not zero, combing will result in rejection of cells slightly larger and slightly smaller than the size of the spheres. This laboratory data involving rejection of inert particles between food peaks is consistent with the drop filter model.

It would appear reasonable to conclude from the above data that the patterns observed are compatible with (or potentially support) the use of at least two different feeding modes by Acartia clausi: the drop filter and the Strickler motion. Data with a broader range of sizes (both field and laboratory) needs to be examined to determine if d^* and β are also variable or are fixed. The high degree of flexibility in feeding response obtained by use of more than one feeding mechanism should not be unexpected for a copepod such as Acartia that often dominates highly variable estuarine environments.

(3) Experimentally defined selective capabilities.

The conceptual idea behind capability experiments is to set up conditions that will elicit selective feeding behavior if that behavior is possible for a given species. Capability experiments (Donaghay and Small, 1979b; Donaghay, 1979) are the most rigorous methods for testing the conceptual (but not mechanistic) validity of the feeding models.

They are also useful in determining the appropriate model(s) and the flexibility of feeding behavior for a particular copepod species. The results of such experiments for Acartia clausi provides the strongest evidence for the drop filter model (Donaghay and Small, 1979b; Donaghay, 1979). The basic method is summarized in Fig. 13 and Table 6.

(4) Codevelopment of structure and behavior with ontogeny.

As copepods develop through their life history stages massive changes occur in their feeding appendages (Marshall and Orr, 1955, 1956). Study of the parallel development of structure and capabilities should allow critical testing of the relationship between behavior and structure, an important foundation of the feeding models. The development of a behavior prior to the development of the structures predicted by the model to be essential for that capability will allow rejection of that mechanism. Development of morphology several stages prior to the first expression of a theoretically associated behavior implies that neurological and physiological development in addition to the required morphology is essential to that behavior. Codevelopment of morphology and behavior as predicted by the model is strong evidence for the mechanistic aspect of that model. Comparison of structure and behavior between species should provide similar, although less critical, tests of the relationship between morphology and function. Although nothing has been published on the codevelopment of behavior and structure, work is in progress in this area (B. Dexter, personal communication).

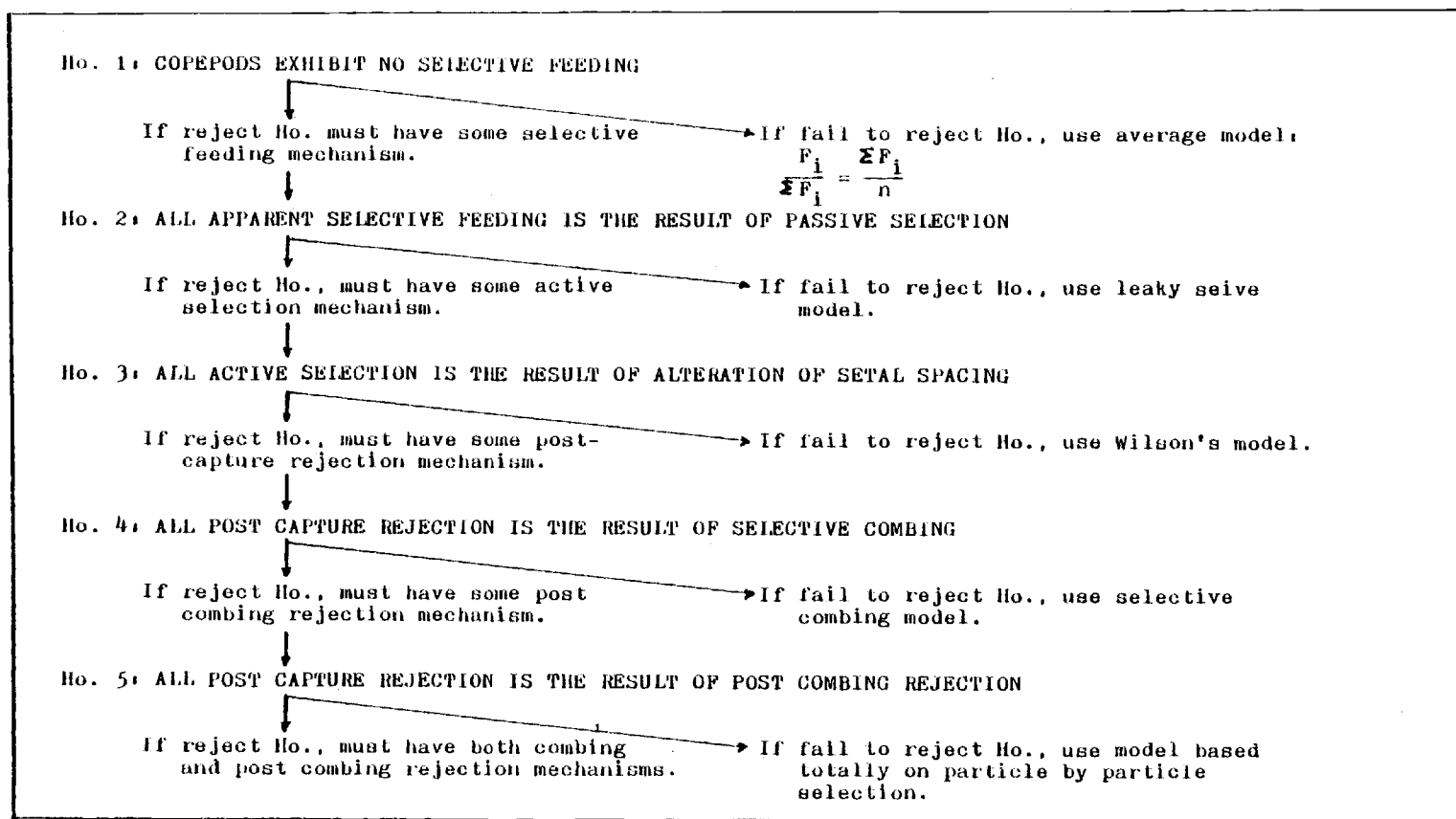


Fig. 13. Serial hypothesis test used to define selectional capabilities of a copepod. Methods for testing each hypothesis are summarized in Table 5. For experimental details of tests 1-3 see Donaghay and Small (1979b); for details of test 4 see Donaghay, 1979a. Test of Ho 5 has not been experimentally evaluated as yet.

Table 6. Method of testing the hypothesis of selective capability shown in Fig. 13.

HYPOTHESIS TESTED	TEST SUB-HYPOTHESIS	EXPERIMENTAL TEST
Ho 1: Copepods exhibit no selective feeding.	Filtering efficiency is constant for all sized particles.	Run ingestion experiments on food mixes of particles ranging in size from 3 to 30um. Calculate apparent filtering rates, F_{ai} . Reject Ho if apparent filtering rates in i^{th} size class differ from the mean of all size classes.
Ho 2: Apparent selective feeding is the result of passive	Previous feeding history does not affect grazing rates or patterns.	Precondition copepods separately on a large and a small single celled diatom. Run ingestion experiments on mixes of both foods. Reject Ho if ingestion rates are unaffected by preconditioning.
Ho 3: Active selection is the result of alteration of setal spacing.	Non-food particles can only be rejected if smaller than food particles.	Precondition copepods separately on a large and a small single celled diatom. Compare the ingestion responses of these preconditioned copepods when offered a mix of both foods with and without an intermediate sized inert sphere. Also compare ingestion responses when a single celled diatom and a larger inert sphere are offered. Reject Ho if diatoms smaller than sphere are ingested but the inert spheres are rejected.
Ho 4: Post capture rejection is the result of selective combing.	Non food particles of the same size as food particles cannot be rejected.	Run ingestion experiments with food preconditioned animals where foods and non food particles of the same size are offered as a mix. Reject Ho if ingest food but not non food particles.
Ho 5: All rejection is via post combing rejection.	Rejection of particles of different sizes than a food and of the same size as a food should have the same time costs, ie, maximum filtering rates at low particle concentrations should be the same in both cases.	Generate filtering rate-food concentration curves with three combinations of particles: (1) food only; (2) food plus larger sphere; and (3) food plus an identical sized sphere. Reject Ho if maximum filtering rates in combination 2 are greater than in combination 3.

PART II: ASSIMILATORY CONTROL OF FEEDING BEHAVIOR

Lehman (1976) suggested that both capture and assimilation processes control observed feeding behavior. The above theoretical arguments define the passive elements of the feeding process and the possible mechanisms whereby active selective choices may be made; however, at the same time they provide no insight into why such active choices might be made. We shall now consider those assimilatory factors that control feeding behavior both quantitatively and qualitatively.

Ingestion is usually described in terms of functional relationships between ingestion rate and food concentration or apparent filtering rate and food concentration. Ingestion rate and apparent filtering rate are mathematically interrelated: ingestion rate equals the product of apparent filtering rate and the exponential mean biomass in the grazing vessel (Donaghay et al., in prep. a). The apparent filtering rate (as measured in a grazing experiment) is equal to the product of the true rate at which water is filtered (processed) by the feeding appendage and the relative efficiency with which particles of a given size are removed from the water. The laboratory experiments of Frost (1972) on Calanus pacificus first demonstrated that the relationship between ingestion and food concentration can be approximated by a rectilinear function (Fig. 14a). In the increasing segment of the curve, the copepod is filtering at the maximum rate possible (Fig. 14b). As a result, ingestion rate increases linearly with increasing particle concentration (Fig. 14a). Above some critical food concentration, the copepod's digestive process appears to become saturated, and ingestion rate becomes constant. The apparent filtering rate decreases with further increases in food concen-

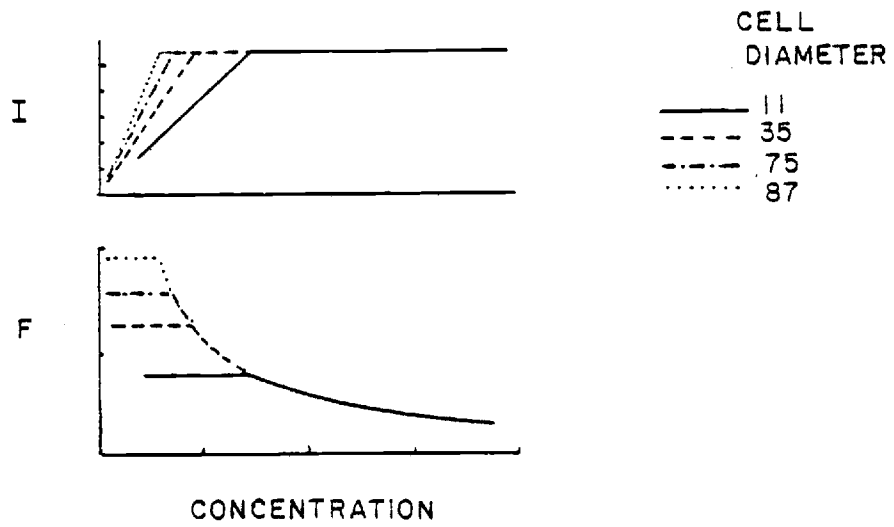


Fig. 14. Functional relationship of ingestion (a) and filtering rate (b) to food concentration. Redrawn from data of Frost (1972) for Calanus pacificus.

tration (Fig. 14b). Thus, below the critical food concentration ingestion for a particular sized particle is totally limited by maximum filtering rate and the relative capture efficiency for that sized particle. The slope of this segment of the curve can change only if (1) particle size is changed, (2) physiological adjustments are made to allow an increase in the maximum filtering rate, or (3) the filter is altered as in the above capture theory in such a way as to alter capture efficiency. The effect of increasing particle size on increasing the slope of the ingestion vs. concentration curve is clear in Frost's (1972) data (Fig. 14a). Whether the other two factors can affect the slope is untested.

Given the above, we may say that there is a capture process controlled segment of the ingestion curve and an internally controlled segment. The question, then, is what sets the limit on the internally controlled segment. Two divergent views have evolved from theoretical and experimental work on the internally controlled segment of the curve: (1) that it is fixed as a function of fixed metabolic needs and is independent of the digestive process or (2) that it is variable and controlled by digestive processes. Frost (1972) provided early experimental evidence and subsequent theoretical evidence (Lam and Frost, 1976; Steele and Frost, 1977) that the maximum ingestion rate, I_{\max} , is fixed. The idea is based on the observation that when Calanus pacificus was given a variety of foods, I_{\max} was food size independent on a carbon basis (Fig. 14a). However, since the different sized cells used in these experiments were all taxonomically very closely related (they were size clones of two species of the genus Thalassiosira), no difference in

digestibility would be expected. Although these data are in agreement with the fixed I_{\max} hypothesis, they are not a critical test of that hypothesis. The fixed I_{\max} model has been used extensively in grazing models (Lam and Frost, 1976; Steele and Frost, 1977).

The alternative viewpoint, that I_{\max} is a function of assimilatory processes, originated from the theoretical model of Lehman (1976). Lehman (1976) pointed out that copepods have very small guts with very rapid maximum gut passage times (~15 minutes). Lehman (1976), therefore considered maximum ingestion rate to be controlled by three factors: (1) the rate at which the volume of a food particle was reduced by digestion; (2) the rate at which energy and general nutrients were released from the food to be absorbed from the gut; and (3) the rate at which critical micronutrients were released from the food and absorbed from the gut. All three of these factors are under digestive enzyme control both quantitatively and qualitatively (although this was not explicitly stated by Lehman [1976]). In Lehman's model, ingestion rate is the net result of the copepod attempting to maximize its gain of energy and materials and minimize its costs of food capture and processing.

Aside from Lehman's purely theoretical arguments, a growing body of laboratory and field data have begun to challenge the fixed I_{\max} hypothesis. In those cases where large numbers of ingestion experiments were done to define a single ingestion curve, greater variability was observed than would be expected from experimental error (Frost, 1972, O'Connors et al., 1976; Robertson and Frost, 1977). The field measurements of zooplankton digestive enzyme activity and substrate concentra-

tion (Mayzaud and Conover, 1976; Mayzaud and Poulet, 1978) showed that there was a strong correlation between zooplankton digestive enzyme activity and substrate concentration, a correlation unexpected if I_{\max} were fixed. The first clear field evidence that I_{\max} was not fixed was provided by Conover (1976). Conover showed for what appears to be a single field population of Pseudocalanus that I_{\max} increased over a period of six days as the concentration of phytoplankton increased. These field results showing a strong effect on ingestion behavior of past feeding history were in strong agreement with our own laboratory results on preconditioning (Donaghay and Small, 1979a,b; Donaghay, 1979).

The above field data, coupled with Lehman's model and our own laboratory work, suggested the following conceptual argument (called the I^* hypothesis). In this hypothesis we are suggesting that within the limits defined by the maximum filtering capacity of the copepod (which increases with particle size), that the assimilatory capacity of the animal will control the ingestion processes both quantitatively and qualitatively.

Theoretical Basis for I^* Hypothesis

Mayzaud and Conover (1976) have shown that the activity of digestive enzymes for a particular food material is directly correlated with concentration of that substrate in the environment (Fig. 15) and that the enzymes can be induced by the presence of those substrates. Conover (1976), drawing directly from the data of Mayzaud and Poulet (1978), has also shown that for natural field populations, the ingestion rate curve

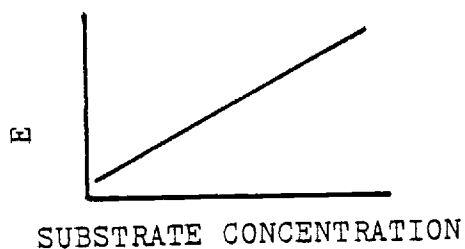


Fig. 15. Relationship between digestive enzyme activity and the concentration of appropriate substrate in the field environment from which the copepods were collected. This figure drawn after Figure 3, Mayzaud and Poulet, 1978.

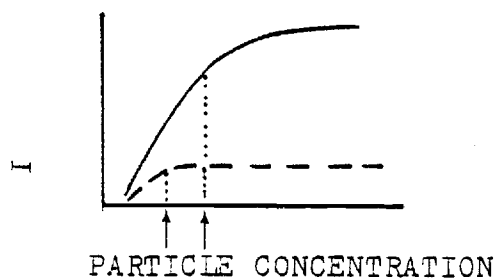


Fig. 16. Ingestion rate curves determined 6 days apart on Pseudocalanus sp. from Bedford Basin, N.S. (from Conover, 1976). Arrows denote ambient concentrations at times of animal collection.

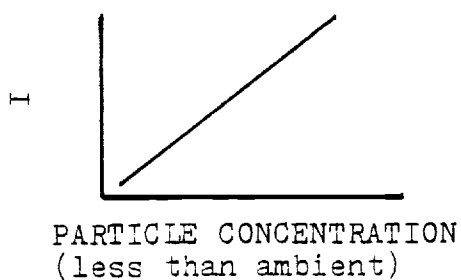


Fig. 17. Relationship between ingestion rate and particle concentration for all levels of food at or below that from which animals were collected. This figure drawn after Figure 1, Mayzaud and Poulet, 1978.

(Ivlev curve) tends to bend over at approximately the ambient food concentration (Fig. 16). As food concentration increases in the field, this inflection point increases in terms of both ingestion rate and particle concentration. As a result of the inflection point occurring at ambient food levels, the relationship between ingestion rate and food concentration for all values of food concentration less than or equal to the ambient concentration is a straight line (Fig. 17). This linear relationship implies that, within the animals' natural system, the animals always have sufficient levels of enzymes to digest or assimilate as fully acclimated animals at ambient concentrations of food. If we denote the inflection point of the rectilinear ingestion curve by I^* (Fig. 18a), and all of the ingestion curves have zero (or constant non-zero) intercepts, then there must exist a single linear (Fig. 18b) or curvilinear (Fig. 18c) relationship between I^* and ambient food concentration at I^* (called C^*). If the amount of food ingested is controlled by the digestive enzyme activity (as implied by I^* occurring at natural concentrations), then I^* must also be close to the food level that the animals can just handle for enzymatic reasons. As a result, I^* should also be a function of digestive enzyme activity in the copepod's gut (Fig. 19). We shall consider below the consequences of the particulate matter changing faster than the animals can acclimate.

If these relationships are in fact generally true, then we should be able to estimate I^* by measuring digestive enzyme activity of grazers in the laboratory or in the field. This estimated I^* value can then be taken to the relationship between I^* and food concentration (Figs. 19b and 19c), and the food concentration at I^* (i.e., C^*) can be determined.

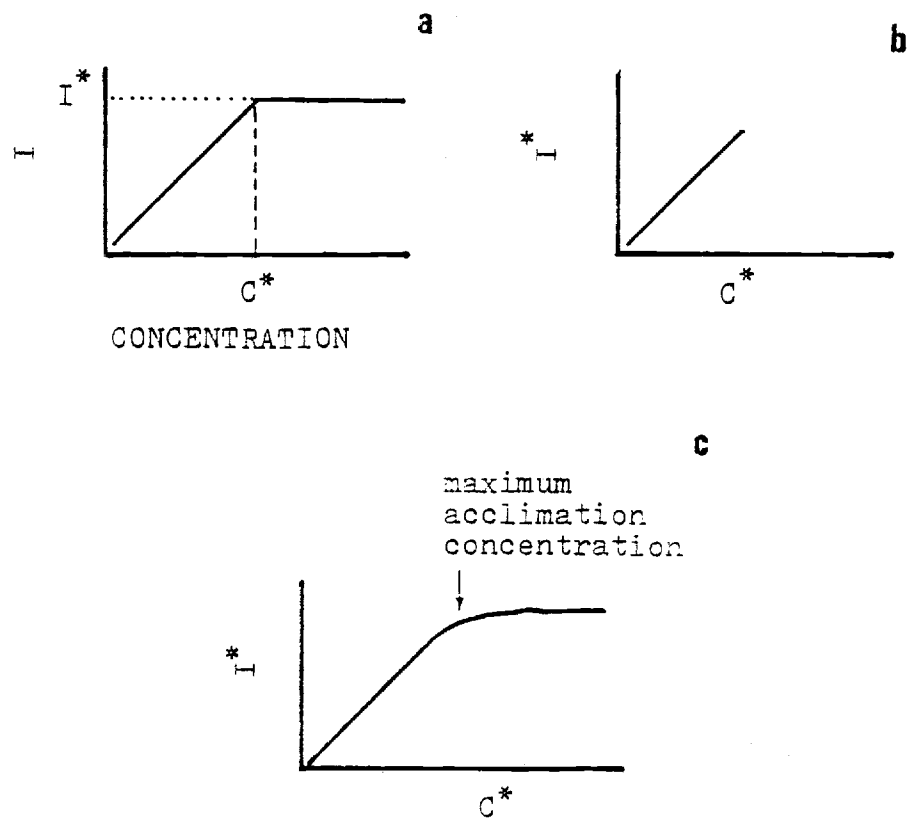


Fig. 18. Hypothesized ingestion rate relationships.

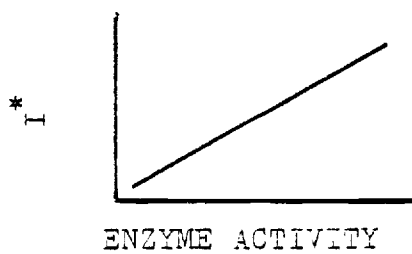


Fig. 19. Hypothesized relationship between I^* and enzyme activity.

Since the rectilinear ingestion function is totally defined by I^* and C^* , the appropriate rectilinear ingestion curve can be generated to predict ingestion rates at any food concentration. These predicted ingestion rates should be correct for all copepod populations with similar grazing prehistories, regardless of the current food concentration. The above argument of course assumes that the rectilinear ingestion function has a fixed point of origin, i.e., a fixed particle concentration greater than or equal to zero. This assumption seems reasonable on two grounds. First, although considerable discussion has occurred about whether a non-zero intercept exists for the ingestion function (Mullin et al., 1975; Frost, 1975; Landry, 1976; Steele, 1976), it is not usually considered to be variable or very large. Second, the assumption seems reasonable since the field data of Mayzaud and Poulet (1978) appear to have very small intercepts that are constant. It does not matter if the intercept is zero or greater, just that it is fixed or very small for the above theoretical argument to be useful.

If the ingestion functions in Fig. 18a are thought of as rectilinear, then two different families of curves can result (Figs. 20a and 20b). [We shall use the rectilinear ingestion function for reasons of its mathematical simplicity; the choice between alternative ingestion functions is somewhat arbitrary at this point since the data variance is too large to make a distinction (Frost, 1975; Mullin et al., 1975).] In the first set (Fig. 20a), the slope of the increasing segment of the ingestion function remains constant and only the maximum ingestion rate increases. This would be expected if only digestive enzymes were involved, i.e., if no other internal physiological or behavioral adjust-

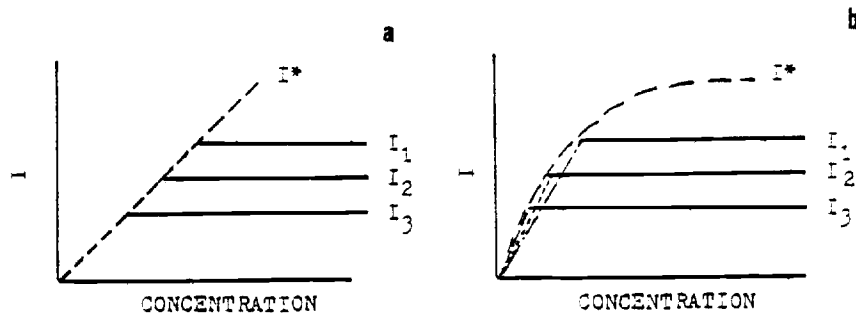


Fig. 20. Hypothesized alternative forms of the ingestion rate function. I_1, I_2, I_3 are hypothesized maximum ingestion rates for animals acclimated at three different food concentrations.

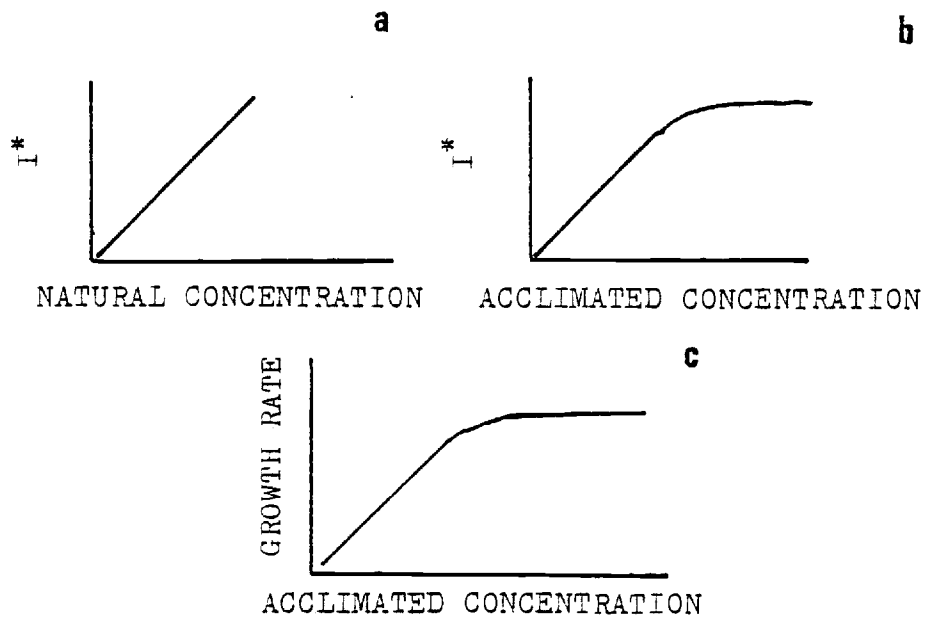


Fig. 21. Hypothesized relationships between I^* and natural (field) particle concentrations (a), I^* and all possible concentrations to which the animals have been acclimated in the laboratory (b), and animal growth rates measured in the laboratory versus acclimated food concentrations (c).

ments were made by the copepod in response to food level changes. This relationship is in agreement with the data in Fig. 17. The apparent discrepancy with Fig. 16 will be considered below. If the maximum ingestion rate increases in time as shown in Fig. 20a, then I^* alone can define the correct rectilinear ingestion curve without having to refer to the I^* vs. concentration curve, Fig. 18b or 18c. As illustrated in Fig. 20b, however, the slope of the increasing segment of the ingestion curve may change as I^* changes. In this case, the increasing segment will not fall along the I^* curve, but the ingestion curve will inflect at its intersection with the I^* curve (dashed line in Fig. 20a and 20b). In this case, it is implied that other physiological or behavioral shifts, in addition to digestive enzyme changes, are occurring within the animals in adjustment to food level. Existing data does not yet allow us to make a distinction between these two cases.

Before proceeding further with this argument, it should be noted that boundary conditions must exist for these relationships; there must be upper limits to the amount of enzymes the animals can synthesize. As a result, I^* may be a linear function of concentration over the range of particle concentrations observed in the field, (Mayzaud and Poulet, 1978) (Fig. 21a), but a theoretical I^* for animals acclimated to a broad enough range of concentrations must eventually bend over (Fig. 21b). As a result, this curve will be the theoretical maximum ingestion curve for acclimated animals and should be qualitatively similar to the growth curve generated by acclimating animals over their entire life span to a given food level (Fig. 21c).

Evidence Supporting the I* Hypothesis

The above theoretical argument can be supported by, and allow reinterpretation of, both laboratory and field data. Mayzaud and Conover (1976), and Mayzaud and Poulet (1978), provide strong evidence for the I* hypothesis. The strength of this evidence arises from the observation that the relationships for field populations shown in Fig. 15 and Fig. 17 are well defined for a variety of enzymes and copepod species taken from Bedford Basin. However, since the I* hypothesis is largely derived from these data and the arguments of Conover (1976), it may be inappropriate to use these data as supportive evidence. Additional supportive evidence for a hypothesis of this type may be obtained by using the conceptual argument to explain previous experiments that deviate from existing theory. Evidence may also be derived if the hypothesis suggests experiments, that, when performed, confirm predictions of the hypothesis. These two kinds of evidence will be described below.

A problem that has long troubled us and has frustrated the incorporation of satisfactory grazing terms in productivity models is an explanation of the large variability in grazing responses shown by Frost (1972) O'Connors et al. (1976), and others. The animals used in the experiments of O'Connors et al. were collected throughout the year. The variability observed in these data is clearly much larger than the variability expected from experimental replication. For example Donaghay and Small (1979a) reported only a 10% coefficient of variation for replicated ingestion rate experiments at any one food concentration. In O'Connors et al. it was suggested that part of the variance was due to

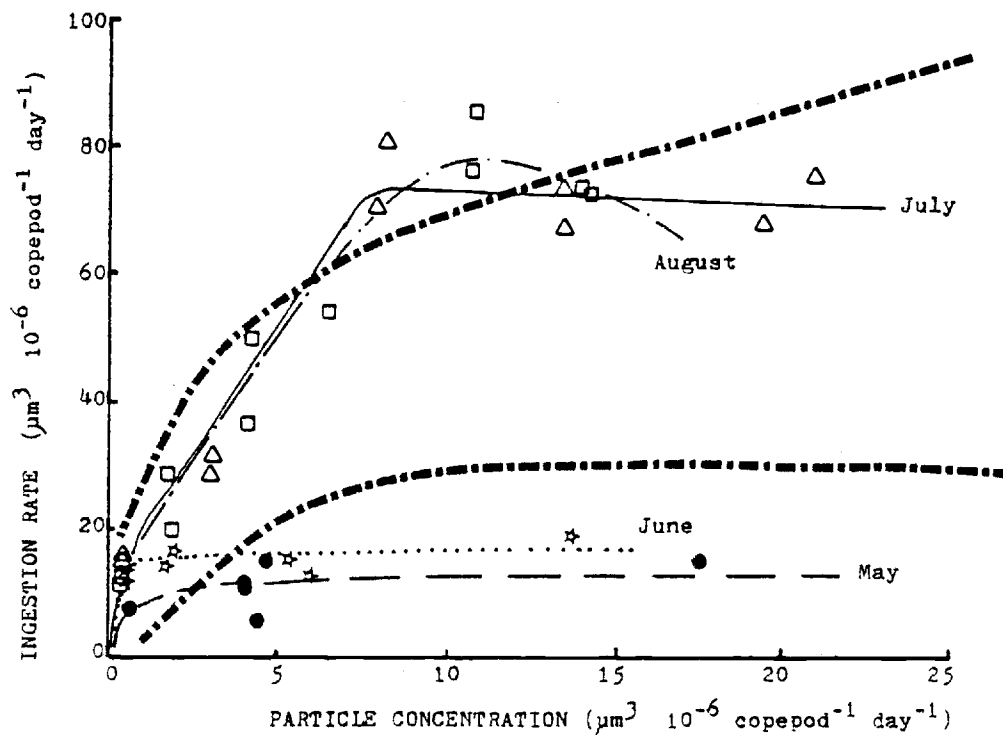


Fig. 22. Seasonal ingestion rates of *Acartia clausi*. Ingestion rates on *T. aestivalis* for large form *A. clausi* collected from Yaquina Bay, Oregon, in May (●), June (✱), July (Δ), and August (□), 1976. The lines through the data points were fitted by eye. The dashed line represents the data envelope of O'Connors et al. (1976) for the same form of *Acartia* grazing on *T. gravida*, a similar sized chain-former.

seasonal changes in the animals' grazing response. To investigate this, a series of ingestion curves were run during the summer of 1976 for the large form of Acartia clausi reported by O'Connors et al. (Fig. 22). From these data (Fig. 22) it is clear that a series of different ingestion curves can be defined. These curves each have a low internal variability (they replicate well), but clearly change with season. The dashed line is the ingestion rate envelope shown in O'Connors et al. (1976) for the large form Acartia clausi. It is clear that the full range of ingestion responses found in O'Connors et al. (1976) can be explained by seasonal variability. Two explanations for this seasonal variability can be offered. First, the seasonal changes in ingestion rate could be the result of changes in ingestion rate due to enzymatic changes, as suggested by the above theory of assimilatory control of feeding. This interpretation would be in agreement with the observations of Mayzaud and Conover (1976) and Mayzaud and Poulet (1978) that enzyme levels also change with season. However, seasonal changes could also be the result of changes in the phenotype of the grazer populations with season as has been shown for rotifers by King (1972) and suggested for Daphnia by Herbert (1974). Although clonal changes are possible for Acartia because of its pattern of production of resting eggs (Uye and Fleminger, 1975; Zillioux and Gonzalez, 1976; Johnson, in press), this possibility seemed unlikely. Phenotypic changes may also occur due to seasonal temperature differences inducing different sized animals (Miller et al., 1977). These different sized animals may be clonally identical, but may have different ingestion rates due purely to size difference (O'Connors et al., 1976).

We performed a preliminary experiment to see how much change could be induced in the ingestion function of Acartia by preconditioning Acartia clausi at two different food levels for a period of three days. Animals were collected from Yaquina Bay, Oregon, separated, and allowed to feed on Thalassiosira fluviatilis at $5 \times 10^6 \mu\text{m}^3 \text{ml}^{-1}$ for about 4 days. This period of feeding was used to condition all of the animals to T. fluviatilis as a food, and to allow the animals to acclimate to the laboratory (Donaghay and Small, 1979a). Two groups of about 600 adult female A. clausi were then separated. The first group was placed in a flask with $2.7 \times 10^6 \mu\text{m}^3 \text{ml}^{-1}$ of T. fluviatilis to precondition the animals to a low food level. The second group was placed in a flask with $16 \times 10^6 \mu\text{m}^3 \text{ml}^{-1}$ of T. fluviatilis to precondition the animals to a high food level. Each day the two food levels were adjusted to maintain the desired levels of food. After three days of preconditioning at these food levels, animals were sorted into groups of 30 animals each. Twenty-four hour ingestion rate experiments were then performed on these animals at a variety of food levels. Ingestion rates were calculated as in Frost (1972). The resulting ingestion curves are plotted for high- and low-food-preconditioned animals (Fig. 23). These results clearly show that two different ingestion curves can be generated by only three days of preconditioning to different concentrations of the same food species. High-food preconditioning clearly gives higher ingestion rates at higher food levels than does low-food preconditioning. The data suggest that the low-food-preconditioned animals are able to maintain higher ingestion rates at low food than high-food-preconditioned animals. If these data are plotted over the data of O'Connors et al. (1976),

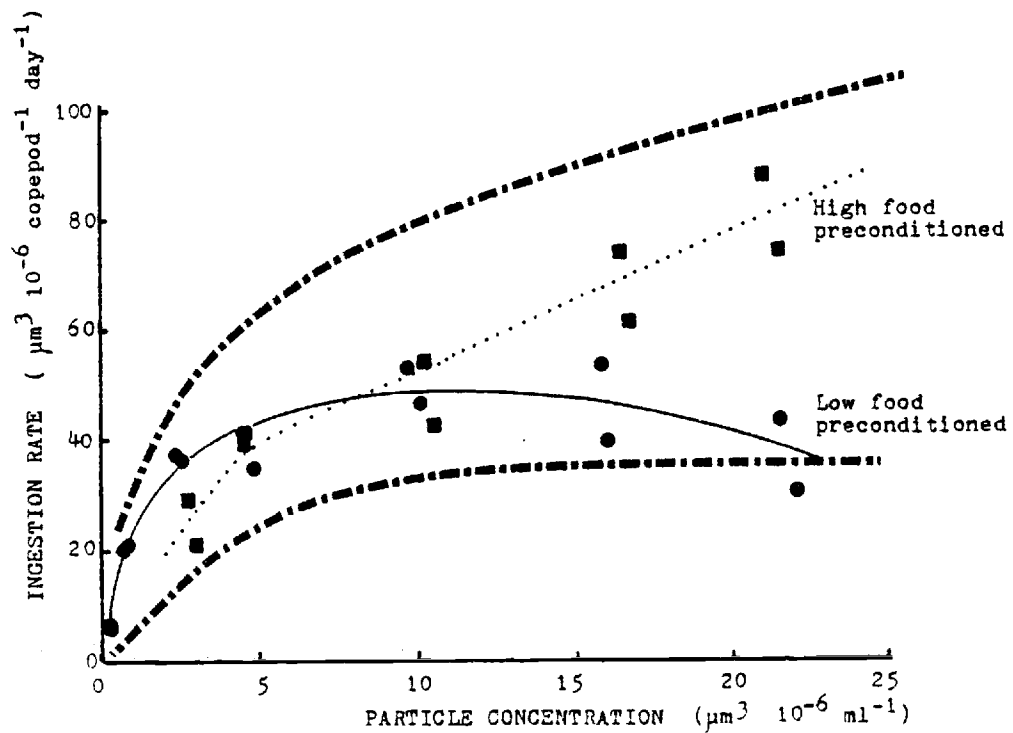


Fig. 23. Preconditioning effects on ingestion rate curves. Ingestion rates for large form *Acartia clausi* females grazing on *T. fluviatilis*. The solid circles are for animals preconditioned for four days at $2.7 \times 10^6 \mu\text{m}^3 \text{ ml}^{-1}$ and the solid squares are for animals preconditioned at a high food level, $16 \times 10^6 \mu\text{m}^3 \text{ ml}^{-1}$. The dashed line (----) represents the ingestion rate envelope of O'Connors et al. (1976) defined for the slightly larger cell *T. gravida*.

it is clear that about 70% of the variance in the data of O'Connors et al. can be accounted for by three days of preconditioning. Mayzaud (personal communication) has indicated that this time period (3 days) is similar to that required for enzyme induction. It is also similar to the time required for grazing behavior to stabilize in the laboratory. These data suggest that enzyme induction is the most likely explanation for ingestion rate variability in Acartia, rather than clonal factors or temperature phenotypes. This hypothesis clearly needs testing by simultaneous measurements of both ingestion rate curve shifts and enzyme level changes.

Critical conditions necessary for experimental testing of I* hypothesis

Experimental testing of the I* hypothesis can be accomplished using any time series of ingestion rate curve and enzyme measurements made on a single population of copepods that have been exposed to a known time series of change in phytoplankton concentration. The above statement requires that three critical conditions be met before the results can be rigorously used.

First, it is absolutely critical that all the animals used for measurements of ingestion rate and enzyme levels be from a single population of copepods that have identical feeding prehistories. For this condition to be met it is necessary to use a single life history stage of a single copepod species. It is necessary to use a single copepod species since there is no reason to assume that all species will be equally acclimated to this food environment and because different species may have different enzyme-substrate relationships. It must be

possible to repeatedly sample that population as food concentrations (and types) change with time and to have records of how those phytoplankton foods have changed in time. Although this condition can easily be met in the laboratory by taking samples over time from a large population of copepods maintained in a large, well mixed tank, it is much more difficult in the field. Two problems exist in the field in meeting this condition: (1) it is often difficult to ensure that one is always sampling from a single population with a uniform feeding prehistory, and (2) because of animal mobility and spatial heterogeneity in phytoplankton quantity and quality, it is necessary to identify to what fraction of the water column a population of copepods are preconditioned. There is some preliminary evidence that copepods are preconditioned to only a small fraction of the total water column (Donaghay and Small, 1979b).

The second critical condition is that the particles used in the experiments to determine the ingestion curves (I^* curves) must be free of confounding due to temporal changes in the qualitative characteristics of those particles. The use of natural particle spectra that change in both size and concentration with time may result in changes in ingestion curves that are both functions of enzymatic changes and size changes. Such apparent confounding need not interfere with the use of field data in testing the I^* hypothesis, however. To the extent to which the relationships between ingestion rate and food concentration (Fig. 14a) shown for Calanus pacificus (Frost, 1972) are generally true, changes in particle size should only affect the slope of the increasing segment of the ingestion curve. The maximum ingestion rates should be size independent and should be under assimilation control rather than

capture control. Thus, our ability to measure I^* (but not C^*) should be equally as good with natural particle spectra as with a single standard food insofar as particle size and the copepods ability to assimilate that food are independent (as shown by Frost, 1972). The observed changes in I_{\max} in field data (Conover, 1976; Mayzaud and Poulet, 1978; O'Connors, personal communication) are thus strong evidence for the I^* hypothesis. However, since the slope of the increasing segment of the ingestion curve is capture process controlled, and has been shown to become steeper with increasing particle size (Fig. 14), the inflection point relative to the concentration axis (C^*) will be strongly affected by particle size changes. This means that the I^* - C^* relationship (Fig. 18b) cannot be evaluated from most field data (see Fig. 24). The results from a hypothetical field experiment will be used to illustrate the point (Fig. 24). Suppose that over the period of a phytoplankton bloom, complete ingestion curves are developed on both natural particle spectra and on a single test food. These experiments are repeated three times (T_1 , T_2 , T_3) as phytoplankton concentration increases. If the I^* hypothesis is valid, the results of the single food experiments will appear as in Fig. 24a and the correct I^* - C^* relationship will be defined (as in Fig. 18b). If the natural particle spectrum increases only in concentration (but not size), as between T_1 and T_2 , the ingestion curve for the natural particle spectrum will be similar to that for the single food. However, if the particle spectrum increases in size as well as concentration, the increasing segment of the ingestion curve should steepen, and C^* will be displaced to a lower concentration than expected (as between T_2 and T_3 , Fig. 24b). Although the I^* values will be cor-

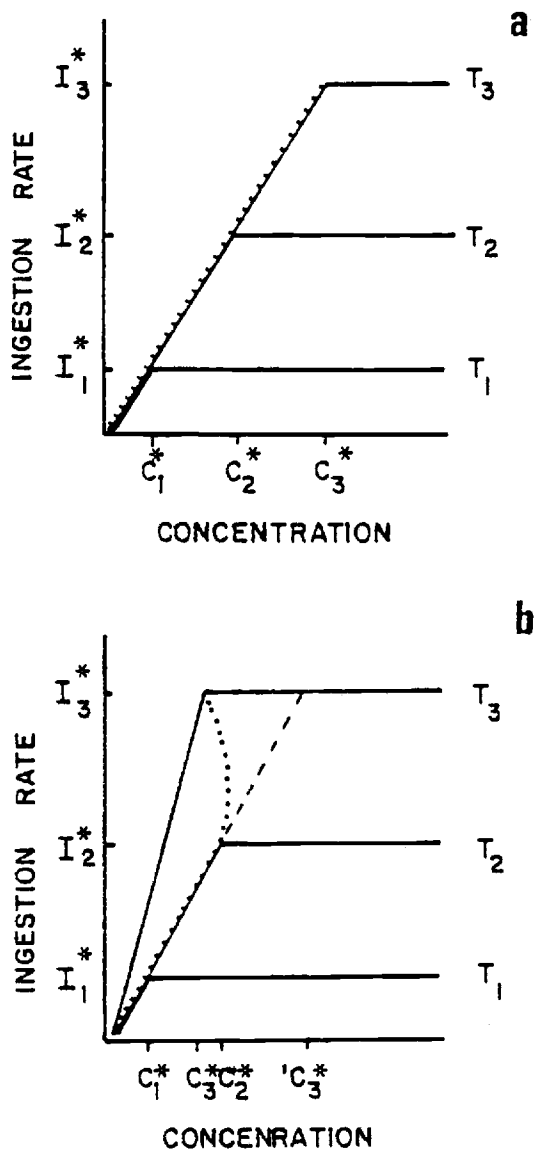


Fig. 24. Expected ingestion rate concentration relationships for copepods exposed to changing phytoplankton concentration with time (T_1 , T_2 , T_3): (a) when fed a single test food, and (b) when fed the natural particle spectra from which they were collected. Solid lines represent expected curves; dotted line represents observed I^*-C^* relationship.

rect (compare I_3^* in Fig. 18a and b), the resultant I^*-C^* relationship will have strong confounding of size and concentration. If both single food and natural spectra experiments are run in a given field situation, changes in slope of the increasing segment becomes a measure of the effects of particle size change on the ingestion relationship, while differences in I_{\max} values indicate differential degrees of assimilatability per unit of food volume between the natural particle spectra and the standard food. Changes in particle size spectra may be the cause of the difference in slope of the increasing segment of the ingestion curves of Conover (1976) shown in Fig. 16 earlier. O'Connors, et al. (in press) using Temora longicornis feeding on natural particle spectra have observed large changes in I^* with season, and some changes in slope of the increasing curve segments that in some cases are correlated with changes in average particle size. Since both the data of O'Connors et al. (in press) and Conover (1976) show strong changes in I^* , these data become field evidence for the I^* hypothesis.

A third critical condition must be met. If the results from field or laboratory experiments are to be used to define the underlying I^*-C^* and I^*-E relationships (Figs. 18b and 19), it is necessary to show that the copepods used in the experiments are fully acclimated to that food concentration at the time of the test. The best way to solve this problem is to determine the relationship between degree of acclimation and rate of increase (k_a) in phytoplankton concentration. The necessary data can be generated from any large time series set of data where copepods have been exposed to a variety of rates of increase in food concentration, and then tested for ingestion and enzyme responses. At

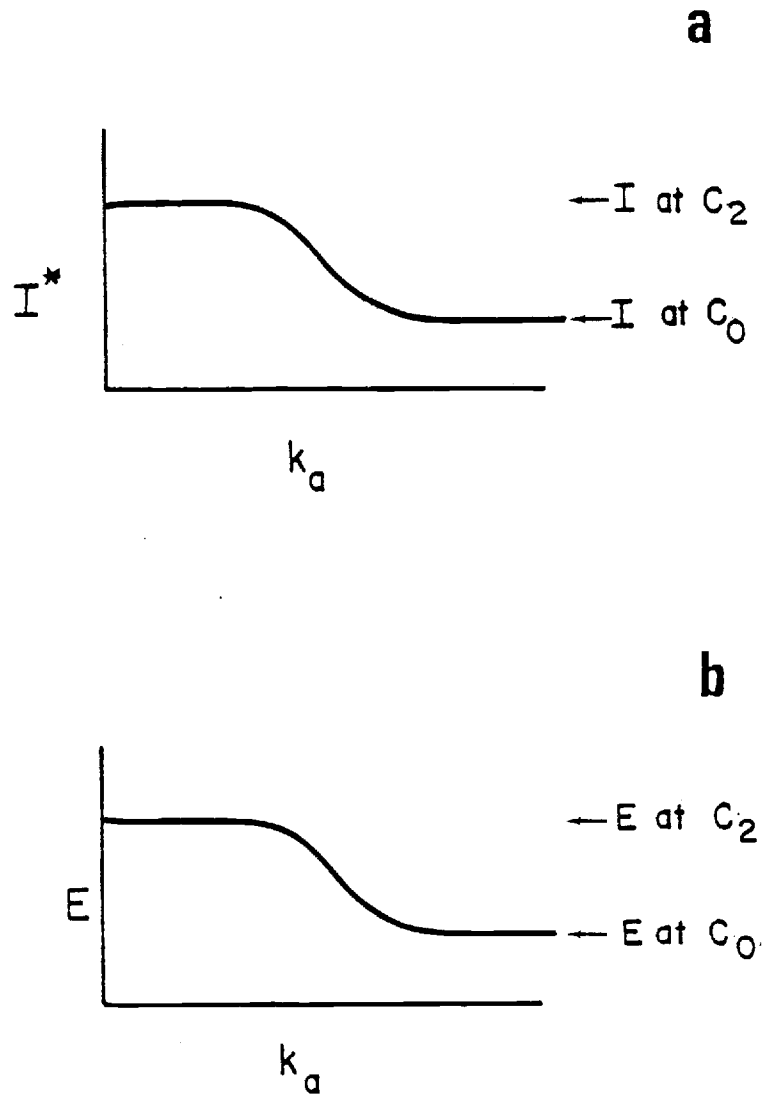


Fig. 25. Hypothesized relationship between (a) I^* and k_a and (b) enzyme activity (E) and k_a .

any given concentration, at all rates of food increase at which the animals can keep up, the responses should be identical; above this maximum rate, the responses should get progressively more and more out of phase with the changing food environments. These ingestion and enzyme measurements (under acclimated conditions) will allow the definition of the theoretical relationship between I^* and food concentration (Fig. 18b), I^* and enzyme activity (Fig. 19) and enzyme activity and substrate concentration (Fig. 20). In addition, if these measurements are repeated at, say, four pre-set food concentrations, a distinction between the two different patterns of ingestion curves shown in Fig. 20a and 20b might be made. If the I^* values are plotted against rates of phytoplankton increases, k_a , at any one of the pre-set food concentrations (Fig. 25a), then I^* should be constant up to the value of k_a above which the animals cannot keep up. In addition, plots of digestive enzyme activity (E) versus k_a can be made (Fig. 25b). For both of these plots, the values of I^* or E should decrease for all values of k_a greater than the animals' maximum rate of adjustment. As k_a becomes very large (i.e., the changes in food concentration approach instantaneous, or as k_a approaches ∞) the values of I^* and enzyme activity should approach the values at the start of the experiment. In other words, as the time it takes to go from the initial food particle concentration (C_0) to some higher concentration (C_2) approaches zero, the I^* and enzyme activity curves should approach the values at C_0 . If both I^* and E curves (Fig. 25a and 25b) begin to decrease at the same values of k_a , then this represents further evidence that the level of enzyme activity is the functional basis for the reduced ingestion rates. In addition,

the inflection values of k_a will tell us the maximum rate of food increase that the copepod species can match. A comparison of the ingestion curves generated at several pre-set food concentrations will allow definition of whether I^* changes with different food preconditioning levels as shown in Fig. 20a or 20b or in some other fashion. If, when the plots of I^* versus k_a and E versus k_a are compared for different preconditioning food concentrations, the inflection point changes, then the maximum rate of copepod adjustment is food concentration dependent. If the relationship between I^* , E and k_a are defined as shown in Fig. 25, these relationships should prove very useful in predicting copepod grazing responses in field studies of non-steady state environments.

Similar experiments can also be performed to determine how fast the copepods can adjust to decreasing food concentrations. The only difference here is that the animals would start at high food levels, and responses would be measured as food levels dropped at different rates. The same type of curves as above can then be defined. Comparison between increasing and decreasing functions could be made to determine what differences, if any, exist between upward and downward adjustment.

Extensive testing of the I^* hypothesis is clearly needed. Although some data already exist to support the hypothesis as noted above, critical tests of the hypothesis in the laboratory and field are needed. Such testing is currently underway. In such testing it is important that the three conditions discussed above be carefully met. If the hypothesis is not rejected by such tests, the resulting model can be used to interpret the results of field and laboratory experiments under all conditions (i.e., not just those necessary for testing the model).

PART III. ECOLOGICAL AND EVOLUTIONARY IMPLICATIONS OF ALTERNATE FEEDING BEHAVIOR

Herein we have proposed a series of alternative grazing models. These have taken the form of alternative capture and assimilation models. Although many of the examples given illustrate the more complex behavioral patterns, this is not meant to imply that all copepods have chosen these strategies. The examples are mostly derived from coastal copepods (Acartia sp.). It is fully recognized that the evolutionary histories and current environments of different species may result in very different capabilities and very different ways of achieving these capabilities. Thus Calanus plumchrus, presumably having evolved in open oceanic environments, may be very different from a neritic species such as Acartia clausi. We shall consider below why different strategies should be expected in animals taken from different environments.

The types of adaptations and capabilities exhibited by a copepod species may vary as a function of the degree of the coupling between the phytoplankton and the copepod. It is generally accepted that both physical factors and the copepod (and to a lesser extent other zooplankton and herbivorous fish) controlled processes of grazing and nutrient regeneration combine in an interactive fashion to control phytoplankton dynamics (Dugdale, 1967; Parsons and Takahashi, 1973). Within the constraints on growth set by temperature, salinity and oxygen, the dynamics of the copepod populations are controlled by food availability, by food quality and by predation. While physical mixing processes often control the initiation of phytoplankton blooms and the amount of "new" (Dugdale, 1967) nitrogen available for such blooms, copepod grazing and

regeneration may strongly control the duration of the bloom, the extent to which such new nitrogen is realized as phytoplankton biomass or transferred to higher trophic levels, as well as total phytoplankton dynamics in periods between mixing events. From a phytoplankton viewpoint, the role of copepods can be visualized as a continuum between two extreme roles: the controller and the exploiter. As nutrient injection events become more frequent and less predictable, the copepod must take more of the role of an exploiter; as such events become increasingly rare, the copepod may exert a greater role as a controller. The exploiter must maximize his own growth and reproduction in periods of high primary production (and extend those periods over time as much as possible) and at the same time develop mechanisms (such as resting eggs) to survive periods of unfavorable conditions. Unfavorable conditions may be defined not only by food, but also by changes in salinity, temperature or predation. The controller, in contrast, must be able not only to exploit the phytoplankton effectively as a food resource at low concentrations, but also to spread the primary production resulting from seasonal injection of new nutrients over a sufficiently long period of time to allow the copepods own life cycle to be completed. This can best be achieved if grazing pressure (i.e., total grazer flux loss) and primary production are as nearly balanced as possible.

For a copepod to be considered an effective controller of phytoplankton biomass and production, it must have a sufficiently fast enzyme induction rate (i.e., $I^* - k_a$ and $E - k_a$) to be totally acclimated over the entire range of k_a possible in its environment. Let us consider why this is necessary. If a copepod can be totally acclimated at all rates

of phytoplankton apparent growth rate, then as the natural concentration of phytoplankton increases, ingestion rate will also increase, i.e., at all phytoplankton concentrations, C^* must be $\geq C$. Furthermore, the fraction of phytoplankton production consumed by copepods will tend to remain constant. As long as this fraction remains constant (assuming that the specific growth rate [k_c] of the phytoplankton remains constant), the apparent rate of increase of the phytoplankton will remain constant. If on the other hand, the copepod is not able to acclimate over the entire range of k_a , then, once k_a exceeds the maximum rate of acclimation, C^* will become less than C . As a result, further increases in phytoplankton concentration will result in no concomitant increase in ingestion rate. Under such conditions grazer flux loss will become an ever decreasing fraction of primary production unless copepod biomass increases sufficiently fast to keep grazer flux loss a constant fraction of primary production. As a result, the apparent phytoplankton growth rate will rapidly accelerate and the phytoplankton biomass will suddenly appear to explode only to crash under ensuing nutrient limitation. Such crashes tend to result in transfer of production (and injected nutrients) from pelagic to benthic consumers and dramatically shorten the duration of the bloom.

Since the total grazer flux loss is a function of both individual copepod ingestion rates and copepod biomass, for a copepod to be an effective controller, the copepod must not only remain acclimated (i.e., $C \leq C^*$), but the copepod must have a sufficiently large biomass such that grazer flux loss is a significant fraction of total production. The sufficiency of the copepod's biomass at any given time during a

phytoplankton bloom will be determined both by its own growth rate (in terms of increase in the number of individuals and weight gain per individual) and by its own population density at the start of the period of increase in primary production. If the copepod's biomass is insufficient, then although k_a may be held constant by increasing individual copepod ingestion rates, grazer flux loss will be such a small fraction of total phytoplankton production as to have little controlling effect on the course of the bloom. On the other hand, if the rate at which a copepod can grow (both as individuals and as a population) is very fast, i.e., if it approaches the k_a of the phytoplankton, then this alone (i.e., without change in individual ingestion capabilities) could theoretically lead to control of primary production. In the field, however, the significance of copepod growth in controlling phytoplankton production is limited by two factors. First, maximum copepod (individual and population) growth rates (copepod k_c 's) are much lower than maximum phytoplankton growth rates. With the exception of Paracalanus and Acartia tonsa (Heinle, 1969; Miller et al., 1977) which have maximum individual growth rates of 0.8, the growth rates of most copepods range between 0.1 and 0.4 $\mu\text{g C gained}/\mu\text{g C body weight/day}$ (Harris and Paffenhöfer, 1976; Peterson, 1979; Marshall, 1973). Second, these growth rates are often not realized in the field due to the effects of temperature, salinity, inadequate food or predation (see review by Heinle, in press for example).

In summary, the effectiveness of a copepod as a controller is a function of (1) the maximum rate of acclimation of the individual copepod relative to the maximum apparent growth rate of phytoplankton; (2)

the biomass of the copepod population present at the initiation of the phytoplankton bloom; and (3) the rate at which the copepod population can increase its own biomass. It should be noted that these three factors may not be completely independent. To the extent to which rapid acclimation of ingestion processes can increase growth rates or increase storage of materials for enduring interbloom periods, initial copepod biomass and copepod growth rates will be coupled to acclimation rates. It should also be noted that the extent to which these three factors combine to keep grazer flux loss a large and constant fraction of primary production, both the duration of the bloom and the rate at which both biomass and chemical changes in phytoplankton composition ensue following nutrient depletion will be affected. As long as grazer flux loss remains a large and constant (or increasing) fraction of total production, the rate of nutrient decline will be dramatically slowed as a result of both a decreased rate of increase in nutrient demand and constantly increasing amounts of nutrient regeneration. The closer grazer flux loss approaches phytoplankton production the more nearly regenerated nutrient will meet nutrient demand. As a result, changes in phytoplankton chemical composition resulting from nutrient deficiency following nutrient depletion should be lessened and the period of bloom should be prolonged.

With the above factors in mind, it is now possible to consider how the degree of control exerted by a copepod is affected by the physical and biological properties of coastal and oceanic environments (summarized in Table 7). Probably the single most important factor is the potential for large variability in the apparent phytoplankton growth

Table 7. Characteristics of coastal and oceanic environments potentially important to the evolution of feeding behavior.

NON-FOOD-RELATED ENVIRONMENTAL FACTORS			
	OCEANIC		COASTAL
(1) Bottom depth	Too deep for resting eggs		Shallow enough for resting egg recovery
(2) Vertical temperature gradient	Large enough to provide cold refuge for diapause and advantage for vertical migration (?)		Too small to use (except fjords)
(3) Frequency of mixing events	Episodic in subtropics, increasingly seasonal poleward		Very frequent, from months to days or less
FOOD-RELATED ENVIRONMENTAL FACTORS			
	NON SEASONAL OCEANIC	SEASONAL OCEANIC	COASTAL
(1) Particle spectra			
organic fraction	even	even to peaked	highly peaked
inorganic fraction	low, even	low, even	decreases exponentially with size
stability	good, slow change	intermediate	poor, rapid changes in time and space
(2) Food Abundance	very low; constant	varies seasonally	rapid change in space and time
(3) Food species diversity	high	intermediate, varies seasonally	low, but dominance rapidly varies
(4) Chemical food quality	slowly changing; may be poor	high to intermediate; varies seasonally	varies over max. range in space and time
(5) Plant production	low, constant	intermediate to low with season	rapid fluctuation over wide range
(6) Long term predictability	excellent	moderate to excellent	poor
(7) Relative phytoplankton growth rates (intra and inter specific in time and space)	relatively small changes	moderate seasonal changes	large differences in both time and space

rate, k_a . The potential for large variability in k_a will exist in those environments in which there is a large range in the physical and chemical factors controlling phytoplankton growth rates (k_c). The three principle factors are temperature, light intensity (both in terms of surface light intensity and light availability to an individual cell over time) and nutrient flux. Nutrient flux is controlled both by the frequency and magnitude of nutrient injection events and by nutrient regeneration by zooplankton (and to a lesser, but unknown, extent by bacteria).

Non-seasonal oceanic areas tend to be typified by relatively constant light-temperature fields with nutrient injection events being rare (i.e., storm caused) (Pomeroy, 1973). The constancy of physical conditions and the tight coupling between nutrient regeneration by zooplankton and primary production make large fluctuations in phytoplankton k_c unlikely and unsustainable if they should occur. As a result, effective control can be maintained by any copepod (or assemblage of copepods) that maintains a relatively constant biomass and diverse age class structure. Reproductive synchronization, rapid growth rates, and rapid ingestion rate acclimation capabilities are of little use. Because of the low levels of food, one would in general expect the evolution of adaptations to enhance capture processes rather than assimilation processes.

As one moves poleward to more seasonal, but still oceanic areas, winter mixing causes injection of large quantities of new nutrients into surface waters. This mixing decouples phytoplankton growth from nutrient regeneration. In addition, the seasonal stabilization of the water

column combined with seasonal changes in light intensity and temperature lead to a wide range of phytoplankton growth rates. In the absence of sufficient grazing pressure these conditions will result in a large spring phytoplankton bloom with very high food availability followed by a long period of low production and phytoplankton biomass more typical of tropical areas. The injected nutrients will be most effectively exploited by copepods only if the dominant copepods have high rates of acclimation, high initial copepod biomass and high copepod growth rates.

Although it is the classical view (see Raymont, 1963 for summary) that copepod biomass and grazing rates do not become large enough to effectively control production until well into the spring bloom, there is some evidence that Calanus plumchrus and Calanus cristatus may have evolved a combination of mechanisms that make them effective controllers in the central north Pacific (ocean station P). It is well established in this region that while growth rate and primary production of phytoplankton vary with season, as would be expected from changes in the physical and chemical environment, phytoplankton biomass remains relatively constant (Beklemishev, 1954; Heinrich, 1962; Parsons, 1965; Larrance, 1971; Anderson and Munson, 1972). This condition has generally been attributed to intensive grazing pressure by planktonic copepods (Beklemishev, 1957; Heindrich, 1961; McAllister et al., 1960; Parsons and Le Brasseur, 1968). In other words, grazer flux loss very closely parallels changes in primary production. By overwintering as adults at depth, and laying eggs before the initiation of the spring bloom, C. plumchrus and C. cristatus start off the bloom with the maximum numerical population of individuals that also have the maximum possible rate

of biomass increase. Thus the high initial numbers and high potential growth rate of each individual allow C. plumchrus and C. cristatus to increase grazer flux loss rapidly as primary production increases, and to thereby keep k_a very low and non-accelerating. Enzyme induction based acclimation may also be involved, but no data exist to test this. The lack of change in phytoplankton concentration with time in the central North Pacific would appear to eliminate the need for rapid enzyme induction on a quantitative basis, or at the very least make detection of its effect on ingestion-concentration relationships very difficult. The animals, however, should have a sufficient diversity of enzyme types to efficiently process the variety of food types that may be encountered. C. plumchrus and C. cristatus may thus be prime examples of successful controller copepods. The phytoplankton bloom at ocean station P is clearly spread over a very long period. The period is sufficiently long so that copepod eggs laid at depth before the initiation of conditions favorable to rapid phytoplankton growth can grow to stage V copepodites, store enough energy and materials to overwinter, then molt to adults and lay eggs the following spring. It should be pointed out that this mechanism will work only if timing of the initiation of the spring bloom is sufficiently predictable (at least to the copepod) so that eggs can be laid at the appropriate time. Laying of the eggs too early may result in starvation of the nauplii before primary production increases; laying of the eggs too late will result in failure to fully control, and fully make use of, the phytoplankton bloom. Either case is potentially disastrous to the copepod. The problem of premature egg laying in C. plumchrus may be partially

alleviated by the large energy reserve in the eggs that permits survival and development of the nauplii with little food present (Heinle, in press). The above pattern of overwintering is also made possible by the properties of the physical environment and physiological adjustments of the copepod. The cold, deep waters provide a refuge from high metabolic rates and a hypothesized refuge from predation (McLaren, 1976). The copepods apparently also go through a series of physiological adjustments to reduce body nitrogen turnover rates to increase carbon stores, and to reduce carbon metabolic rates (see review by Heinle, in press).

In coastal waters, differences in environmental conditions make control much more difficult. The physical and chemical conditions tend to vary over a wider range resulting in a wider range of phytoplankton growth rates. Nutrient injection events occur in an unpredictable fashion throughout the year rather than just during the winter. Because nutrient injection can occur during seasons other than winter, the phytoplankton growth rates at the beginning of any non-spring bloom may be much larger and more variable, though the bloom itself may be of much shorter duration than the spring bloom. As a result, the responses of the copepod must be much faster if control is to be maintained. The large oscillations in phytoplankton biomass in most coastal waters are evidence that no uniquely successful mechanism (such as that of Calanus plumchrus) has evolved to control the phytoplankton stocks. However, two less successful strategies appear to be used. In shallow waters, resting eggs produced during previous periods favorable to copepod growth (Johnson, in press; Uye and Fleminger, 1976) may be resuspended by the same physical mixing process that initiates the phytoplankton

bloom. The success of this mechanism is limited by the time lag between resuspension of the resting eggs and the appearance of feeding naupliar stages. In deeper waters, copepods with stored energy reserves can endure periods unfavorable to growth by migrating to depth at stage V copepodites. At the start of the bloom, stage V copepodites can migrate to the surface, feed, molt to adult, and lay large numbers of eggs. Here, again, the lag between initiation of the bloom and first grazing by nauplii may be sufficient to prevent control. However, if growth rates of these individuals are sufficiently large, and if acclimation to changing food levels occurs sufficiently fast, grazing flux loss can begin to exceed production and control might be established later in the season. Both resting eggs and vertical migration have the potential to be effective mechanisms to endure unfavorable periods varying in length from inter-bloom periods of several weeks to seasonal periods of many months.

Regardless of the reason that copepods are unable to totally control biomass in coastal systems, such failure will lead (in conjunction with changes in the physical-chemical environment) to large oscillations in both the quality and quantity of phytoplankton food available. Aside from possible advantages of bloom prolongation by control, there would seem to be direct benefits to the individual copepod that can rapidly acclimate to changing food conditions. To the extent to which such rapid acclimation can lead to higher individual growth rates (for pre-adult stages), reproductive rates, or enhanced individual fitness, there will be a strong chance for the evolution of such mechanisms. The increase in I^* as phytoplankton concentration changes allows such a

copepod to exploit the blooms that it experiences. The sharp changes in food chemical composition (quality) as phytoplankton go from nutrient sufficiency to deficiency and back can best be exploited if the copepod can rapidly acclimate qualitatively as well as quantitatively. In sharp contrast to the conditions where biomass is more or less constant with time, one would expect in general that evolution in coastal systems would favor adaptations to enhance assimilation processes rather than efficiency of capture processes.

Thus far we have considered the effect of variability of phytoplankton growth rate as an average for all species present. However, since different phytoplankton species have widely divergent growth rate responses under any given set of conditions, it is necessary to consider the effect of grazing pressure on the individual species as well as on the average. If specific growth rates vary only slightly between species at any one time, then grazing pressure exerted at a constant level for all species will have very little effect on phytoplankton species diversity. Such constant grazing pressure will only be observed if the filtering efficiency function is highly flattened; i.e., d^* occurs at very small sizes and $\beta = 0$. Although some oceanic copepods appear to have such flattened filtering functions (Schnack, personal communication), others clearly do not (Frost, 1972). If a controller copepod has a steeply increasing filtering efficiency curve with size ($\alpha, \beta \gg 0$), grazing pressure will tend to eliminate large celled phytoplankton. This effect will be amplified, if as has been suggested (Steele and Frost, 1977), phytoplankton growth rates tend to decrease with increasing size. The elimination of larger, slower growing cells in such a

situation will result in a decrease in average cell size and an increase in average specific growth rate for the phytoplankton assemblage. This in turn will result in decreased capture efficiency for the copepods. If such conditions persist over long times, an eventual equilibrium will result between the average growth rate of a given phytoplankton species and the average grazing pressure on that species. The above results will occur only if the grazers involved are predominantly passive selectors and if the filtering efficiency function is seasonally constant. If, as with Calanus plumchrus in the North Pacific, there is a single cohort of copepods per year, then selective pressures on phytoplankton species will seasonally change to the extent to which filtering efficiency curves change with developmental stage. Thus knowledge of the shape of the adult filtering efficiency curve is insufficient to predict selectional effects. The tendency for extinction of phytoplankton species will also be reduced, if as a result of changes in environmental conditions, the growth rate of a given species differentially changes with time. Even with a controller copepod dominating such a system, such phytoplankton species specific growth rate variability in time will cause shifts in the significance of grazing pressure to a given phytoplankton species over time, and thus may preclude the extinction of that species.

Thus far we have considered only the effects of passive selection on phytoplankton species diversity. There has been a strong tendency in such discussions to emphasize possible mechanisms whereby the extinction by grazing of certain types of species can be avoided. Active selection, however, can be a strong force for maintenance of phytoplankton

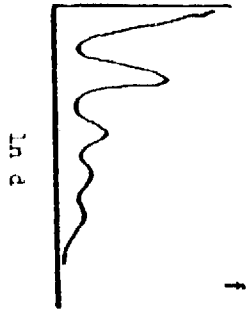
diversity. Active selection by copepods for the most rapidly growing and/or the most abundant phytoplankton species will have a strong tendency to enhance phytoplankton species diversity rather than decrease it. There is a growing body of evidence from our own work that growth rate based selection can occur in some coastal copepods (Donaghay et al., in prep.). There is extensive field evidence (Poulet, 1978; Richman et al., 1977) that filtration rates are highest on the most abundant particle size peak regardless of the size of the particles comprising that peak. Richman et al. (1977) refers to such behavior as "tracking" and Poulet (1978) calls it "opportunistic feeding." Regardless of the name, such feeding behavior will maintain the diversity of the phytoplankton in that grazing pressure will be sharply reduced on those species lying outside the dominant sized peak. Such active selective feeding on the dominant and/or most actively growing peak will tend to enhance the ability of the copepod to control the phytoplankton bloom by concentrating grazing pressure on the most rapidly growing segment of the phytoplankton assemblage. There are some direct individual benefits of such behavior to the copepod that will be considered below.

In the preceding argument about controllers and exploiters we have mentioned the shape of the filtering curve, but only in the sense that it might affect selective pressures on phytoplankton. The filtering curves for coastal copepod species have been repeatedly shown to be logarithmically increasing functions of particle diameter. Such a logarithmic shape gives significant benefits for coastal species, but severe drawbacks for controllers. A logarithmic filtering function for controllers has the disadvantage that it provides a reduced predation

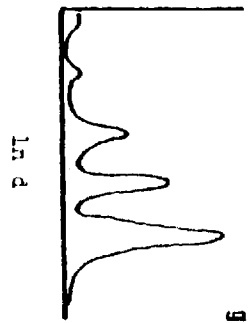
pressure advantage for small phytoplankton, thus tending to drive phytoplankton populations to smaller sizes. These smaller sizes in turn are less efficiently filtered. However, for coastal species a logarithmic filtering function has an advantage. In the above discussion, we have suggested that exploiters are basically highly selective. As discussed in the filter theory section above and by Donaghay et al. (in prep. a), the ability to make selective decisions is based on encounter frequencies. Encounter rate is determined not only by absolute abundance but also by filter design. Natural coastal particle number spectra tend to be exponential decay functions of particle diameter, particularly the non-biogenic fractions (such as suspended sediments) (Fig. 26a). Thus the combination of a logarithmically decreasing particle number spectrum and a logarithmically increasing filtering efficiency function (Fig. 26b) will tend to reduce the encounter frequency of small particles and enhance that of large particles (Fig. 26c). Since the large particles both have more food volume per particle (Fig. 26d) and are more likely to be food (i.e., to not be inorganic material, Fig. 26e and 26a), the reduced total encounter rate, and enhancement of high food value particles in those particles captured, greatly enhances the selective capability of such a copepod. In other words, the logarithmically increasing filtering function can radically alter the particle spectra we see to one dominated by large and more likely food particles (Fig. 26f and 26g). In offshore environments, however, these advantages rapidly disappear because (1) particle concentrations are in general lower, (2) large numbers of inert small particles are absent, and (3) as noted above, being a controller with a logarithmic filtering function is

Fig. 26. Potential interactions of filter design and particle size spectra in coastal waters. All curves are hypothetical. (a) Relative frequency by particle number of sediment (area below dashed line) and biogenic materials plus sediment (area below solid line). Area between dashed and solid lines is relative frequency of biogenic materials. Biogenic spectra (not shown) may have discrete peaks. (b) Filtering efficiency as a function of size over the limited range of 0.1 μm to 15 μm (all models Fig. 8 and 9). (c) Expected encounter rate for a copepod with filtering efficiency curve (b) feeding in an environment with particle spectra (a). (d) Food value per particle for living (biogenic) particles only. Slope of line is steepened if all particles included. (e) Probability of a particle of a given size in environment (a) being non-food (i.e., sediment). (f) Particle volume spectra as measured by Coulter counter and (g) as viewed by a copepod with filter efficiency curve (b).

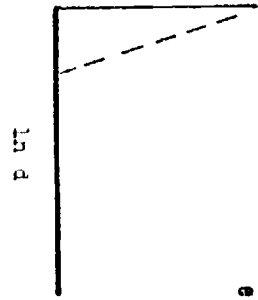
PARTICLE VOLUME
(Coulter Counter)



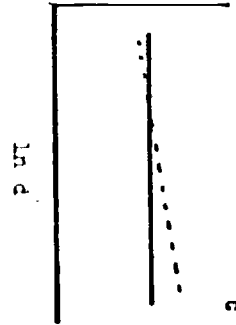
PARTICLE VOLUME
(copepod captured)



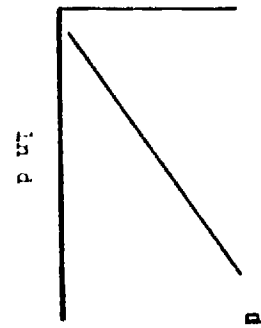
PROBABILITY OF
PARTICLE BEING
SEDIMENT



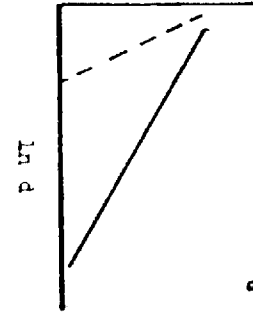
EXPECTED ENCOUNTER
RATE



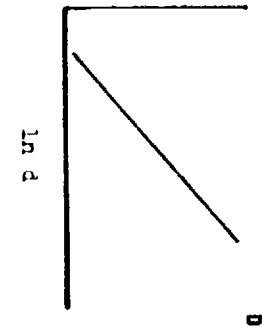
FOOD VOLUME PER
BIOGENIC PARTICLE



PARTICLE NUMBER
(relative frequency)



FILTERING EFFICENCY



difficult. What is suggested here is that strong evolutionary forces might be at work selecting for flat filtering functions offshore and steeply increasing ones inshore. In fact, it can be argued that offshore animals like C. plumchrus that have flattened filtering functions (Frost, 1979) should be easily excluded from nearshore systems, while highly selective estuarine types should be excluded from central gyres. Thus, while the injection of small non-food particles into an environment might have a small effect on Acartia, it might be disastrous for a controller type copepod (see review by Moore [1977] for example for this).

The degree of selectivity observed may be further explained by additional differences between oceanic and coastal environments. Oceanic gyres often have a high diversity of phytoplankton species with a relatively flat or featureless stable particle size spectra (Sheldon et al., 1972, 1973). The combination of low food concentration, high food diversity, and lack of clear abundance peaks make selection based on a limited number of food characteristics very difficult, and may have led to reduced filter based selective capacity in animals from non-seasonal oceanic environments. The high particle encounter rates required by the large size of some of these animals has probably further limited the evolution of selective capability. For a variety of reasons, many large boreal oceanic species have developed mechanisms for storage of energy in oil-sacs (see Heinle, in press, for review). This storage capacity allows them to very effectively use foods high in carbon or nitrogen. Foods high in carbon can be used to increase energy stores, while foods high in nitrogen can be used to enhance growth and

reproduction. Because of the ability to use foods of a wide range of C/N ratios, there might be little evolutionary pressure for the development of extensive chemosensory capability in these animals.

In contrast to the above, coastal systems are often typified by one or two dominant, but temporally and spatially variable, particle size peaks. These peaks are often dominated by one or a few similar phytoplankton species. Such patterns make size-based selection very useful for making food choices, yet relatively simple to achieve. Selective feeding by tracking such peaks (Richman et al., 1977) has the advantage of obtaining improved food quality for the grazer insofar as such peaks are caused by rapidly growing cells. Such peaks will also have lower ratios of inorganic to biotic particles, thus reducing the need for postcombing selection to avoid such particles. As far as the particles in such peaks are biochemically similar [as would be expected if such peaks are dominated by one or two species of rapidly growing cells (Richman et al., 1977)], and tend to persist over time, the tracking of such peaks should enhance enzymatic adaptation to the use of such foods. Work in our laboratory indicates that significant reproductive benefits may ensue from such tracking. The high diversity of species composition of phytoplankton over large time and space scales in both oceanic and coastal systems would tend to inhibit the development of species specific chemosensory cues on which to base selection. However, the wide variability in chemical food quality in coastal systems, when combined with the specific nutritional needs of exploiter copepods, may have resulted in the evolution of chemosensory mechanisms in coastal copepods based on chemical food quality. The high growth and reproductive rates

of many coastal species in conjunction with their apparent inability to store energy (Dagg, 1977; Heinle, in press), provide strong evolutionary advantage to the development of methods to select foods rich in nitrogen. Thus the chemosensory selective mechanisms found in coastal copepods would be expected to be quite divergent from the single prey specific attractant sensing mechanisms in many insects (Feeney, 1978).

Most of the above argument leads to the conclusion that oceanic controller species should have less well developed selective mechanisms and in general different feeding behavior, compared to coastal species. This hypothesis clearly needs to be tested. In the above discussion we have considered only the extremes. There undoubtedly are large and very important areas of the ocean in which there are intermediate cases, or cases that differ from one of the extremes in only a few ways. The expected differences can be logically deduced, as has been done for the above cases. They need not therefore be considered herein. What appears to be most needed at this point is a rigorous testing of many of the theoretical mechanisms proposed herein on a variety of copepods from different habitats and with potentially different evolutionary backgrounds.

REFERENCES

- Anderson, G. C. and R. E. Munson. 1972. Primary productivity studies using merchant vessels in the North Pacific Ocean, p. 245-251. In A. Y. Takenouti (ed.), *Biological oceanography of the northern North Pacific Ocean*. Idemitsu Shoten.
- Batchelor, G. K. 1967. *An Introduction to Fluid Dynamics*, Cambridge University Press, Cambridge, England. 615 pp.
- Beklmeishev, K. V. 1954. [The feeding of some common planktonic copepods in far eastern seas.] *Zool. Zh.* 33:1210-1229. (Transl. from Russian).
- Boyd, C. M. 1976. Selection of particle sizes by filter feeding copepods: A plea for reason. *Limnol. Oceanogr.* 21:175-180.
- Cannon, H. G. 1928. On the feeding mechanisms of the copepods Calanus finmarchicus and Diaptomus gracilis. *Brit. J. Exp. Biol.* 6:131-144.
- Conover, R. J. 1956. Oceanography of Long Island Sound, 1952-1954. VI. Biology of Acartia clausi and A. tonsa. *Bull. Bingham Oceanogr. Coll.* 15:156-233.
- _____. 1976. Feeding interactions in the pelagic zone. *Joint Oceanogr. Conf. Edinburg*. (Unpublished manuscript).
- Dagg, M. 1977. Some effects of patchy food environments on copepods. *Limnol. Oceanogr.* 22:99-107.
- Donaghay, P. L. 1979. Grazing interactions in the marine environment. Proceedings of the International Symposium on Zooplankton Community Structure. Dartmouth College, Hanover, N.H. August 20-25, 1978.
- _____ and L. F. Small. 1979a. Long-term food modification by Acartia clausi: a preliminary view. *Mar. Biol.* 52:129-136.
- _____ and _____. 1979b. Food selection capabilities of the estuarine copepod Acartia clausi. *Mar. Biol.* 52:137-146.
- _____, _____ and R. D. Leatham. In prep. (a). A comparison of grazing functions from phytoplankton and zooplankton viewpoints: An algorithm.
- _____, _____ and R. D. Leatham. In prep. (b). Effects of ammonium regeneration on algal-grazer interactions: Part I. Eurytemora affinis.
- Dugdale, R. C. 1967. Nutrient limitation in the sea: dynamics, identification and significance. *Limnol. Oceanogr.* 12:685-695.

- Feeney, P. 1976. Plant apparency and chemical defense. In: J. Wallace and R. Marshall (eds.), *Recent Advances in Phytochemistry*. 10:1-40.
- Friedman, M. M. and J. R. Strickler. 1975. Chemoreceptors and feeding in calanoid copepods (Arthropoda: Crustacea). *Proc. Nat. Acad. Sci. USA* 72(10):4185-4188.
- Frost, B. 1972. Effects of size and concentration of food particles on the feeding behavior of the marine planktonic copepod Calanus pacificus. *Limnol. Oceanogr.* 17:805-815.
- _____. 1975. A threshold feeding behavior in Calanus pacificus. *Limnol. Oceanogr.* 20:263-266.
- _____. 1977. Feeding behavior of Calanus pacificus in mixtures of food particles. *Limnol. Oceanogr.* 22:472-491.
- _____. 1979. Zooplankton grazing controls phytoplankton growth in the open subarctic Pacific Ocean. ASLO meetings held at Marine Sciences Research Center, Stony Brook, New York June 18-21, 1979.
- Gauld, D. T. 1966. The swimming and feeding of planktonic copepods. In Some Contemporary Studies in Marine Science. H. Barnes (ed.) George Allen and Unwin, Ltd. pp. 313-334.
- Heinle, D. R. 1969. Effects of temperature on the population dynamics of estuarine copepods, Ph.D. dissertation, Univ. Maryland 132 pp.
- _____. In press. Zooplankton in Physiological responses to stress, E. J. Vernberg.
- Heinrich, A. K. 1962. On the production of copepods in the Bering Sea. *Int. Rev. Ges. Hydrobiol.* 47:465-469.
- Herbert, P. D. N. 1974. Ecological differences between genotypes in a natural population of Daphnia magna. *Heredity* 33:327-337.
- Johnson, J. K. In press. Effects of temperature and salinity on production and hatching of dormant eggs of Acartia californiensis (Copepoda) in an Oregon Estuary. *Fishery Bull.* 77(3).
- Kalmijn, Ad. J. 1974. The detection of electric fields from inanimate and animate sources other than electric organs. in A. Fessard (ed.) Handbook of Sensory Physiology. 3:147-201, Springer-Verlag, New York.
- King, C. E. 1972. Adaptation of rotifers to seasonal variation. *Ecology* 53:408-418.
- Lam, R. K., B. W. Frost. 1976. Model of copepod filtering response to changes in size and concentration of food. *Limnol. Oceanogr.* 21:490-500.

- Landry, M. R. 1976. The structure of marine ecosystems: an alternative. *Marine Biology* 35:1-7.
- Larrance, J. D. 1971. Primary productivity in the mid-subarctic Pacific Ocean region, 1966-1968. *Fish. Bull.* 69:595-613.
- Lehman, J. T. 1976. The filter-feeder as an optimal forger, and the predicted shapes of feeding curves. *Limnol. Oceanogr.* 21:501-516.
- Marshall, S. M. 1973. Respiration and feeding in copepods. *Adv. Mar. Biol.* 11:57-120.
- _____ and A. P. Orr. 1955. *The Biology of a Marine Copepod.* Oliver & Boyd, London. 188 pp.
- _____ and _____. 1956. On the biology of *Calanus finmarchicus*. IX. Feeding and digestion in the young stages. *J. Mar. Biol. Assoc. U.K.* 35:587-603.
- Mayzaud, P., R. J. Conover. 1976. Influence of potential food supply on the digestive enzyme activity of neritic copepods. In *Proceed. of the 10th Europ. Mar. Biol. Symp.* Astond, Belg. 2:415-427. Ed. by G. Persoone and E. Jaspers Wetteren, Belgium, Universa Press.
- _____ and S. A. Poulet. 1978. The importance of the time factor in the response of zooplankton to varying concentrations of naturally occurring particulate matter: *Limnol. Oceanogr.* 23:1144-1154.
- McAllister, C. D., T. R. Parsons and J. D. H. Strickland. 1960. Primary productivity and fertility at Station "P" in the north Pacific Ocean. *J. Cons. Int. Explor. Mer.* 25:240-259.
- McLaren, I. A. 1974. Demographic strategy of vertical migration by a marine copepod. *Am. Nat.* 108:91-102.
- Miller, C. G., J. K. Johnson and D. R. Heinle. 1977. Growth rules in the marine copepod genus *Acartia*. *Limnol. Oceanogr.* 22:326-335.
- Mullin, M. M., E. F. Steward and F. J. Fuglister. 1975. Ingestion by planktonic grazers as a function of concentration of food. *Limnol. Oceanogr.* 20:259-262.
- Nival, P. and S. Nival. 1973. Efficacite de filtration des copepodes planctoniques. *Ann. Inst. Oceanogr.* 49:135-144.
- _____ and _____. 1976. Particle retention efficiencies of an herbivorous copepod, *Acartia clausi* (adult and copepodite stages): Effects on grazing. *Limnol. Oceanogr.* 21:34-38.
- O'Connors, H. B., L. F. Small and P. L. Donaghay. 1976. Particle-size modification by two size classes of the estuarine copepod *Acartia clausi*. *Limnol. Oceanogr.* 21:300-308.

- _____, D. C. Biggs and D. V. Ninivaggin. in press. Particle size dependent maximum grazing rates for Temsoira longicornis fed natural phytoplankton.
- Paffenhöfer, G. B. and R. P. Morris. 1976. Feeding, growth and reproduction of the marine planktonic copepod Pseudocalanus elongatus Boeck. J. Mar. Biol. Ass. U.K. 56:327-344.
- Parsons, T. R. 1965. A general description of some factors governing primary production in the Strait of Georgia, Hecate Strait and Queen Charlotte Sound, and the N.E. Pacific Ocean. Fish. Res. Bd. Canada, MS Reprt. Ser. (Oceanogr. Limnol.) 193.
- _____ and R. J. LeBrasseur. 1968. A discussion of some critical indices of primary and secondary production for large scale ocean surveys. Calif. Mar. Res. Comm. CAFCOFI Rept. 12:54-63.
- _____ and M. Takahashi. 1973. Biological Oceanographic Processes. Pergamon Press, New York. 186 pp.
- Peterson, W. T. 1979. Life history and ecology of Calanus marshallae Frost in the Oregon Upwelling Zone. Ph.D. dissertation, OSU. 200 pp.
- Pomeroy, L. R. 1970. The strategy of mineral cycling. Annual Review of Ecology and Systematics. 1:171-190.
- Porter, K. G. and J. R. Strickler. In Prep. The mechanisms of selective feeding in Daphnia.
- Poulet, S. A. 1978. Comparison between five coexisting species of marine copepods feeding on naturally occurring particulate matter. Limnol. and Oceanogr. 23:1126-1144.
- _____ and P. Marsot. 1978. Chemosensory grazing by marine calanoid copepods (Arthropoda: Crustacea). Science 200:403-405.
- _____ and _____. 1979. Chemosensory grazing and food gathering in marine copepods. Proceedings of the International Symposium on Zooplankton Community Structure. Dartmouth College, Hanover, NH. August 20-25, 1978.
- Raymont, J. E. 1963. Plankton and Productivity in the Oceans. Pergamon Press, Ltd. London, England. 660 pp.
- Richman, S., D. R. Heinle and R. Huff. 1977. Grazing by adult estuarine copepods of the Chesapeake Bay. Mar. Biol. 42:69-84.
- Robertson, S. B. and B. W. Frost. 1977. Feeding by an omnivorous planktonic copepod Aestiveus divergens Bradford. J. exp. Mar. Biol. Ecol. 29(231-244).

- Rubenstein, D. I. and M. A. R. Koehl. 1977. The mechanisms of filter feeding: some theoretical considerations. *Amer. Natur.* 111:981-994.
- Schnack, S. 1975. Untersuchungen zur nahrungsbiologie der Copepoden (Crustacea) in der Kieler Bucht. Ph.D. thesis, Kiel. 144 p.
- Schoener, T. W. 1971. Theory of Feeding Strategies. *Am. Rev. Ecol. Syst.* 2, 369-404.
- Sheldon, R. W., A. Prakash and W. H. Sutcliffe, Jr. 1972. The size distribution of particles in the ocean. *Limnol. and Oceanogr.* 17(3):327-340.
- Steele, J. H. 1976. The role of predation in ecosystem models. *Mar. Biol.* 35:9-11.
- _____ and B. W. Frost. 1977. The structure of plankton communication. *Phil. Trans. Royal Soc. London* 280:485-534.
- Strickler, J. T. 1977. Observations of swimming performances of planktonic copepods. *Limnol. Oceanogr.* 22:165-170.
- _____ and G. Rosenberg. 1977. Visual observation of filter-feeding by copepods. 40th annual meeting ASLO E. Lansing.
- _____ and G. A. Paffenhofer. 1979. A cinematographic study of grazing by Eucalanus crassus. Proceedings of the International Symposium on Zooplankton Community Structure. Dartmouth College, Hanover, N.H. August 20-25 1978.
- Uye, S. and A. Fleminger. 1976. Effects of various environmental factors on egg development of several species of Acartia in Southern California. *Mar. Biol.* 38:253-262.
- Wilson, D. S. 1973. Food size selection among copepods. *Ecology* 54:909-914.
- Zilloux, E. J. and J. G. Gonzales. 1972. Egg dormancy in a neritic calanoid copepod and its implications to overwintering in boreal waters. *Proc. European Mar. Biol. Symp.* (5th) Padova. pp. 217-230.